

ABSTRACT

Title of dissertation: CLASSICAL ANALOGIES
 IN THE SOLUTION OF
 QUANTUM MANY-BODY PROBLEMS

Aydin Cem Keser, Doctor of Philosophy, 2017

Dissertation directed by: Professor Victor M. Galitski
 Department of Physics

We consider three quantum many-body systems motivated by recent developments in condensed matter physics, namely topological superconductivity, strongly interacting Bose-Einstein condensates and many-body localization with periodically driven systems. In each of the three problems, an analogy with classical mechanics is employed in the solution of the problem and the interpretation of results. These analogies, in addition to facilitating the solution, illustrate how unique features of classical mechanics or macroscopic phenomena such as macroscopic order parameter and observables, hydrodynamics, spacetime curvature, noise and dissipation, chaos and delocalization emerge out of quantum mechanics. The three problems we study are as follows.

In the first problem, we use quasiclassical methods of superconductivity to study the superconducting proximity effect from a topological p -wave superconductor into a disordered quasi-one-dimensional metallic wire. We demonstrate that the corresponding Eilenberger equations with disorder reduce to a closed nonlinear

equation for the superconducting component of the matrix Green's function. Remarkably, this equation is formally equivalent to a classical mechanical system (i.e., Newton's equations), with the Green's function corresponding to a coordinate of a fictitious particle and the coordinate along the wire corresponding to time. This mapping allows us to obtain exact solutions in the disordered nanowire in terms of elliptic functions. A surprising result that comes out of this solution is that the p -wave superconductivity proximity induced into the disordered metal remains long range, decaying as slowly as the conventional s -wave superconductivity. It is also shown that impurity scattering leads to the appearance of a zero-energy peak.

In the second problem, we consider a system of bosons in the superfluid phase. Collective modes propagating in a moving superfluid are known to satisfy wave equations in a curved spacetime, with a metric determined by the underlying superflow. We use the Keldysh technique in a curved spacetime to develop a quantum geometric theory of fluctuations in superfluid hydrodynamics. This theory relies on a “quantized” generalization of the two-fluid description of Landau and Khalatnikov, where the superfluid component is viewed as a quasi-classical field coupled to a normal component – the collective modes/phonons representing a quantum bath. This relates the problem in the hydrodynamic limit to the “quantum friction” problem of Caldeira-Leggett type. By integrating out the phonons, we derive stochastic Langevin equations describing a coupling between the superfluid component and phonons. These equations have the form of Euler equations with additional source terms expressed through a fluctuating stress-energy tensor of phonons. Conceptually, this result is similar to stochastic Einstein equations that arise in the theory

of stochastic gravity. We formulate the fluctuation-dissipation theorem in this geometric language and discuss possible physical consequences of this theory.

In the third problem, we investigate dynamical many-body localization and delocalization in an integrable system of periodically-kicked, interacting linear rotors. The linear-in-momentum Hamiltonian makes the Floquet evolution operator analytically tractable for arbitrary interactions. One of the hallmarks of this model is that depending on certain parameters, it manifests both localization and delocalization in momentum space. We present a set of “emergent” integrals of motion, which can serve as a fundamental diagnostic of dynamical localization in the interacting case. We also propose an experimental scheme, involving voltage-biased Josephson junctions, to realize such many-body kicked models.

CLASSICAL ANALOGIES IN THE SOLUTION OF QUANTUM MANY-BODY PROBLEMS

by

Aydin Cem Keser

Dissertation submitted to the Faculty of the Graduate School of the
University of Maryland, College Park in partial fulfillment
of the requirements for the degree of
Doctor of Philosophy
2017

Advisory Committee:

Professor Victor M. Galitski, Chair/Advisor

Professor Theodore L. Einstein

Professor Theodore Jacobson

Professor Dionisios Margetis, Dean's Representative

Professor Ian Spielman

© Copyright by
Aydin Cem Keser
2017

Dedication

to my father

Acknowledgments

This thesis would not have been possible without people who contributed with their ideas to my research projects, and people who accompanied me through out my graduate school years.

First and foremost, I want to thank my advisor Victor Galitski. He gave me a chance to join his group and to work on a set of diverse, interesting and challenging problems. He taught me that being a scientist is about forging a character that exhibits courage in the face of the unknown, candid curiosity and integrity, in addition to acquiring knowledge and skills.

I would also like to thank the thesis defense committee members for their efforts to carefully read and comment on this thesis.

I would like to thank my collaborators, Valentin Stanev, Sriram Ganeshan and Gil Refael. Their ideas, guidance and support were essential for the research I am presenting in this thesis. I am also grateful to the Condensed Matter Theory Center, its director Sankar Das Sarma, and the Joint Quantum Institute for providing great environment for doing physics. The people who work here, and frequent seminars and talks were very inspiring and helpful. I also want to mention my officemates (chronologically): Sergey Pershoguba, Juraj Radic, Hilary Hurst, Yahya Alavirad. I enjoyed our time together and all the conversations and discussions about physics or life in general. I am also grateful to all the other Galitski group members with whom I spent my time at UMD.

In addition to this I would like to thank my mother and father for their endless

support. I would like to commemorate my late uncle and late grandfather, both immigrant workers at some point in their lives. Your legacy will live on.

I would like to thank Natalia Budyldina for all the years we spent together, and for carrying the emotional burden of graduate school with me.

Likewise, I would like to thank my roommates. It has been great sharing the same living space with them.

I would also like to thank my friends in the area: Ali and Helen and of course Benjamin Yapici for making me a member of their family, Berk Gurakan and Maya Kabkab, Caner Celik and Sinem Kilic, Burak Cesme, Ugur Cetiner, Bahrom Oripov, Lori Sen, Gokce Basar and Tania Marie, Murat Mercan and all the members of the METU alumni association in DC and the Pir Sultan Abdal Cultural Association of DC.

I would like to thank Monash University and Mannix College for their generous hospitality and Dr. Simon Caterson, whom I had the chance to meet during the amazing time I spent in Australia.

Finally, I would like to mention my endless gratitude to Sarah Black for transforming me from a hesitant and risk averse young dreamer towards a resolutely persistent man.

Table of Contents

| | |
|---|-----|
| Dedication | ii |
| Acknowledgments | iii |
| Table of Contents | v |
| List of Figures | vii |
| List of Abbreviations | ix |
| List of Publications | x |
| 1 Introduction | 1 |
| 1.1 Classical and Quantum mechanics | 1 |
| 1.1.1 Macroscopic wave functions and order parameter fields | 5 |
| 1.1.2 Chaos and localization | 7 |
| 1.2 Keldysh contour and nonequilibrium quantum theory | 10 |
| 1.2.1 Keldysh field integral for bosons | 11 |
| 1.2.2 Quantum particle in contact with an environment | 14 |
| 1.2.3 Keldysh field integral for fermions | 17 |
| 1.2.4 BCS theory of superconductivity in the Keldysh formalism | 20 |
| 2 Long range p -wave proximity effect into a disordered metal | 24 |
| 2.1 Introduction | 24 |
| 2.2 The s -wave case | 26 |
| 2.3 The p -wave case | 29 |
| 2.4 Classical particle analogy | 32 |
| 2.5 The p -wave wire with normal segment | 34 |
| 2.6 Conclusion | 41 |
| 3 Analogue stochastic gravity in strongly interacting Bose-Einstein condensates | 43 |
| 3.1 Introduction | 43 |
| 3.2 The model and energy scales | 48 |
| 3.3 Background field formalism on the Keldysh contour for Bogoliubov quasiparticles | 52 |
| 3.3.1 Covariant phonon action | 57 |
| 3.4 Analogue Einstein equations and two-fluid hydrodynamics | 61 |

| | | |
|-------|---|-----|
| 3.4.1 | Hilbert stress-energy operator of the covariant phonon field . . | 63 |
| 3.4.2 | Semiclassical analogue Einstein equations and the “phonon matter” | 64 |
| 3.4.3 | Canonical versus covariant conserved currents | 65 |
| 3.4.4 | Mass-energy-momentum balance and the covariant conservation of stress-energy operator | 69 |
| 3.5 | Stochastic analogue Einstein equations | 74 |
| 3.5.1 | Linear response and the covariant stress-energy correlator . . . | 74 |
| 3.5.2 | Global thermal equilibrium and fluctuation dissipation relation | 76 |
| 3.5.3 | Hydrodynamic fluctuations around a deterministic solution . | 80 |
| 3.5.4 | Stochastic analogue Einstein equation | 82 |
| 3.5.5 | Procedure to compute background metric fluctuations from the analogue Einstein equation | 82 |
| 3.6 | Equilibrium ‘Minkowski’ fluctuations | 84 |
| 3.7 | Conclusions and outlook | 87 |
| 4 | Dynamical many-body localization in an integrable model | 92 |
| 4.1 | Introduction | 92 |
| 4.2 | The Model | 95 |
| 4.3 | Main Results | 96 |
| 4.3.1 | Energy dynamics | 96 |
| 4.3.2 | Momentum dynamics | 97 |
| 4.3.3 | Integrals of motion | 98 |
| 4.4 | Dynamical many-body localization and the structure of $\vec{\alpha}$ | 100 |
| 4.4.1 | Case I: $\alpha_1 \dots \alpha_d$ are distinct generic irrationals | 100 |
| 4.4.2 | Case II: $\alpha_1 = \alpha_2$ and $\alpha_2 \dots \alpha_d$ are distinct generic irrationals . | 101 |
| 4.4.3 | Case III: $\alpha_1 = 1/2$ and $\alpha_2 \dots \alpha_d$ are distinct generic irrationals | 102 |
| 4.5 | Derivation of main results | 103 |
| 4.5.1 | Derivation of the evolution of energy and momentum averages | 104 |
| 4.5.2 | Construction of integrals of motion | 106 |
| 4.5.3 | Floquet Hamiltonian and quasienergy eigenstates | 107 |
| 4.6 | Experimental proposal | 108 |
| 4.7 | Conclusions | 109 |
| 5 | Conclusions | 112 |
| A | Mapping between Quantum Kicked Rotor and the tight-binding model | 116 |
| A.1 | Lattice model of single quantum kicked rotor | 116 |
| A.2 | d -dimensional lattice model | 117 |
| B | Derivation of the canonical conservation law | 120 |
| C | Noise and response kernels | 122 |
| | Bibliography | 125 |

List of Figures

| | | |
|-----|---|----|
| 2.1 | The potential landscape of a classical particle with motion describing the Green's function, for a normal metallic segment, in contact with a superconductor. Depending on the superconductor (s or p -wave) potential is either V_s or V_p . In the clean limit both converge to V^{clean} . | 33 |
| 2.2 | Contour plot of the DOS of an infinite wire. There is moderate disorder ($\beta = 1$) in the normal segment ($x > 0$). The solid yellow marks the regions that are beyond the plot range (where $N/N_0 > 3.5$). Notice the zero-energy peak in the normal segment. | 37 |
| 2.3 | DOS at the junction of infinite normal and superconducting segments. Three cases for the disorder in the normal segment are plotted: weak ($\beta = 0.1$, blue), moderate ($\beta = 1$, purple), and strong ($\beta = 10$, red). Notice the suppression of DOS with the increase of disorder strength. | 38 |
| 2.4 | Components of \hat{g} , (g_1 : blue, g_2 : purple, g_3 : red) for a wire with infinite p -wave section and finite disordered section of length $L = 5\xi_0$. Top panel: weak disorder ($\beta = 1/(2\tau_{imp}\Delta_0) = 0.1$). Middle panel: moderate disorder ($\beta = 1$). And bottom panel: strong disorder ($\beta = 10$). The Matsubara frequency is set to $\omega = \Delta_0/2$. | 40 |
| 2.5 | The weight of the zero-energy mode $\mathcal{M}(x)$ in a normal section with length $L = 5\xi_0$ for three disorder strengths (blue: $\beta = 0.1$, purple: $\beta = 1$, red: $\beta = 10$). | 41 |
| 3.1 | The Keldysh contour and its forward/backward branches labeled by the path index $s = \pm$: Each degree of freedom and the associated sources are defined twice, one on each branch. The values are matched at t_f , for example $\rho_f^+ = \rho_f^-$. | 53 |
| 3.2 | The Keldysh contour for the phonon field. The metric tensor depends on the background variables ρ_0^\pm and θ_0^\pm and therefore is also defined twice. | 60 |

- 4.1 (Top panel) Plots showing evolution of the root mean square deviation of energy, $\sigma(E) = \sqrt{\langle H_0^2 \rangle - \langle H_0 \rangle^2}$, as a function of time, labeled by the number of kicks, N . (Bottom Panel) Plots showing evolution of the root mean square deviation of individual momenta in an ensemble of 10 particles $\sigma(p_i) = \sqrt{\langle p_i^2 \rangle - \langle p_i \rangle^2}$ as a function of time, labeled by the number of kicks, N . The initial states of the rotors are assumed to be definite momentum states. The total number of particles in this interacting ensemble is $d = 10$ and circular boundary conditions apply. We consider two body interaction term to be $J_{ij} = \cos(\theta_i - \theta_j)$. The periodic kicking potential is given by $K(\theta) = \sum_{m=1}^{\infty} k_m \cos(m\theta)$ for all particles. The m -th Fourier coefficient is fixed by $k_m = \tilde{z}/m^2$, where \tilde{z} is a random complex number with real and imaginary parts uniformly distributed in the interval $[0,1]$. We make sure that $K(\theta)$ is real. We choose $\vec{\alpha}$ corresponding to three scenarios: Figs. (AI, AII): If φ denotes the golden ratio, $\alpha_j = (j/d)\varphi - (1/2)\varphi$ are all irrationals for $j = 1 \dots 10$. Figs. (BI, BII): We consider α_j distinct irrationals as in Case A, but set $\alpha_1 = \alpha_2$, which results in the resonant growth of $\sigma(p_1)$ and $\sigma(p_2)$, while $\sigma(E)$ is bounded. Figs. (CI, CII): We consider α_j as in Case A and set $\alpha_1 = 1/2$, which results in the resonant growth of $\sigma(E)$ and $\sigma(p_i)$ 99
- 4.2 Schematic of chain of voltage-biased (V_i) superconducting grains coupled to each other (J_i) using Josephson junctions. Each grain is connected (K_i) to a grounded common macroscopic superconductor stroboscopically through a strong Josephson coupling. 109

List of Abbreviations

| | |
|-------|-------------------------------------|
| BCS | Bardeen-Cooper-Schrieffer |
| BEC | Bose-Einstein Condensate |
| BBGKY | Bogoliubov-Born-Green-Kirkwood-Yvon |
| BdG | Bogoliubov-de Gennes |
| IOM | Integral of Motion |
| MBL | Many Body Localization |
| ODE | Ordinary Differential Equation |
| PDE | Partial Differential Equation |
| QFT | Quantum Field Theory |
| RMS | Root Mean Square |

List of Publications

The dissertation is based on the following publications:

1. Aydin Cem Keser, Valentin Stanev, and Victor Galitski. Long range p -wave proximity effect into a disordered metal. *Phys. Rev. B* *91*, 094518 (2015) .
2. Aydin Cem Keser, Sriram Ganeshan, Gil Refael, and Victor Galitski. Dynamical many-body localization in an integrable model. *Phys. Rev. B* *94*, 085120 (2016).
3. Aydin Cem Keser, and Victor Galitski. Analogue Stochastic Gravity in Strongly-Interacting Bose-Einstein Condensates. *arXiv:1612.08980* (2017).

Chapter 1: Introduction

1.1 Classical and Quantum mechanics

In this thesis, we will solve or extend the solution of three quantum many-body problems. These problems in addition to their practical value in the context of recent developments in condensed matter physics, such as zero-energy modes in topological systems, strongly interacting Bose condensates and many-body localized systems, serve an auxiliary purpose as well. Each model is connected to a seemingly unrelated analogous classical system that elucidates the underlying physics or helps us address a broader issue in modern physics, such as the emergence of classical degrees of freedom, spacetime and quantum chaos. Before introducing these three problems, we will give a very brief qualitative review of the relation between classical and quantum mechanics.

Classical mechanics is a theory of nature that describes the motion of an N -body system in the $6N$ dimensional phase space. All observables are functions of $3N$ configuration space variables and their $3N$ conjugate momenta. [1, 2] The $N \rightarrow \infty$ limit leads to an idealization called the classical field and is the subject of continuum mechanics. The geometry of spacetime on which physical systems live is thought of as a continuum itself whose dynamics is determined by the Einstein

equation. [3] When the gravitational field is weak, the solution to this equation approaches the Minkowski geometry. [4] In this geometry, phenomena are described by the Lorentz covariant equations of motion. For example, electrodynamics is described by Maxwell's equations. Finally, when the typical speeds are slow compared to the speed of light, Galilean relativity, Newton's laws of motion and universal gravitation hold to a good approximation. In situations where it is impossible to exactly locate the system in phase space, the equations of motion for a probability distribution is written [5]. Finally where the number of constituents are too numerous and undergo random collisions, aggregate quantities are described by thermodynamics. [6]

Ever since the conception of quantum theory, the problem of how the classical description of nature emerges out of quantum mechanics has attracted a great deal of interest, and it is still at the heart of many interesting physical problems. [7, 8] Roughly speaking, classical mechanics is thought of as the $\hbar \rightarrow 0$ limit of quantum theory. (The numerical value of the Planck constant measured in terms of the typical scales of the system is small). Depending on the mathematical formalism that describes quantum mechanics, this limit manifests itself in myriad ways. In the path integral quantization, the ratio of the action functional to Planck constant appears in a complex exponential that represents the amplitude of a matter wave. When this quantity grows, the path integral tends to zero due to a rapidly oscillating integrand, except for classical trajectories, for which the action is extremized. [9] In the canonical quantization, the fundamental commutation relation tends to zero, which means that the expectation value of a product of position and momentum

operators reduces to the product of their expectation values, each of which obeys the classical equation of motion by Ehrenfest's principle. [10, 11] In phase space formulation, the Moyal bracket reduces to the Poisson bracket, and the equations of motion for observables obey Hamilton's equation of motion. [12]

To get a grasp of the situation, consider a harmonic oscillator made up of a mass of 1 kg and spring constant of 1 kg s⁻². Assuming that a sinusoidal mode with an amplitude of 1 m is excited, the energy is 0.5 J and the time scale is 1 s. Compare the product of energy and time scales to the metric value of reduced Planck constant which is 34 orders of magnitude smaller. Alternatively, we can compute the quantum of energy $\hbar\omega$ in the system to find the occupation number to be on the order of 10³³ particles (phonons). In other words, the quanta are too small to be perceived.

An important issue worth noting is the measurement problem. So long as one stays in the classical realm where \hbar is small, as everybody did till the 20th century, the above considerations roughly (we will explain this further 1.1.2) explain the emergence of classical mechanics. However, the problem deepens when one considers a quantum system, typically surrounded by an experimental physicist and her apparatus which are both in the classical realm. As in Schroedinger's thought experiment [13], the result of a quantum phenomenon might trigger a macroscopic classical event, for example the death of a cat. How the quantum state collapses to a definite classical outcome is the so-called measurement problem that is at the heart of many scientific and philosophical issues in quantum theory. [8, 14]

In the many-body context, quantum mechanics is responsible for many macro-

scopic electromagnetic and thermal phenomena, and the problem of how macroscopic observables follow from the many-body wave function encompasses an entire branch of physics called condensed-matter physics.

Therefore, the transition to classical mechanics, or emergence of classical degrees of freedom, is complicated through interactions that entangle the underlying quantum degrees of freedom. This seems to indicate that the measurement problem is related to how a quantum system is interacting with its environment, which can be a macroscopic measurement device or simply the rest of the particles in the system. This, we believe, should convince the reader that the quantum to classical transition is essentially a many-body phenomenon.

The process of classicalization of a system due to interactions with an environment or a ‘bath’ is called decoherence. One interpretation is that only classical looking degrees of freedom survive the decoherence process. [8] A simple toy model is a quantum particle that is coupled to a thermal bath i.e. a family of oscillators. The so called Caldeira-Leggett model, that we will solve in the Keldysh field integral method, describes how classical equations of motion, dissipation and noise can be calculated from quantum mechanics, assuming that decoherence takes place. [15] The complete resolution of the measurement problem and transition to classical mechanics is beyond the scope and aims of this thesis, therefore we refer the reader to the above references. However, as in the Caldeira-Leggett model, the models we consider in this thesis will help us understand how various unique features of classical mechanics can come out of the many-body quantum mechanics at least from an operational point of view.

1.1.1 Macroscopic wave functions and order parameter fields

At low temperatures a many-body quantum system, due to the vast number of its constituents, is approximated by a quantum field. [15] (This ‘low’ temperature can be as large as thousands of Kelvins in metals due to the vast number of electrons that occupy high energy states as a result of the exclusion principle). The quantum field is described as modes (quasiparticles) excited over a vacuum state. The concept of a vacuum state of a many-body system is intimately connected to the phases of matter. In metals it is an incompressible sea of electrons; in a BEC, it is a macroscopic wave function, that behaves like a fluid through Madelung’s description. In any case, the typical procedure is to start from a phase (that forms by spontaneously breaking a symmetry) and consider the excitations above the vacuum defined by the phase. [16]

One of the holy grails of the condensed matter theory is the phases of matter that has macroscopic quantum properties, such as superfluids and superconductors. In these systems, a macroscopic number of fermions or bosons get locked and form a single giant wave function (a classical matter wave similar to a classical light field). This classical wave is called the order parameter field of the phase. The many-body wave function is, by the above mentioned general picture, described by the quantum field of quasiparticles that are excited over the vacuum defined by the order parameter. The order parameter field, together with correlation functions of the quasiparticle field, obeys a set of partial differential equations [17, 18]. The resulting description predicts how macroscopic observables arise from quantum mechanics;

hence, it answers the quantum to classical transition question for the system at hand. Furthermore, once a PDE is obtained, one can conjure up an unrelated classical system that mimics its behavior.

In Part 2, we consider a superconductor, where the order parameter (Cooper field), together with the matrix of two-point correlation functions, satisfies the PDE called the Gorkov equation supplemented by a self-consistency condition. Further simplification is obtained by considering the slow varying dynamics of the correlation functions. In thermal equilibrium, the PDE reduces to a set of three ODE's with non-linear terms due to the disorder in the superconductor. By identifying a hidden constant of motion, we reduce the ODE system to a single second-order ODE, that can be thought of as the equation of motion of a classical particle moving in a potential. Using this simple and intuitive system, we compute the Green's function of a topological superconducting wire in contact with a dirty lead, a problem of great practical interest in the field of topological quantum computing. Our calculation reveals the smoking gun for the long-sought Majorana zero mode in this system.

In Part 3, we start with a bosonic system in the superfluid phase. Writing the superfluid wave function in hydrodynamic variables, we write the fluid equations of motion that describe the interplay between the superfluid 'classical' degrees of freedom and the quantum field of excitations, that is phonons. As in the Caldeirra-Leggett model, the bath of quasaiparticles create dissipative and noisy dynamics on the background field. Another interesting layer of analogy appears due to the effective covariance of the phonon field. Phonons in this theory appear as though they are propagating in a pseudo-Riemannian metric defined by the background flow.

In this respect, the momentum, mass and energy conservation laws of the superfluid are analogous to Einstein's equations and the covariant conservation of the stress energy tensor for matter. We use this analogy to compute the noise correlator and transport coefficients in the system in a manifestly covariant form. This analogy provides a hint for the emergence of the classical spacetime from the yet-to-be-found quantum theory of everything. Moreover, one can discuss the vacuum energy, cosmological constant and other quantum gravitational phenomena such as black holes, Hawking radiation and covariance anomalies in this context.

1.1.2 Chaos and localization

Even for macroscopic objects, the $\hbar \rightarrow 0$ limit does not straightforwardly explain classical behavior all together, because the limit is singular. [19] When $\hbar = 0$ strictly, classical mechanics predicts chaos. Differential equations that describe classical systems with positive Lyapunov exponents is ubiquitous. A positive Lyapunov exponent means that the distance between two particles in the system or in the ensemble grows exponentially with time, despite being infinitesimally small at the beginning. The linearity and the unitarity of quantum mechanics and the ensuing integrability prohibits this behavior for isolated systems. [20] Although, at first the phase space distribution of a quantum system explores the phase space in a way similar to a classical ensemble at a certain time scale quantum effects take over and the phase space diffusion stops. [21, 22] This time scale, the Ehrenfest time, is perceivably short even for astronomical bodies, despite the fact that \hbar is extremely

small yet non-zero. For example, the inverse Lyapunov exponent i.e. time scale for chaos to develop for the rotation of Hyperion, the non-round moon of Saturn is approximately 30 days. The Ehrenfest time for Hyperion is 37 years. However, chaotic motions of macroscopic bodies persist. [23]

The resolution is again hidden in the decoherence process. The rotation angle of Hyperion is not a quantum variable. Hyperion is showered by a variety of particles that causes decoherence on a time scale of order 10^{-53} s. [24] The environment restores chaos.

Prohibition of chaos in quantum mechanics has an important consequence in many-body physics: Anderson localization. In a disordered lattice, the diffusion of a wave packet stops due to quantum destructive self-interference. The Ehrenfest time is replaced by the localization length. [25, 26]

An illustrative model, dubbed the Maryland Model, that connects the prevention of dynamical chaos in quantum mechanics and localization was put forward by Fishman, Grempel and Prange. [25] The quantized version of a quintessential chaotic system, the standard map that describes the motion of a rotor kicked with a constant period, is mapped onto a tight binding model. The sites of the lattice are angular momentum quantum numbers, so that dynamical chaos maps to delocalization. It is shown that, unless certain resonances are avoided, the phase space diffusion comes to a halt, in other words wave functions of the lattice are localized. An integrable version of the Maryland model was also proposed, where localization is controlled by the rotation number of the rotor, i.e. the number of turns it completes between each kick. [27, 28]

For a given subsystem located deep inside a many-body system, the environment is the rest of the system itself. So far, it has been believed that localization would be destroyed due to the interacting system acting on its components as a bath. As a result electron transport has been expected to be restored, just as the chaotic orbit of Hyperion persists due to decoherence enforced by the showering light and cosmic particles. This process of an interacting system acting as a bath to its subsystems is called thermalization and it is what makes the predictions of equilibrium statistical mechanics applicable to a quantum many-body system. [29–31]

However, recently a class of interacting models have been proposed where thermalization does not occur, causing a phenomenon called many-body localization. [32–39] A many-body localized system can not be described by equilibrium statistical mechanics because it does not thermalize; instead, it is described by a set of local conserved quantities that remember their initial values. [40]

In Part 4, inspired by the Maryland model, we consider a set of interacting integrable rotors and discuss localization in the context of integrals of motion and resonances in the energy-momentum transfer due interactions and kicking.

Quite surprisingly, the quantum and classical behavior of the integrable Maryland model are very similar. [41] For this reason, as a side note, a similar Hamiltonian is proposed as a building block for a deterministic quantum theory. [42]

1.2 Keldysh contour and nonequilibrium quantum theory

The goals we laid out in the introduction requires formulating quantum theory of fields and particles and, extracting classical/macrosopic observables. The path integral formulation is an ideal candidate for this. Moreover, choosing a closed time integration contour provides great utility in non-equilibrium and disordered systems, as well as noisy and dissipative scenarios. In this section we will provide a brief review of Keldysh field integral.

Nonequilibrium quantum field theory is developed by the pioneers of the quantum theory such as Schwinger, Kadanoff, Baym, Konstantinov, Perel and Keldysh around the same time that Matsubara developed the thermal field theory technique. [43–46] The method is applied to a variety of problems in non-equilibrium statistical mechanics, quantum Brownian motion, transport problems and disordered systems and it forms the backbone of nonequilibrium kinetic theory. [15, 47] The technique we refer to as Keldysh formalism is also referred to as Closed Time Path formalism due to the choice of the integration contour of the path integral. Calzetta and Hu applied this formalism to fields on curved spacetime [48] and the marriage between non-equilibrium fields and gravity gave rise to the stochastic gravity paradigm. [49].

In the Keldysh formalism one replaces the vacuum persistence amplitude of the “in-out” formalism with the following partition function,

$$Z[V] = \text{Tr} \left\{ \hat{U}_C(\hat{V}) \hat{\rho}(-\infty) \right\} \quad (1.1)$$

In this equation $\hat{\rho}(-\infty)$ is the (normalized) density matrix of the system at an early time, and $\text{Tr}\hat{\rho}(-\infty) = 1$. The operator \hat{U}_C is the evolution operator path ordered on a closed time contour. The closed time contour starts at an early time $t \rightarrow -\infty$, extends to $t \rightarrow \infty$, forming the forward branch of the contour, and reverses back to $t \rightarrow -\infty$, forming the backward branch of the contour. The Hamiltonian for the evolution is $\hat{H} = \hat{H}_0 + \hat{V}^\pm(t)$ where the external time dependent potential is allowed to be different on the forward and backward branches of the contour. If $\hat{V}^\pm(t)$ denotes the forward and backward values of the external potential, $V^+(t) = V^-(t)$ renders $U_C = 1$ and the partition function becomes $Z = 1$. This has a technical advantage over the usual in/out formalism, where $Z = \langle \text{in} | \text{out} \rangle$ is not necessarily unity and should be accounted for while computing amplitudes.

1.2.1 Keldysh field integral for bosons

Specifically, suppose we have a scalar real massless free field ϕ that obeys the scalar wave equation. The partition function is then written as a functional integral over the closed time path C , and it reads

$$Z = \int \mathcal{D}[\phi] e^{i \int_C d^4x d^4x' \bar{\phi}(x) \hat{D}^{-1}(x, x') \phi(x')} \quad (1.2)$$

where D is the Green's function. The objective is to determine the Green's function, given the initial density matrix. Let ϕ^\pm denote the values of the forward/backward values of the field, thereby effectively doubling the number of degrees of freedom in the problem. Let S denote the classical action of the field ϕ . Labeling the initial

and final values of the fields as $\phi_i^\pm = \phi^\pm(-\infty)$ and $\phi_f^\pm = \phi^\pm(+\infty)$, respectively, we can write the Feynman path integral representation of Z in Eq. (1.1) as

$$Z = \int \mathcal{D}[\phi^\pm] \varrho[\phi_i^+, \phi_i^-] \delta(\phi_f^+ - \phi_f^-) e^{i(S[\phi^+] - S[\phi^-])} \quad (1.3)$$

Here S , the action integral, is taken from $t \rightarrow -\infty$ to $t \rightarrow +\infty$. Notice that we explicitly imposed the initial and final conditions on the fields. Keldysh discovered that the initial and final value constraints can be handled by constructing the fields

$$\phi^{c(q)} = \frac{1}{2} (\phi^+ \pm \phi^-) \quad (1.4)$$

$\phi^{c(q)}$ are classical and quantum components of the field. Defining $\vec{\phi} = (\phi^c \ \phi^q)^T$ and absorbing the density matrix into the action and the Jacobian of the transformation in Eq. (1.4) in the integration measure we get the following path integral for the field vector:

$$Z = \int \mathcal{D}[\vec{\phi}] \exp \left[\frac{i}{2} \int d^4x d^4x' \vec{\phi}^T(x) \hat{D}^{-1}(x, x') \vec{\phi}(x') \right] \quad (1.5)$$

where the inverse Green's function matrix reads

$$\hat{D}^{-1}(x, x') = \begin{pmatrix} 0 & [D^A]^{-1} \\ [D^R]^{-1} & [D^{-1}]^K \end{pmatrix}_{x, x'} \quad (1.6)$$

The retarded (advanced) Green's functions $D^{R(A)}$ are lower(upper) triangular matrices in the time domain that are independent of the initial density matrix. They are formally written as:

$$-i \langle \phi^{c(q)}(x) \phi^{q(c)}(x') \rangle = D^{R(A)}(x, x') = \frac{1}{2} \{ (i\partial_t \pm i0)^2 + \nabla_{\vec{r}}^2 \}^{-1} \delta(x - x') \quad (1.7)$$

So we can write them as a Fourier integral over 4-momentum

$$D^{R(A)}(x, x') = \frac{1}{2} \int \frac{d^4 k}{(2\pi)^4} \frac{e^{-ik(x-x')}}{(k^0 \pm i0)^2 - |\vec{k}|^2} \quad (1.8)$$

and therefore

$$D^R(x - x') = D^R(y) = -\frac{1}{4\pi} \theta(y^0) \delta(y^\mu y_\mu) \quad (1.9)$$

They satisfy the properties

$$[D^A]^T = D^R \quad (1.10a)$$

$$D^A(k^0, \vec{k}) = D^R(-k^0, \vec{k}) = [D^R]^*(k^0, \vec{k}) \quad (1.10b)$$

$$D^{A(R)}(y^0 = 0, \vec{y}) = 0 \quad (1.10c)$$

The last one means, in the continuum limit the step function in Eq. (1.9) is regularized as $\theta(0) = 0$.

The Keldysh Green's function contains the information about the initial correlations, and it is the correlator

$$D^K(x, x') = -i \langle \phi^c(x) \phi^c(x') \rangle \quad (1.11)$$

It is parametrized by using an antisymmetric kernel F

$$D^K(x - x') = D^R \circ F - F \circ D^A \quad (1.12a)$$

$$[D^{-1}]^K = [D^R]^{-1} \circ F - F \circ [D^A]^{-1} \quad (1.12b)$$

$$F^T = -F \quad (1.12c)$$

Here $F(x, x')$ contains the initial correlations hence it depends on $\hat{\varrho}(-\infty)$ and the symbol \circ means convolution. The Wigner transform of F is the distribution function

and in equilibrium it is $F(\epsilon) = \coth(\epsilon - \mu)/2T$, a manifestation of the Fluctuation-Dissipation Relation (FDR). For real bosons, $F(\epsilon)$ is real and odd; therefore, the chemical potential vanishes.

Note that the action in Eq. (1.5) vanishes when quantum components of fields are put to zero,

$$S_0|_{\phi^q} = 0 \quad \text{and} \quad \left. \frac{\delta S_0}{\delta \phi^q} \right|_{\phi^q=0} = 0 \quad (1.13)$$

gives the classical equation of motion for the field ϕ^c . This justifies the names chosen for the field components ϕ^c, ϕ^q . The above properties of the Keldysh action and its Green's functions are collectively referred as the 'causality structure'. The causality structure is intact when external potentials or interactions are switched on.

1.2.2 Quantum particle in contact with an environment

Here we will derive the Langevin equation for the Brownian motion of a quantum particle in contact with a bath. The particle has the following action in the Keldysh formalism:

$$S_p[X] = \int_C dt \frac{1}{2} \dot{X}^2 - V(X) \quad (1.14)$$

Denoting the coordinate over the forward/backward branches as X^\pm and performing the rotation to classical and quantum components

$$X^cl = \frac{1}{2}(X^+ + X^-); \quad X^q = \frac{1}{2}(X^+ - X^-) \quad (1.15)$$

the action reads

$$S_p[X] = \int_{-\infty}^{\infty} dt \, 2\dot{X}^{cl} \dot{X}^q - V(X^{cl} + X^q) + V(X^{cl} - X^q) \quad (1.16)$$

Note that variational derivative with respect to X^q at the limit $X^q \rightarrow 0$ gives the classical equation of motion

$$\ddot{X}^{cl} + V'(X^{cl}) = 0 \quad (1.17)$$

In addition to the particle, we have the heat bath, commonly assumed to be a collection of bosonic degrees of freedom with a wide spectrum, i.e. a collection of harmonic oscillators with characteristic frequencies indexed by s . The action for the bath and bath-system coupling will be taken as

$$S_{bath}[\vec{\phi}_s] = \frac{1}{2} \sum_s \int_{-\infty}^{\infty} dt \vec{\phi}_s^T D_s^{-1} \vec{\phi}_s \quad (1.18a)$$

$$S_{coupling} = \sum_s g_s \int_C dt X \phi_s = \sum_s g_s \int_{-\infty}^{\infty} dt \vec{X}^T \sigma_1 \vec{\phi}_s \quad (1.18b)$$

The choice for the form of the couplings make the partition function amenable to Gaussian integration so that

$$Z = \int \mathcal{D}[\vec{\phi}_s] \mathcal{D}\vec{X} e^{i[S_p + S_{bath} + S_{coupling}]} = \int \mathcal{D}[\vec{X}] e^{i[S_b + S_{diss}]} \quad (1.19)$$

where the resulting dissipative term reads

$$S_{diss} = \frac{1}{2} \int \int dt dt' \vec{X}^T(t) \mathcal{D}^{-1}(t - t') \vec{X}(t') \quad (1.20)$$

with the dissipative kernel

$$\mathcal{D}^{-1}(t - t') = -\sigma_1 \left(\sum_s g_s^2 D_s(t - t') \right) \sigma_1 \quad (1.21)$$

The kernel \mathcal{D} inherits its causality structure from the bosonic Green's function D . The retarded and advanced components in Fourier space reads

$$[\mathcal{D}^{-1}(\omega)]^{R(A)} = -\frac{1}{2} \sum_s \frac{g_s^2}{(\omega \pm i0)^2 - \omega_s^2} \quad (1.22)$$

The spectral density of the path is defined as

$$J(\omega) = \pi \sum_s (g_s^2 / \omega_s) \delta(\omega - \omega_s) \quad (1.23)$$

and it is assumed to behave as $J(\omega) = 4\gamma\omega$ at low frequencies. With this definition the dissipative kernel becomes

$$[\mathcal{D}^{-1}(\omega)]^{R(A)} = 4\gamma \int \frac{d\omega'}{2\pi} \frac{\omega'^2}{\omega'^2 - (\omega \pm i0)^2} = \text{const} \pm 2i\gamma\omega \quad (1.24)$$

The constant contributes to the definition of the classical potential in which the particle is moving. In thermal equilibrium the Keldysh component follows from these as

$$[\mathcal{D}^{-1}(\omega)]^K = ([\mathcal{D}^{-1}(\omega)]^R - [\mathcal{D}^{-1}(\omega)]^A) \coth \frac{\omega}{2T} = 4i\omega\gamma \coth \frac{\omega}{2T} \approx 8iT\gamma \quad (1.25)$$

where the approximation holds in the classical limit where $\hbar\omega/kT \ll 1$.

All in all the total action in real space after integrating out the bath reads:

$$S_{tot}[\vec{X}] = \int_{-\infty}^{\infty} dt \, 2\dot{X}^{cl} \dot{X}^q - V(X^{cl} + X^q) + V(X^{cl} - X^q) - 2X^q \gamma \dot{X}^{cl} + 8iT\gamma (X^q)^2 \quad (1.26)$$

The variational derivative around $X^1 = 0$ will produce a damped equation of motion. The full Langevin equation can be obtained by decoupling the $(X^q)^2$ by using an auxiliary noise variable.

$$Z = \int \mathcal{D}[\vec{X}] e^{iS_{tot}} = \int \mathcal{D}[\vec{X}, \xi] e^{\frac{i}{4\gamma T} \int dt \xi^2} e^{-i \int dt 2X^q (\ddot{X}^{cl} + V'(X^{cl}) + \gamma \dot{X}^{cl} - \xi)} \quad (1.27)$$

where, the higher terms in the external potential are dropped, as they don't contribute to the equations of motion. The Langevin equation immediately follows after applying Eq. (1.13) to Eq. (1.27).

$$\ddot{X} + V'(X) + \gamma \dot{X} = \xi \quad (1.28)$$

The correlation function of noise can be computed from Eq. (1.27) as

$$\langle \xi(t) \xi(t') \rangle = 2\gamma T \delta(t - t') \quad (1.29)$$

The fluctuation dissipation relation manifests itself in this equation, as the noise correlator is proportional to the friction coefficient γ .

1.2.3 Keldysh field integral for fermions

The path integral for a fermionic field is written in terms of two independent Grassmann fields ψ and $\bar{\psi}$. On a closed time path contour C , the functional integral for a free fermion field with Green's function G reads

$$Z = \int \mathcal{D}[\bar{\psi}\psi] e^{i \int_C d^4x d^4x' \bar{\psi}(x) \hat{G}^{-1}(x, x') \psi(x')} \quad (1.30)$$

Similar to the boson case, let ψ^\pm and $\bar{\psi}^\pm$ denote the forward/backward values of the Grassmann fields. The following Keldysh parametrization

$$\psi_1 = \frac{1}{\sqrt{2}} (\psi^+ + \psi^-), \quad \psi_2 = \frac{1}{\sqrt{2}} (\psi^+ - \psi^-) \quad (1.31a)$$

$$\bar{\psi}_1 = \frac{1}{\sqrt{2}} (\bar{\psi}^+ - \bar{\psi}^-), \quad \bar{\psi}_2 = \frac{1}{\sqrt{2}} (\bar{\psi}^+ + \bar{\psi}^-) \quad (1.31b)$$

proposed by Larkin and Ovchinnikov and defining

$$\vec{\Psi} = \begin{pmatrix} \psi_1 \\ \psi_2 \end{pmatrix}, \quad \vec{\bar{\Psi}} = \begin{pmatrix} \bar{\psi}_1 \\ \bar{\psi}_2 \end{pmatrix} \quad (1.32)$$

brings the action into the following

$$Z = \int \mathcal{D}[\vec{\Psi}\vec{\bar{\Psi}}] \exp \left[i \int d^4x d^4x' \vec{\bar{\Psi}}^T(x) \hat{G}^{-1}(x, x') \vec{\Psi}(x') \right] \quad (1.33)$$

where the inverse Green's function matrix reads

$$\hat{G}^{-1}(x, x') = \begin{pmatrix} [G^R]^{-1} & [G^{-1}]^K \\ 0 & [G^A]^{-1} \end{pmatrix}_{x, x'} \quad (1.34)$$

The components of the Green's function satisfy the following symmetry properties

$$G^A = [G^R]^\dagger, \quad G^K = -[G^K]^\dagger \quad (1.35)$$

Therefore, the Keldysh component can be parametrized by using a hermitian matrix

$F = F^\dagger$ as

$$G^K = G^R \circ F - F \circ G^A \quad (1.36)$$

where the symbol \circ means convolution. In thermal equilibrium the Green's function depends only on the difference between time components, due to the time translational symmetry. Fourier transform in this time coordinate produces the equilibrium distribution function F as a function of energy ϵ as

$$F(\epsilon) = 1 - 2n_F(\epsilon) = \tanh \frac{\epsilon - \mu}{2T} \quad (1.37)$$

To be more specific, consider the free gas of electrons under a uniform Zeeman field H_Z that has the Hamiltonian

$$\hat{H} = \frac{\hat{p}^2}{2m} + \vec{H}_Z \cdot \vec{\hat{s}} \quad (1.38)$$

With the spin degrees of freedom $\sigma, \sigma' = \pm$, the Keldysh action of the free Fermi gas reads

$$S_0 = \sum_{\sigma, \sigma'} \int d^4x d^4x' \vec{\Psi}_\sigma^T(x) \hat{G}_{\sigma\sigma'}^{-1}(x, x') \vec{\Psi}_{\sigma'}(x') \quad (1.39)$$

Choosing the direction of H_Z as the z axis and using the fact that energy, momentum and the z -component of spin are good quantum numbers, and defining the Fourier decomposition of the fermion fields as

$$\psi(\vec{r}, t) = \sum_{\vec{k}} \psi(\vec{k}, t) e^{i\vec{k} \cdot \vec{r}}, \quad \bar{\psi}(\vec{r}, t) = \sum_{\vec{k}} \bar{\psi}(\vec{k}, t) e^{-i\vec{k} \cdot \vec{r}} \quad (1.40)$$

the bare Green's functions can be immediately written down as

$$G_{\sigma\sigma'}^{R(A)}(\vec{k}, \epsilon) = \delta_{\sigma\sigma'} \left(\epsilon - \epsilon_{\vec{k}, \sigma} \pm i0 \right)^{-1} \quad (1.41a)$$

$$G_{\sigma\sigma'}^K(\vec{k}, \epsilon) = -2\pi i \delta_{\sigma\sigma'} F(\epsilon) \delta(\epsilon - \epsilon_{\vec{k}, \sigma}) \quad (1.41b)$$

where

$$\epsilon_{\vec{k}, \sigma} = \frac{|\vec{k}|^2}{2m} + \sigma H_Z \quad (1.42)$$

1.2.4 BCS theory of superconductivity in the Keldysh formalism

The free electron gas is just an idealization, as collisions and momentum transfer between electrons occur due to interactions. The two-body interaction term can be captured by including the interaction term in the action $S = S_0 + S_{int}$ where in reciprocal space we have

$$S_{int} = -\frac{1}{2} \int_C dt \sum_{\vec{q}, \vec{k}, \vec{k}'} \sum_{\sigma \sigma'} U(\vec{q}) \bar{\psi}_{\vec{k}, \sigma} \bar{\psi}_{\vec{k}', \sigma'} \psi_{\vec{k} + \vec{q}, \sigma'} \psi_{\vec{k} - \vec{q}, \sigma} \quad (1.43)$$

Depending on the magnitudes of the momenta of the incoming electrons, we can have three classes of scattering events. First, the incoming electrons have momenta comparable to the Fermi momentum so that $k, k' \sim k_F$ and the transferred momentum $q \ll k_F$ is small. Second, the sum of the incoming momenta $|\vec{k} + \vec{k}'| \sim 2k_F$ is close to twice Fermi momentum; and third, the difference of the momenta $|\vec{k} - \vec{k}'| \sim 2k_F$ is nearly twice Fermi momentum. In the last two cases, the momentum transfer is on the order of k_F .

The second type, where $|\vec{k} - \vec{k}'| \sim 2k_F$ is the most important, as it produces Cooper pairs in the following way. Relabeling the momenta so that the transferred momentum is exactly $|\vec{k} + \vec{k}'|$, we get

$$S_{BCS} = -\frac{1}{2} \int_C dt \sum_{\vec{q}, \vec{k}, \vec{k}'} \sum_{\sigma \sigma'} U(\vec{k} + \vec{k}') \bar{\psi}_{\vec{k}, \sigma} \bar{\psi}_{-\vec{k} + \vec{q}, \sigma'} \psi_{\vec{k}' + \vec{q}, \sigma'} \psi_{-\vec{k}', \sigma} \quad (1.44)$$

where the subscript *BCS* stands for Bardeen-Cooper-Schrieffer theory that is based on the idea that interactions that flip the momenta of the incoming pair binds them

into bosonic pairs. In BCS theory, the interaction between electrons are mediated by phonons with momentum $\sim k_F$ is frequency independent and attractive and is $-\lambda/\nu$ where ν is the density of states at Fermi energy and $\lambda > 0$. Indeed, in this case, the interaction is of pairing type because the interaction vanishes due to fermionic commutation relations when the spins of the interacting electrons are the same. Defining the Cooper pair fields as:

$$\Phi(\vec{q}, t) = \sum \psi_{\vec{k}+\vec{q}\downarrow}(t)\psi_{-\vec{k}\uparrow}(t), \quad \bar{\Phi}(\vec{q}, t) = \sum \bar{\psi}_{-\vec{k}\uparrow}(t)\bar{\psi}_{\vec{k}+\vec{q}\downarrow}(t) \quad (1.45)$$

The interaction in real space reads

$$S_{BCS} = \frac{\lambda}{\nu} \int_C d^4x \bar{\Phi}(x)\Phi(x) \quad (1.46)$$

A bosonic degree of freedom Δ is introduced so that the total action becomes quadratic in the fermionic fields. This effectively decouples the Cooper fields at expense of creating a bosonic condensate Δ . To do this observe that, BCS action can be written as

$$\exp(iS_{BCS}) = \int \mathcal{D}[\Delta] e^{i \int_C d^4x [-\frac{\nu}{\lambda} |\Delta|^2 + \Delta \bar{\Phi} + \Delta^* \Phi]} \quad (1.47)$$

Now, the partition function for the free and interacting parts $S_0 + S_{BCS}$ can be expressed in terms of a single quadratic action, the Bogoluibov de Gennes action S_{BdG}

$$\int \mathcal{D}[\bar{\psi}\psi] e^{(iS_0 + iS_{BCS})} = \int \mathcal{D}[\Delta] e^{-\frac{\nu}{\lambda} i \int_C d^4x |\Delta|^2} \int \mathcal{D}[\bar{\psi}\psi] e^{iS_{BdG}} \quad (1.48)$$

where

$$S_{BdG} = \int_C d^4x \begin{pmatrix} \bar{\psi}_\uparrow & -\psi_\downarrow \end{pmatrix} \begin{pmatrix} i\partial_t + \frac{1}{2m}(\nabla_r + i\vec{A})^2 - V_{dis} & \Delta \\ -\Delta^* & -i\partial_t + \frac{1}{2m}(\nabla_r - i\vec{A})^2 - V_{dis} \end{pmatrix} \begin{pmatrix} \psi_\uparrow \\ \bar{\psi}_\downarrow \end{pmatrix} \quad (1.49)$$

The crystal dislocations and non-magnetic impurities impose a disordered electric potential on the system, which we call V_{dis} . In addition, we assumed the Zeeman coupling is small and ignored it.

This 2×2 kernel is defined in the particle-hole or the so-called Nambu space. In a general situation coupling terms exist between the particle hole spinor $(\psi_\uparrow, \bar{\psi}_\downarrow)$ and the spinor with opposite spin structure $(\psi_\downarrow, -\bar{\psi}_\uparrow)$. So the BdG kernel is 4×4 acting on bi-spinors that live in the direct product of Nambu and spin spaces. Here, due to the absence magnetic impurities and spin orbit coupling, the spin space becomes trivial and we get two copies of the Nambu space.

However, we still need to enlarge the kernel if we want to double the degrees of freedom to account for the closed-time contour. So we are working in the product of Nambu and Keldysh spaces. In this space, we can write

$$\vec{\Psi} = \begin{pmatrix} \psi_{1\uparrow} & \bar{\psi}_{1\downarrow} & \psi_{2\uparrow} & \bar{\psi}_{2\downarrow} \end{pmatrix}^T, \quad \vec{\bar{\Psi}} = \begin{pmatrix} \bar{\psi}_{1\uparrow} & -\psi_{1\downarrow} & \bar{\psi}_{2\uparrow} & -\psi_{2\downarrow} \end{pmatrix} \quad (1.50)$$

$$S_{BdG} = \int \int d^4x d^4x' \vec{\bar{\Psi}}(x) \left[\hat{G}_0^{-1}(x, x') - \hat{V}_{dis}(x, x') \right] \vec{\Psi}(x') \quad (1.51)$$

where G_0 is the Green's function of the clean superconducting system and the dis-

order potential $\hat{V}_{dis}(x, x') = V(x)\delta(x - x')\mathbf{1}$ i.e. it is diagonal in spacetime as well as Keldysh and Nambu spaces. The derivation of Gorkov equations for the Green's function and quasiclassical Green's functions for a disordered superconductor follows from the Keldysh BdG action in Eq. (1.51). [50]

Chapter 2: Long range p -wave proximity effect into a disordered metal

2.1 Introduction

Superconducting heterostructures have attracted a lot of attention recently as possible hosts of Majorana fermions [51–59]. One of the important outstanding questions in the studies of these heterostructures is the interplay between topological superconductivity and disorder [60–63]. Here we explore this issue, focusing on the leakage of p -wave superconductivity into a disordered metal. Naïvely, it may not appear to be a particularly meaningful question, because unconventional superconductivity is known to be suppressed by disorder per Anderson’s theorem [64]. However, Anderson’s theorem is only relevant to an intrinsic superconductor and has little to do with a leakage of superconductivity.

The linearized Usadel equations are standard tools in studies of proximity effects [65, 66]. Their derivation, however, assumes that an anisotropic component of the superconducting condensate’s wave function is small compared to the isotropic one, which is not the case in the systems we are interested in. Here, we focus on the more general Eilenberger equations [18, 67], which allow us to straightforwardly model systems with complicated geometries and varying degree of disorder. (In the context of topological superconductivity, similar approach has been used in

Refs. [68–71].)

In this work, we consider an infinite quasi-one-dimensional system (nanowire), at least part of which is superconducting. To describe the electronic correlations in the system we utilize the quasiclassical Green’s function \hat{g} – a matrix in Nambu and spin space [18]. It is obtained from the full microscopic Green’s function and faithfully captures the long length scale features of the system. For a recent comparison between quasiclassical and fully microscopic calculation of the same structure, see, for example [72]. In a one-dimensional model, \hat{g} depends on the Matsubara frequency (ω), the center-of-mass coordinate of the pair (x), and the direction of the momentum at the Fermi points ($\zeta \equiv \mathbf{p}_x/p_F$ is $+1/-1$ for right/left going particles). It obeys the Eilenberger equation [18, 66, 67]

$$\zeta v_F \partial_x \hat{g} = -[\omega \hat{\tau}_3, \hat{g}] + i[\hat{\Delta}, \hat{g}] - \frac{1}{2\tau_{imp}}[\langle \hat{g} \rangle, \hat{g}]. \quad (2.1)$$

Here $\hat{\tau}$ are the Pauli matrices in Nambu space. The effects of impurities enter the equation through the last term, in which τ_{imp} is the mean time between collisions, and $\langle \dots \rangle$ denotes an average over the Fermi surface (actually, two disconnected points in the one-dimensional case). Since we are interested in wires in which superconductivity is induced by a proximity with a bulk superconductor, we treat $\hat{\Delta}$ as an external parameter, which, furthermore, we assume constant throughout the wire. This allows us to ignore self-consistency, and simplifies the calculations.

The outline of this chapter is as follows. In Sec. 2.2 and Sec. 2.3, we obtain exact solutions of Eq. (2.1) for s -wave and p -wave order parameters respectively. In Sec. 2.4 we introduce an intuitive picture for the behavior of the solution by mapping

the equations to the equation of motion of a classical particle in an external force field. In Sec. 2.5 we study superconducting correlations induced by proximity in a metallic wire. In particular, we demonstrate that the p -wave correlations can be surprisingly long-ranged, even in the presence of disorder. We also show that impurity scattering produces a zero-energy peak in the density of states (DOS). We summarize the results of our work in Sec 2.6. Although self-consistency is not relevant for the experimental setup we are considering, in the Appendix we provide for completeness the solutions of the fully self-consistent Eilenberger equations for both s -wave and p -wave quasi-one-dimensional superconductors.

2.2 The s -wave case

We decompose \hat{g} in Nambu space using the Pauli matrices τ_i : $\hat{g} = -ig_1\hat{\tau}_1 + g_2\hat{\tau}_2 + g_3\hat{\tau}_3$. The off-diagonal scalar functions g_1 and g_2 describe the superconducting particle-particle correlations, whereas the diagonal component g_3 contains the particle-hole correlations. These functions have to satisfy the normalization condition $-g_1^2 + g_2^2 + g_3^2 = 1$.

In the case of an s -wave superconductor, $\hat{\Delta}$ is a spin-singlet and, ignoring the spin indices, it can be written as $\Delta_0 i\tau_2$ – this is equivalent to choosing the order parameter to be purely real. We ignore self consistency and assume that Δ is constant in space. The function g_2 is in the same channel as $\hat{\Delta}$, and thus encodes the s -wave pairing correlations. The g_1 function has more interesting origin – it describes the p -wave, odd-frequency superconducting correlations, induced by boundaries or

other inhomogeneities, and disappearing in bulk uniform superconductors [73–76].

The component g_1 is odd in momentum; therefore, its Fermi surface average vanishes identically: $\langle g_1 \rangle = 0$. The components g_2 and g_3 are even in momentum; therefore, $\langle g_2 \rangle = g_2$ and $\langle g_3 \rangle = g_3$ are satisfied. With these considerations, Eq. 2.1 can be now written as a set of three coupled first order differential equations for the scalar functions g_i :

$$\zeta v_F \partial_x g_1 = -2\omega g_2 + 2\Delta g_3, \quad (2.2a)$$

$$\zeta v_F \partial_x g_2 = -2\omega g_1 - \frac{1}{\tau_{imp}} g_1 g_3, \quad (2.2b)$$

$$\zeta v_F \partial_x g_3 = 2\Delta g_1 + \frac{1}{\tau_{imp}} g_1 g_2. \quad (2.2c)$$

To be integrable this system of equations has to have two constants of integration. The norm of \hat{g} , which is $-g_1^2 + g_2^2 + g_3^2 = 1$ is one of them. We have identified another constant C_s , given by

$$C_s = g_1^2 / (2\tau_{imp}) + 2\Delta g_2 + 2\omega g_3, \quad (2.3)$$

and obeying $\partial_x C_s = 0$. Note that the value of C_s can be fixed using the appropriate boundary conditions. Using it we can reduce the system given by Eq. (2.2) to a single second-order differential equation for g_1 :

$$v_F^2 \partial_x^2 g_1 = \left(4\omega^2 + 4\Delta^2 + \frac{C_s}{\tau_{imp}} \right) g_1 - \frac{1}{2\tau_{imp}} g_1^3. \quad (2.4)$$

Let us note several interesting limits for this equation. The $\tau_{imp} \rightarrow \infty$ is the clean superconductor limit, which was considered in Refs. [73, 74]. The $\tau_{imp} \rightarrow 0$ is the

strong disorder limit, in which Eq. (2.4) leads to results equivalent to those obtained by the Usadel equations [66]. Finally, $\Delta \rightarrow 0$ is the normal metal limit, where non trivial (proximity) solutions follow from superconducting boundary conditions.

The bulk superconducting energy Δ_0 is a convenient energy scale for the system. Even in a normal metal, where $\Delta = 0$, non-trivial solutions can appear because of proximity with a superconductor. In this case we can still use Δ_0 , the bulk gap parameter value in the neighboring superconductor, as a convenient energy scale. To streamline the notation we denote the coefficient from Eq. (2.4) by $\alpha_s = \omega^2 + \Delta^2 + C_s/(4\tau_{imp})$, and normalize C_s and α_s by the superconducting energy Δ_0 , to get $\tilde{C}_s = C_s/\Delta_0$ and $\tilde{\alpha}_s = \alpha_s/\Delta_0^2$. We also introduce the dimensionless coordinate $\tilde{x} = x/\xi_0$ (where $\xi_0 \equiv v_F/\Delta_0$ is the superconducting coherence length) and the dimensionless disorder strength $\beta = 1/(2\Delta_0\tau_{imp})$. With these substitutions we can write Eq. (2.4) as

$$\partial_{\tilde{x}}^2 g_1 = 4\tilde{\alpha}_s g_1 - 2\beta^2 g_1^3. \quad (2.5)$$

Once the boundary values of the Green's function components are given, the value of C_s and therefore α_s is fixed. Then we can solve Eq. (2.5) without *explicit* reference to the other components of \hat{g} . Multiplying both sides of Eq. (2.5) with $\partial_{\tilde{x}} g_1$, the solution can be obtained implicitly as an integral:

$$\int_{g_1(\tilde{x}_1)}^{g_1(\tilde{x}_2)} \frac{dg_1}{\pm \left[4\tilde{\alpha}_s g_1^2 - \beta^2 g_1^4 + 2\tilde{E}_s \right]^{1/2}} = \zeta \tilde{x}_2 - \zeta \tilde{x}_1. \quad (2.6)$$

Here, \tilde{E}_s is a constant of integration (in itself a function of C_s), about which we will have more to say in Sec. 2.4. Note that the Fermi index $\zeta = \pm 1$ appears on the right side of Eq. (2.6), therefore the function g_1 is manifestly odd in momentum. We

determine the plus/minus sign in front of the integrand by demanding consistency with the boundary conditions and the integration path so that the signs of both sides in Eq. (2.6) match. We will present an intuitive way to understand this solution in Sec. 2.4 and show that only monotonic solutions are physically acceptable. For a solution that starts from $\tilde{x} = 0$, it is convenient to recast the integral in Eq. (2.6) in terms of the inverse elliptic function sn^{-1} , which leads to

$$\text{sn}^{-1} \left(\frac{g_1(\tilde{x}')}{(\rho_s^+)^{1/2}} \middle| \frac{\rho_s^+}{\rho_s^-} \right) \bigg|_0^{\tilde{x}} = \pm \zeta \beta \tilde{x} [-\rho_s^-]^{1/2}, \quad (2.7a)$$

$$\rho_s^\pm = \frac{1}{\beta^2} \left(2\alpha_s \pm \left[4\alpha_s^2 + 2\tilde{E}_s \beta^2 \right]^{1/2} \right). \quad (2.7b)$$

where \tilde{x}' is a dummy variable.

Once we have $g_1(x)$, we can obtain the other components by using the constant of integration C_s and the system in Eq. (2.2), to get

$$g_2(x) = \frac{\tilde{\Delta} \left(\tilde{C}_s - \beta g_1^2(x) \right) - \tilde{\omega} \zeta \partial_{\tilde{x}} g_1(x)}{2 \left(\tilde{\omega}^2 + \tilde{\Delta}^2 \right)}, \quad (2.8a)$$

$$g_3(x) = \frac{\tilde{\omega} \left(\tilde{C}_s - \beta g_1^2(x) \right) + \zeta \tilde{\Delta} \partial_{\tilde{x}} g_1(x)}{2 \left(\tilde{\omega}^2 + \tilde{\Delta}^2 \right)}. \quad (2.8b)$$

2.3 The p -wave case

In the case of a p -wave wire we consider spinless fermions. As in the previous section, we decompose \hat{g} using the Pauli matrices $\hat{\tau}_i$. The order parameter can be written as $\zeta \Delta_0 i \tau_2$, and we again assume that Δ is a constant in space. The difference from the s -wave case arises from the fact that now g_2 is p -wave, and g_1 contains the secondary s -wave (odd-frequency) correlations [76, 77], and references therein.

The components of \hat{g} again obey three coupled differential equations, which differ from the s -wave case, due to the Fermi surface averaging in the last term of Eq. (2.1). In the p -wave case the order parameter has p -wave symmetry; therefore, we get $\langle g_1 \rangle = g_1$, $\langle g_2 \rangle = 0$. Note that $\langle g_3 \rangle = g_3$ applies (particle-hole correlations are s -wave-like). With these we have

$$\zeta v_F \partial_x g_1 = -2\omega g_2 + 2\zeta \Delta g_3 - \frac{1}{\tau_{imp}} g_2 g_3, \quad (2.9a)$$

$$\zeta v_F \partial_x g_2 = -2\omega g_1, \quad (2.9b)$$

$$\zeta v_F \partial_x g_3 = 2\zeta \Delta g_1 - \frac{1}{\tau_{imp}} g_1 g_2. \quad (2.9c)$$

In the clean case, these equations are linear and easily solved [70, 73, 74]. Impurities introduce nonlinear coupling, proportional to $1/\tau_{imp}$. Nevertheless, as we demonstrate, these equations can be treated analytically. The next several steps closely follow the discussion in the preceding section. We have again identified a constant C_p obeying $\partial_x C_p = 0$. It is given by

$$C_p = -g_2^2/(2\tau_{imp}) + 2\zeta \Delta g_2 + 2\omega g_3. \quad (2.10)$$

Using it we can derive from the system in Eqs. (2.9) a single second-order equation for g_2 :

$$v_F^2 \partial_x^2 g_2 = -2\zeta \Delta C_p + 4\alpha_p g_2 - \frac{3\zeta \Delta}{\tau_{imp}} g_2^2 + \frac{g_2^3}{2\tau_{imp}^2}, \quad (2.11)$$

where for convenience we have introduced $\alpha_p = \omega^2 + \Delta^2 + C_p/(4\tau_{imp})$. Notice the difference with Eq. (2.4), which is for g_1 .

Again, we use the energy scale Δ_0 (see Sec. 2.2 for more explanation) to introduce normalized coordinate $\tilde{x} = x/\xi_0$ (where $\xi_0 \equiv v_F/\Delta_0$), dimensionless disorder

strength $\beta = 1/(2\Delta_0\tau_{imp})$, and normalize C_p and α_p as $\tilde{C}_p = C_p/\Delta_0$ and $\tilde{\alpha}_p = \alpha_p/\Delta_0^2$.

With these substitutions Eq. (2.11) becomes

$$\partial_{\tilde{x}}^2 g_2 = -2\zeta\tilde{\Delta}\tilde{C}_p + 4\tilde{\alpha}_p g_2 - 6\zeta\beta\tilde{\Delta}g_2^2 + 2\beta^2 g_2^3. \quad (2.12)$$

Now we integrate the equation Eq. (2.12), which can be done without any explicit reference to the other two components:

$$\int_{g_2(\tilde{x}_1)}^{g_2(\tilde{x}_2)} \frac{dg_2}{\left[-4\zeta\tilde{\Delta}\tilde{C}_p g_2 + 4\tilde{\alpha}_p g_2^2 - 4\zeta\tilde{\Delta}g_2^3 + \beta^2 g_2^4 + 2\tilde{E}_p\right]^{1/2}} = \pm\zeta(\tilde{x}_2 - \tilde{x}_1) \quad (2.13)$$

The Fermi momentum appears on the right hand side of equation Eq. (2.13) and g_2 is odd in momentum, as it should. We determine the plus/minus sign of the integral in Eq. (2.13) in order to be consistent with the boundary conditions and the integration path.

In this chapter, we are interested in the behavior of the solution in a disordered normal metal next to a superconductor, so we consider the special case $\Delta = 0$, and recast the integral in Eq. (2.13) in terms of the inverse elliptic function sn^{-1} to get Eq. (2.14):

$$\text{sn}^{-1} \left(\frac{g_2(\tilde{x}')}{(\rho_p^+)^{1/2}} \middle| \frac{\rho_p^+}{\rho_p^-} \right) \bigg|_0^{\tilde{x}} = \pm \frac{\zeta\beta\tilde{x}}{\xi_0} [\rho_p^-]^{1/2}, \quad (2.14a)$$

$$\rho_p^\pm = \frac{1}{\beta^2} \left(-2\alpha_p \pm \left[4\alpha_p^2 - 2\tilde{E}_p\beta^2 \right]^{1/2} \right). \quad (2.14b)$$

Once we have $g_2(x)$, we can obtain $g_1(x)$ and $g_3(x)$ by using the constant of

integration C_p and the system in Eq. (2.9), to get

$$g_1(x) = \frac{-\zeta \partial_{\tilde{x}} g_2(x)}{2\tilde{\omega}}, \quad (2.15a)$$

$$g_3(x) = \frac{\tilde{C}_p + \beta g_2(x)^2 - 2\zeta \tilde{\Delta} g_2(x)}{2\tilde{\omega}}. \quad (2.15b)$$

2.4 Classical particle analogy

There is a surprising but intuitive way to understand the results from the previous two sections. We can think of Eq. 2.6 as an equation of motion of a classical particle with coordinate g_1 , in an external force field. In this interpretation the normalized position $\zeta \tilde{x}$ takes the role of the dynamical time of this classical particle. The Hamiltonian of the classical particle is given by the following equation:

$$H_s[g_1] = \frac{1}{2}(\partial_{\tilde{x}} g_1)^2 - 2\tilde{\alpha}_s g_1^2 + \frac{\beta^2}{2} g_1^4. \quad (2.16)$$

This Hamiltonian describes a particle in a double-well potential $V_s[g_1] = -2\tilde{\alpha}_s g_1^2 + \beta^2 g_1^4/2$, as shown in Fig. 2.1. We denote the conserved energy of this Hamiltonian as \tilde{E}_s . We can furnish the solution to the “equation of motion” by inverting the integral in equation Eq.(2.6) that sums up to the elapsed time $\zeta \tilde{x}_2 - \zeta \tilde{x}_1$ between initial and final coordinates $g_1(\tilde{x}_1)$ and $g_2(\tilde{x}_2)$, respectively.

The double well potential $V_s[g_1]$, allows non-monotonic solutions. However, the classical turning points of this potential scale as $\pm(\omega \tau_{imp})$ at high frequency, and for both $\omega \rightarrow \infty$ or $\tau_{imp} \rightarrow \infty$ the non-monotonic motion has unbounded amplitude; hence, these solutions are not physical. Therefore, we will only consider the monotonic solutions. If we denote the poles of the integrand as ρ_s^\pm then we can

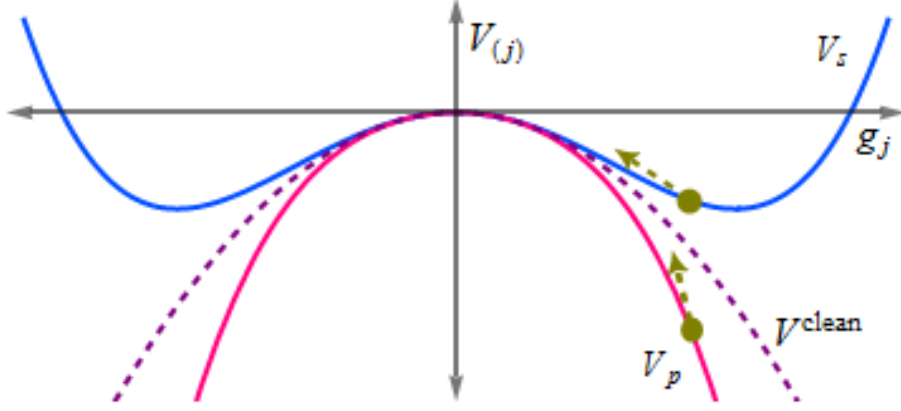


Figure 2.1: The potential landscape of a classical particle with motion describing the Green's function, for a normal metallic segment, in contact with a superconductor. Depending on the superconductor (s or p -wave) potential is either V_s or V_p . In the clean limit both converge to V^{clean} .

conveniently write the integral in Eq. (2.6) with monotonic integration path that starts from the point $g_1(\tilde{x} = 0)$, in terms of the inverse Jacobi elliptic function sn^{-1} as in equation Eq. (2.7).

In a similar manner, we can interpret Eq. (2.12) as the equation of motion of a classical particle with coordinate g_2 , moving in an external potential. The Hamiltonian of this classical particle is given in Eq. (2.17)

$$H_p[g_2] = \frac{1}{2}(\partial_{\tilde{x}}g_2)^2 + 2\zeta\tilde{\Delta}\tilde{C}_pg_2 + 2\tilde{\alpha}_pg_2^2 - 2\zeta\tilde{\Delta}g_2^3 + \frac{\beta^2}{2}g_2^4. \quad (2.17)$$

The Hamiltonian given by equation Eq. (2.17) describes the particle in the external potential potential $V_p[g_2] = 2\zeta\tilde{\Delta}\tilde{C}_pg_2 + 2\tilde{\alpha}_pg_2^2 - 2\zeta\tilde{\Delta}g_2^3 + \beta^2g_2^4/2$. We denote the conserved energy of this Hamiltonian as \tilde{E}_p . We can again find the solution to the “equation of motion” by inverting the integral in equation Eq.(2.6) that sums

up to the elapsed time $\zeta\tilde{x}_2 - \zeta\tilde{x}_1$ between initial and final coordinates $g_2(\tilde{x}_1)$ and $g_2(\tilde{x}_2)$, respectively.

In the special case of interest, where we are solving the equations in a disordered metal, $\Delta = 0$, therefore the potential $V_p[g_2]$, shown in Fig. 2.1, permits only monotonic solutions (given in Eq. (2.14)).

2.5 The p -wave wire with normal segment

We now proceed to study the leakage of superconductivity in a metallic wire. We consider an infinite wire extending along the x -axis with two segments that meet at $x = 0$. The infinite segment on the left ($x < 0$) is made of clean p -wave superconductor with order parameter $\zeta\Delta_0$. The segment on the right ($x > 0$) is made of a diffusive normal metal (the order parameter is zero). We are, in fact, considering a quasi-one-dimensional system, with several conducting channels, rather than a truly one-dimensional wire, which would be in an insulating state even for infinitesimal disorder strength.

We want a solution that for $x \rightarrow -\infty$ reproduces the mean field result for a uniform clean p -wave superconductor. Introducing the parameter B and the dimensionless variables $\tilde{\Omega} = \Omega/\Delta_0$, $\tilde{\omega} = \omega/\Delta_0$, we can write such a solution [70, 78, 79]:

$$g_1(x) = (1/\tilde{\omega})[1 - \tilde{\Omega}B] \exp(2\tilde{\Omega}x/\xi_0), \quad (2.18a)$$

$$g_2(x) = \zeta(1/\tilde{\Omega}) \left(1 - [1 - \tilde{\Omega}B] \exp(2\tilde{\Omega}x/\xi_0) \right), \quad (2.18b)$$

$$g_3(x) = \left\{ [1 - \tilde{\Omega}B]/(\tilde{\Omega}\tilde{\omega}) \right\} \exp(2\tilde{\Omega}x/\xi_0) + \tilde{\omega}/\tilde{\Omega}. \quad (2.18c)$$

B has to be determined from the boundary conditions at the junction ($x = 0$). For simplicity, we consider the case of perfectly transparent boundary, which guarantees the continuity of the Green's functions at the junction (More realistic modeling of the boundary requires more complicated boundary conditions) [80, 81]. (Note that Eqs. (2.18) were derived under the assumption that the order parameter is constant in the clean p -wave superconductor.)

Now we consider the diffuse normal segment with infinite length. Then, for $x \rightarrow \infty$ we have $g_1 \rightarrow 0$, $g_2 \rightarrow 0$ and $g_3 \rightarrow \text{sgn}(\omega)$, and using the constant of integration $\tilde{C}_p(x = 0) = \tilde{C}_p(x \rightarrow \infty) = 2|\tilde{\omega}|$ we get a quadratic equation, with one of the two solutions given as:

$$B = \frac{1}{\beta} \left[-1 + \sqrt{1 + 2\beta(\tilde{\Omega} - \tilde{\omega})} \right], \quad (2.19)$$

and we discard the other solution because it leads to a non-monotonic solution. We can understand intuitively the behavior of g_2 by invoking the classical analogy. The particle in potential V_p starts at “position” $g_2(0) = \zeta B$, with velocity $\partial_{\tilde{x}} g_2(0) = -2\tilde{\omega}\zeta g_1(0) = -2\zeta(1 - \tilde{\Omega}B)$, and moves towards its unstable equilibrium point $g_1(+\infty) = 0$, gradually slowing down until $\partial_{\tilde{x}} g_2(+\infty) = 0$, from which we deduce $\tilde{E}_p = 0$. Indeed, it takes infinite amount of time for the particle to reach the point $g_2 = 0$, a fact we see from the diverging integral in Eq. (2.13) for $\tilde{E}_p = 0$, as $g_2 \rightarrow 0$.

For $\tilde{E}_p = 0$ the elliptic integral leads to inverse hyperbolic functions, and defining the dimensionless constant $\kappa = [1 + \beta^2 B^2 / (4\tilde{\alpha}_p)]^{1/2}$, we can write the solution

for g_2 :

$$g_2(x) = \frac{\zeta B}{\cosh(x/\xi') + \kappa \sinh(x/\xi')}. \quad (2.20)$$

Here $\xi' = \xi_0/(2\tilde{\alpha}_p^{1/2})$ gives the effective decay length of the solution (at $T = 0$). In physical units it is

$$\xi' = \frac{v_F}{\sqrt{4\omega^2 + 2|\omega/\tau_{imp}|}}. \quad (2.21)$$

In the dirty limit we have $\xi' = \sqrt{D/|\omega|}$, where D is the diffusion coefficient. Finally, in the clean limit g_2 converges to $\zeta B \exp(-2|\tilde{\omega}|x/\xi_0)$, as expected [70].

The other two components of the Green's function can be derived from g_2 using \tilde{C}_p and the Eilenberger equations: $g_1 = -\zeta\xi_0\partial_x g_2/(2\tilde{\omega})$ and $g_3 = \text{sgn}(\tilde{\omega}) + \beta g_2^2/(2\tilde{\omega})$. As expected, impurities suppress g_2 relative to g_1 . However, they both decay in the normal segment over the *same* length scale, given by Eq. (2.21). This decay is long-range, and furthermore, with exactly the same length scale obtained for the case of s -wave order parameter [73, 74]. Thus, the naïve expectation of strong suppression of the p -wave correlations is misleading in this case. This is one of the main points of this chapter (Also, note that the order parameter amplitude Δ_0 appears only in the boundary conditions at $x = 0$. Thus, even a complete self-consistent treatment of the superconducting segment would not change the decay length, only the overall prefactor), and it is also supported by the fact that the same decay length scale appears also in the case of an s -wave superconductor with magnetic disorder [75], which is known to be analogous in some ways to a p -wave superconductor with potential disorder.

We can now obtain the DOS of the system from $\text{Re}[g_3(\omega \rightarrow -i\epsilon + \delta)]$ [70].

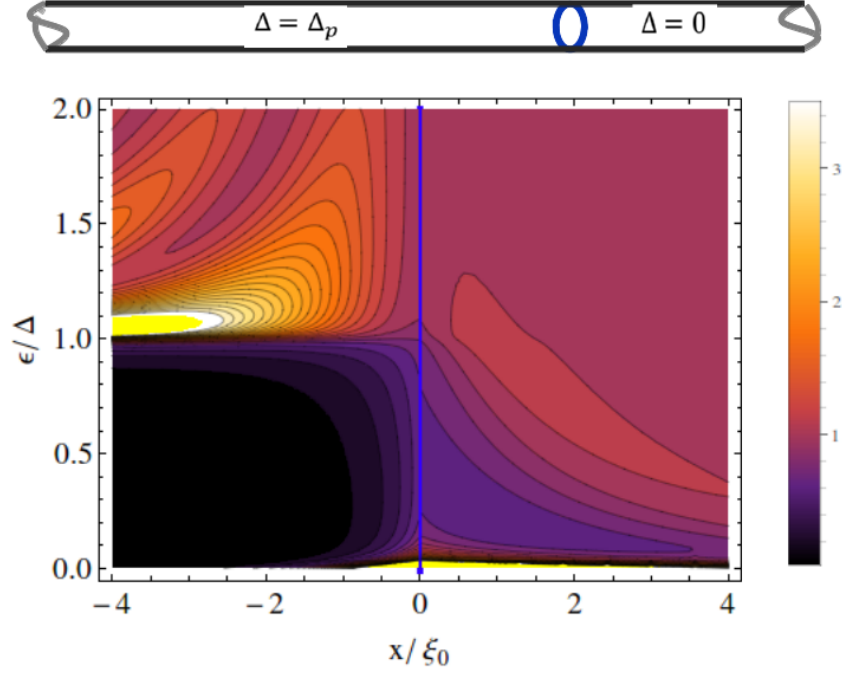


Figure 2.2: Contour plot of the DOS of an infinite wire. There is moderate disorder ($\beta = 1$) in the normal segment ($x > 0$). The solid yellow marks the regions that are beyond the plot range (where $N/N_0 > 3.5$). Notice the zero-energy peak in the normal segment.

On Fig. 2.2 we show it for a system with moderate disorder. Several things are apparent from this plot. First, for low energies there is a significant decrease in the DOS of the normal segment, caused by the proximity effect; however, it is not a real gap, since the DOS stays finite. This decrease is entirely due to the impurities, which “trap” the superconducting correlations close to the boundary (in the clean case the DOS is constant for $x > 0$ [70]). The impurity-induced term in g_3 also has a divergence in the limit of small frequencies ($g_3 \sim 1/\omega$), which leads to an infinite peak in the DOS (see Fig. 2.3). This zero-energy peak has the same origin as the Majorana edge state (namely, the sign change in the order parameter [78, 79, 82]).

From Eq. (2.20), we can see that the weight of the zero-energy peak has a power-law decay $\sim (1 + \beta Bx/\xi_0)^{-2}$ into the metallic segment.

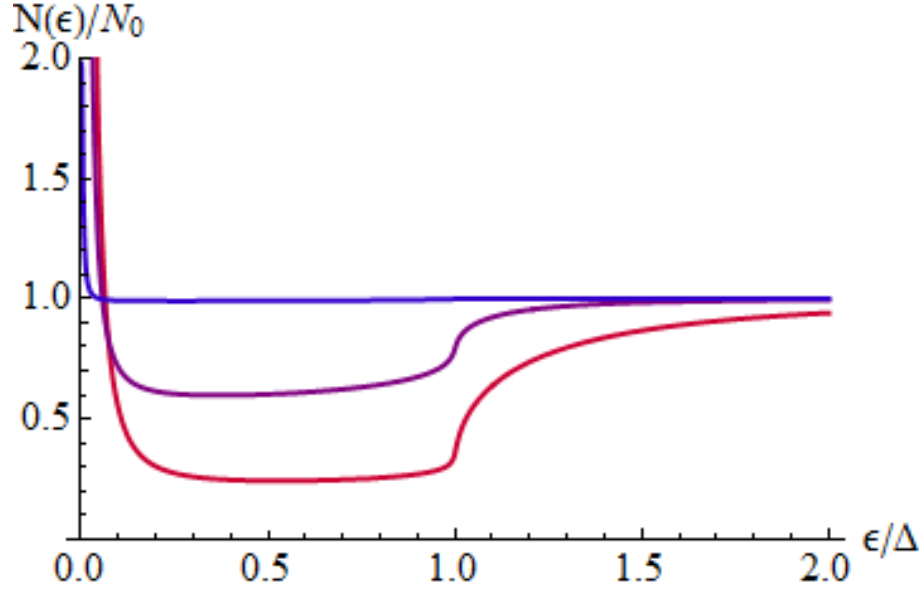


Figure 2.3: DOS at the junction of infinite normal and superconducting segments. Three cases for the disorder in the normal segment are plotted: weak ($\beta = 0.1$, blue), moderate ($\beta = 1$, purple), and strong ($\beta = 10$, red). Notice the suppression of DOS with the increase of disorder strength.

As a side note, in the case of an s -wave superconductor, the solution of Eq. (2.4) is $g_1 = \zeta A [\cosh(x/\xi') + \kappa_s \sinh(x/\xi')]^{-1}$, with A and κ_s that can be derived by matching the solutions at the junction. However, unlike the p -wave case, the g_1 component at the boundary is proportional to $\tilde{\omega}$. This dependence on $\tilde{\omega}$ changes the behavior of the DOS. From $g_3 = \text{sgn}(\tilde{\omega}) - \beta/(2\tilde{\omega})g_1^2$, we can see that the low frequency limit is finite, and there is no zero-energy peak in the s -wave case (Analogous calculation in the s -wave case leads not to a peak, but linear suppression of DOS at low energies. The overall DOS profiles are very similar to those obtained earlier numerically) [83].

If the normal segment has finite length L , we impose the condition $g_2(L) = 0$ (the p -wave component is suppressed by boundary reflection). Then the solution follows immediately from Eq. 2.14 as $g_2(x) = \zeta(\rho_p^+)^{1/2} \text{sn}[\beta(\rho_p^-)^{1/2}(x - L)/\xi_0]$, with elliptic parameter $m = \rho_p^+/\rho_p^-$. However, this expression has limited value, since B_L , which should be obtained from matching the two solutions for g_2 at $x = 0$, enters the expression through the parameters ρ_p^\pm , and is difficult to find. Fortunately, an approximate analytic form for B_L can be obtained. Numerical investigation suggests that B_L can be approximated by $B[1 - \exp(-2L/\lambda_B)]$, with $\lambda_B = B\xi_0$ (it controls how quickly B_L approaches to the infinite wire limit). Once we have B_L , we can write g_2 in a form that manifestly converges to that of the $L = \infty$ case [84]. The common elliptic parameter of the elliptic functions is $(\rho_p^- - \rho_p^+)/\rho_p^-$, and it lies in the interval $[0, 1]$. With these definition we get:

$$g_2(x) = \zeta \frac{B_L \text{dn}\left(\beta|\rho_p^-|^{1/2} \frac{x}{\xi_0}\right) - \text{sn}\left(\beta|\rho_p^-|^{1/2} \frac{x}{\xi_0}\right) \text{cn}\left(\beta|\rho_p^-|^{1/2} \frac{x}{\xi_0}\right) \sqrt{|\rho_p^+| + B_L^2} \sqrt{1 + B_L^2/|\rho_p^-|}}{\text{cn}^2\left(\beta|\rho_p^-|^{1/2} \frac{x}{\xi_0}\right) - (B_L^2/|\rho_p^-|) \text{sn}^2\left(\beta|\rho_p^-|^{1/2} \frac{x}{\xi_0}\right)}. \quad (2.22)$$

We can again obtain the two other components from g_2 by using: $g_1 = -\zeta\xi_0\partial_x g_2/(2\tilde{\omega})$ and $g_3 = (\tilde{\alpha}_p - \tilde{\omega}^2)/(\beta\tilde{\omega}) + \beta g_2^2/(2\tilde{\omega})$. Figure 2.4 shows the components g_1, g_2, g_3 of the quasiclassical matrix Green's function \hat{g} , for varying disorder strengths, over a semi infinite wire with disordered section.

As $L \rightarrow \infty$, the elliptic functions are replaced by their hyperbolic counterparts, and we recover Eq. 2.20. This convergence is exponential, so the wire is effectively infinite when $L/(B\xi_0) \gg 1$. Conversely, if $L/(B\xi_0) \ll 1$, $g_2(x)$ decays linearly in the normal metal. Again, it is the impurity-induced contribution to g_3 that is of most

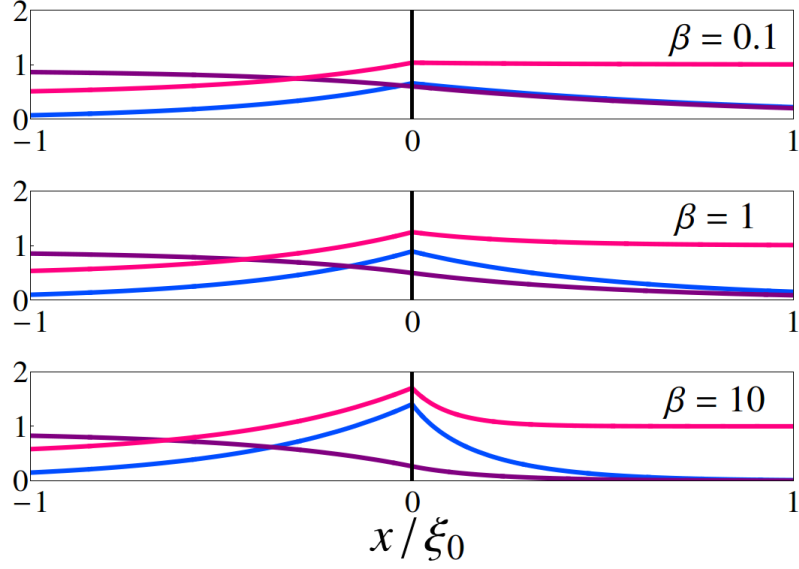


Figure 2.4: Components of \hat{g} , (g_1 : blue, g_2 : purple, g_3 : red) for a wire with infinite p-wave section and finite disordered section of length $L = 5\xi_0$. Top panel: weak disorder ($\beta = 1/(2\tau_{imp}\Delta_0) = 0.1$). Middle panel: moderate disorder ($\beta = 1$). And bottom panel: strong disorder ($\beta = 10$). The Matsubara frequency is set to $\omega = \Delta_0/2$.

interest. After analytic continuation we can write the zero-energy limit as

$$g_3(x) = \frac{1}{\pi} \delta(\epsilon) \mathcal{M}(x). \quad (2.23)$$

Here, $\mathcal{M}(x)$ describes the x -dependent weight of the zero-energy mode, and can be extracted from Eq. (2.22):

$$\mathcal{M}(x) = \frac{\alpha_p}{\beta} + \frac{\beta}{2} \left(\frac{B_L - \sqrt{\frac{\alpha_p}{2\beta^2}} \left(1 + \frac{\beta^2 B^2}{2\alpha_p} \right) \sin \left(\beta |\rho_p^-|^{1/2} \frac{x}{\xi_0} \right) \cos \left(\beta |\rho_p^-|^{1/2} \frac{x}{\xi_0} \right)}{\cos^2 \left(\beta |\rho_p^-|^{1/2} \frac{x}{\xi_0} \right) - \frac{\beta^2 B^2}{2\alpha_p} \sin^2 \left(\beta |\rho_p^-|^{1/2} \frac{x}{\xi_0} \right)} \right)^2. \quad (2.24)$$

It is monotonically decreasing function, and its values at the ends of the wire are $\mathcal{M}(0) = 1 - B_L$ and $\mathcal{M}(L) = \mathcal{M}(0) - \beta B_L^2/2$ respectively. Figure 2.5 shows $\mathcal{M}(x)$ in the normal section with length $L = 5\xi_0$, for various disorder strengths. As can be seen, it becomes peaked closer to $x = 0$ as the disorder in the normal section increases. On the other hand, for weak disorder, $[\mathcal{M}(0) - \mathcal{M}(L)]/(L/\xi_0)$ is small, so the zero-energy peak is delocalized over the entire normal segment.

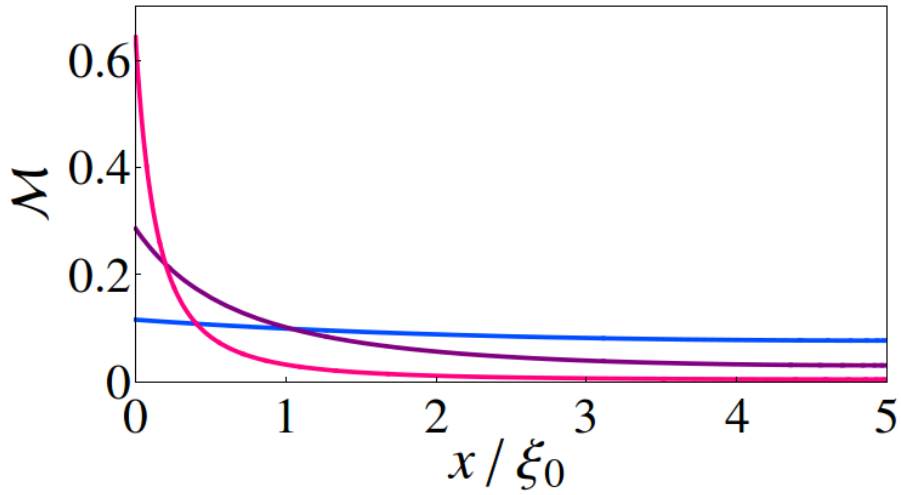


Figure 2.5: The weight of the zero-energy mode $\mathcal{M}(x)$ in a normal section with length $L = 5\xi_0$ for three disorder strengths (blue: $\beta = 0.1$, purple: $\beta = 1$, red: $\beta = 10$).

2.6 Conclusion

We presented a quasiclassical description of a quasi-one-dimensional superconductor. The appropriate Eilenberger equations of the system were solved *exactly*. Surprisingly, we discovered that this problem can be mapped to a one-dimensional classical particle moving in an external potential. In view of the recent interest

in superconducting heterostructures, we studied the proximity effects in a normal segment, attached to a clean p -wave wire. We discovered that despite the presence of impurities, the proximity-induced superconducting correlations are long-range. We also found that impurity scattering leads to the appearance of a delocalized zero-energy peak.

Chapter 3: Analogue stochastic gravity in strongly interacting Bose-Einstein condensates

3.1 Introduction

The idea that a curved spacetime is an emergent structure has a long history [85, 86] and has been discussed in various physical contexts [87] from classical fluid mechanics [88, 89] and crystals with defects [90] to quantum entanglement [91]. While in the context of fundamental gravity, the emergent scenario remains speculative at this stage, there has been a number of concrete realizations of various aspects of general relativity in “analogue gravity” models, where a non-trivial curved spacetime metric arises naturally in the description of collective modes relative to a background solution of the field equations [87, 92]. A prominent example of such analogue theory is a strongly correlated superfluid [93], where the phonon modes, propagating relative to a (generally inhomogeneous and non-stationary) superflow, satisfy a wave-equation in an effective curved spacetime

$$\partial_\mu (\sqrt{-g} g^{\mu\nu} \partial_\nu \phi) = 0, \tag{3.1}$$

where $\phi(\vec{r}, t)$ is the phonon field – a small deviation from a “mean-field” configuration, $g = \det g_{\mu\nu}$ is the determinant and $g^{\mu\nu}$ is the matrix inverse of the metric

$$g_{\mu\nu} = \frac{\rho}{c} \begin{pmatrix} c^2 - v^2 & \vec{v}^T \\ \vec{v} & -\mathbf{I}_{3 \times 3} \end{pmatrix} \quad (3.2)$$

which is determined by the underlying superflow (\vec{v} and c are the superfluid velocity and the speed of sound, ρ is the density of the fluid including the excitations). Many exciting general-relativistic effects immediately follow from this observation, including the formation of sonic horizons and black hole-type physics [92], analogue Hawking radiation [94], proposed by Unruh [88] and recently reported by Steinhauer to have been observed in cold-atom Bose-Einstein condensates [95], and a unifying principle for cosmology and high energy physics discussed extensively by Volovik [93, 96].

This geometric theory of excitations in a superfluid, that this work focuses on and develops further, is an alternative formulation of the phenomenological Landau-Khalatnikov two-fluid theory of superfluidity [97, 98], which has been originally developed as a macroscopic description of superfluid Helium. As the name suggests, this theory separates the fluid flow into two components – one being the zero entropy, zero viscosity superflow and the other being the entropy-carrying, dissipative normal flow. The two-fluid theory relies on the conservation laws for mass, energy, and momentum in a Galilean-invariant continuum made up of these two components. In addition to being an accurate macroscopic description of superfluid helium, the two-fluid theory can be viewed as the first historical example of a long wavelength hydrodynamic limit of a strongly interacting quantum field theory. The low energy

effective field theory paradigm offers a number of powerful techniques to analyze strongly interacting field theories and the hydrodynamic limit of high energy theories (e.g., the AdS/CFT and string theory) [99–102].

The main idea of this work relies on a conceptual analogy between the quantum generalization of the Landau-Khalatnikov two-fluid description and the Caldeira-Leggett-type theories of “quantum friction”, where a closed system is separated into two components – a quantum “particle” and a bath to which it is coupled [15, 103]. Integrating out the bath leads to classical equations of motion for the particle, which necessarily feature a friction force and a stochastic Langevin force, connected to each other via a fluctuation-dissipation theorem. For a strongly correlated BEC, this analogy associates the superfluid order parameter field with the Caldeira-Leggett “particle” and the Bogoliubov excitations with the bath. The question we ask here is what are the corresponding Langevin equations of motion that arise? We develop and use a combination of the aforementioned geometric theory of excitations and Keldysh field-theoretical methods in a curved spacetime to answer this question. The main result is the following stochastic equations of motion

$$\partial_t \rho + \nabla \cdot (\rho \vec{v}) = \frac{1}{2} \nabla \cdot \left[\sqrt{-g} \left(\langle \hat{T}_{\mu\nu} \rangle + \xi_{\mu\nu} \right) \frac{\delta g^{\mu\nu}}{\delta \vec{v}} \right], \quad (3.3a)$$

$$\partial_t \theta + \frac{1}{2} v^2 + \mu(\rho) = \frac{\sqrt{-g}}{2} \left(\langle \hat{T}_{\mu\nu} \rangle + \xi_{\mu\nu} \right) \frac{\delta g^{\mu\nu}}{\delta \rho}, \quad (3.3b)$$

where ρ is the density of the fluid, θ is the superfluid flow potential, $\vec{v} = \nabla \theta$ is the irrotational flow fluid of the superfluid component, $\mu(\rho)$ is the chemical potential of the fluid, $g^{\mu\nu}$ is the matrix inverse of the metric tensor (3.2), $\sqrt{-g} = |\det(g_{\mu\nu})|^{1/2}$ is the spacetime volume measure, $\hat{T}_{\mu\nu}(x)$ is the stress-energy tensor operator of the

phonons (here x is a short-hand for the $(3+1)$ -spacetime variable and the Einstein summation convention is in use) and $\xi_{\mu\nu}(x)$ is a stochastic tensor field, describing its fluctuations around the average $\langle \hat{T}_{\mu\nu}(x) \rangle$. That is, the statistics of the Gaussian noise with zero average is determined by the correlator

$$\langle \xi_{\mu\nu}(x) \xi_{\mu'\nu'}(x') \rangle = \frac{1}{2} \langle \{ \hat{t}_{\mu\nu}(x), \hat{t}_{\mu'\nu'}(x') \} \rangle,$$

where $\hat{t}_{\mu\nu}(x) = \hat{T}_{\mu\nu}(x) - \langle \hat{T}_{\mu\nu}(x) \rangle$ and $\{\cdot, \cdot\}$ is the anti-commutator. The averages here are calculated relative to a deterministic background. What these equations actually describe are fluctuations in the superfluid, e.g. they yield statistics of density and velocity fluctuations, which in turn determine a stochastic metric. In this sense, there is a strong similarity to the stochastic Einstein equations discussed in the context of stochastic gravity [49, 104].

While these stochastic Einstein equations are interesting in and of themselves, their derivation presents a technical challenge (a non-trivial generalization of the non-equilibrium Keldysh techniques for a curved spacetime is required) [48] and gives rise to a number of additional interesting results along the way, as discussed below. This chapter is structured as follows:

In Sec. 3.2, we discuss the applicability of the metric description of a superfluid by analyzing the relevant length and energy scales. In analogy with cosmology, the geometric description breaks down at an effective “Planck energy,” where both the linear dispersion of phonons and the hydrodynamic description break down.

In Sec. 3.3, we use the background field formalism to write down the Keldysh quantum field theory of quasiparticles. We emphasize that the Keldysh description

is necessary for taking the dynamical fluctuations of the phonon field into account.

In Sec. 3.4, we derive the analogous Einstein equation that governs the background and the excitations – “matter field.” We establish equivalence of the analogue Einstein equation and the covariant conservation law for the phonons to the two-fluid conservation laws of Landau and Khalatnikov. We prove the equivalence of the two descriptions by reducing the covariant conservation law down to the Noether current of the two-fluid system by using the equations of motion. In Appendix B, we provide the technical details of this derivation.

In Sec. 3.5, we take the analogy between the superfluid system and general relativity further to the domain of stochastic fluctuations. We write the response and dissipation kernels in the covariant language, and give the details of this in Appendix C. In global thermal equilibrium, we discuss the notion of temperature on curved spacetime. We prove the fluctuation dissipation relation for a metric with globally time-like Killing vectors, that is for a flow that can be brought to a stationary form after a Galilean transformation.

Finally in Sec. 3.6, we linearize the stochastic analogue Einstein equation and obtain a Langevin-type equation for the stochastic corrections to the background. We show that the symmetries of the flow determine the structure of the Langevin equation, by considering the Minkowski case.

Throughout this chapter, we will use the Einstein summation convention for the indices, unless otherwise stated. The spacetime indices are in lower case Greek letters while the space indices are in lower case Latin letters. We use the sign convention $(+ - - -)$. In addition, the fluid dynamics equations are written in

terms of Cartesian tensors, where there is no distinction between covariant and contravariant tensors.

3.2 The model and energy scales

In this section, we review the energy scales involved in the analysis of an interacting system of bosons and its excitations. The analogue “general relativistic” description is an approximation to the exact theory and its applicability is controlled by our ability, or lack thereof, to neglect a quantum pressure term discussed below. The main conclusion of this section is that the stronger the repulsive interactions between bosons composing the superfluid, the less important the quantum pressure term and correspondingly the wider the domain of applicability of the general-relativistic approximation (in the sense of a range of energies and length-scales where the description applies). We discuss these “Planck” energy and length-scales below.

Our starting point is just the standard Lagrangian of interacting bosons

$$\mathcal{L}[\Phi, \Phi^*] = \Phi^* i\hbar \partial_t \Phi - \frac{\hbar^2}{2m} |\nabla \Phi|^2 - \varepsilon(|\Phi|^2), \quad (3.4)$$

where $\Phi(\vec{r}, t) \equiv \Phi(x)$ is the boson field, m is the mass of a boson, and the energy $\varepsilon(|\Phi|^2)$ describes an external potential and density-density repulsion between the bosons. Though, at this stage we do not specify the external potential and interaction potential between bosons, for $\varepsilon = \frac{g}{2}|\Phi|^4 + V|\Phi|^2$, the saddle point of this Lagrangian, satisfies the Gross-Pitaevskii or non-linear Schrödinger equation:

$$i\hbar \partial_t \Phi = -\frac{\hbar^2}{2m} \nabla^2 \Phi + V(\vec{r}, t)\Phi + g|\Phi|^2\Phi. \quad (3.5)$$

The first step in deriving the hydrodynamic theory is the Madelung transformation of the boson field [105], which is a change of variables to polar coordinates in each point of spacetime:

$$\Phi(x) = \sqrt{\frac{\rho(x)}{m}} e^{im\theta(x)/\hbar}. \quad (3.6)$$

The new variables are the density, ρ , and the phase θ , which in effect is a “flow potential” for the superfluid, that gives rise to the irrotational flow velocity field

$$\vec{v} = \nabla\theta.$$

In terms of these variables, the Lagrangian (3.4) takes the form

$$-\mathcal{L} = \rho\partial_t\theta + \frac{1}{2}\rho\vec{v}^2 + \varepsilon(\rho) + \underbrace{\frac{1}{8}\left(\frac{\hbar}{m}\frac{\nabla\rho}{\sqrt{\rho}}\right)^2}_{\text{“quantum pressure”}}. \quad (3.7)$$

Classically, the long-wavelength description of this system in local thermodynamic equilibrium is fluid dynamics. This description can be extended to the quantum regime, where a macroscopic order exists as in the case of a condensate. This macroscopic order is a non-trivial vacuum that solves the mean field fluid equation Eq. (3.8), which is just the Gross-Pitaevskii equation Eq. (3.5) in the Madelung parametrization:

$$\partial_t\rho + \nabla \cdot (\rho\vec{v}) = 0, \quad (3.8a)$$

$$\partial_t\theta + \frac{1}{2}\vec{v}^2 + \frac{\partial\varepsilon}{\partial\rho} = \frac{1}{2}\frac{\hbar^2}{m^2}\frac{1}{\sqrt{\rho}}\nabla^2\sqrt{\rho}. \quad (3.8b)$$

These are the Euler equations for an ideal, zero entropy fluid, with an additional energy per unit mass appears in the right-hand side of Eq. (3.8b) due to the quantum potential term $\sim (\nabla\sqrt{\rho})^2$ in Eq. (3.7). Together with the continuity equation

Eq. (3.8a), the gradient of (3.8b), when multiplied by the density ρ , produces a momentum balance equation. In this equation, the quantum potential leads to a pressure gradient, hence this potential is called “quantum pressure” in Eq. (3.7).

The excitations over this non-trivial vacuum state are the Bogoliubov quasiparticles. These quasiparticles can be thought of a quantum field propagating on top of the ground state manifold. When treated semiclassically, the quasiparticles constitute sources to the hydrodynamic equations (3.8), in the spirit of the two-fluid hydrodynamics. Moreover, the entropy-carrying quasiparticle quantum field acts as a bath on the background system. In addition to momentum and energy flux and stresses, the quantum bath creates a noise to the evolution of the background, leading to a stochastic Langevin component.

We now show, by analyzing the appropriate scales, that when the repulsive interactions between the bosons are strong, the quantum pressure term is suppressed. Such a fluid is the basis of the gravitational analogy, as it simulates the spacetime on which the matter field – that is, the phonon field – propagates [93, 96].

If we momentarily ignore the quantum pressure proportional to $\nabla\sqrt{\rho}$, we get the Lagrangian density of a vortex free perfect fluid with flow velocity $\vec{v} = \nabla\theta$. The excitations of this system are obtained by linearizing the equations of motion and are the sound waves with speed $c^2 = \rho d^2\varepsilon/d\rho^2$ at equilibrium density. When quantized, the excitations have the linear spectrum $E_p = \hbar ck$. Therefore, the dimensional parameters characterizing the vortex free quantum hydrodynamics are the Planck constant, \hbar , the equilibrium density ρ_e , and the equilibrium speed of sound, c_e . The relevant energy scale of this theory is $E_Q = (\hbar^3 c_e^5 \rho_e)^{1/4}$. Since the energy density

is $\sim \rho_e c_e^2$, the characteristic length scale is $d_Q = (\rho_e c_e / \hbar)^{-1/4}$. Therefore, the mass scale is $\rho_e d_Q^3 = M_Q = (\rho_e \hbar^3 / c_e^3)^{1/4}$ and the time-scale is $t_Q = d_Q / c_e = (\rho_e c_e^5 / \hbar)^{-1/4}$.

With the addition of the quantum pressure term, the spectrum of Bogoliubov phonons receives a correction as $E_p = \hbar c_e k \sqrt{1 + \hbar^2 k^2 / (4m^2 c_e^2)}$. Therefore the linear spectrum of phonons breaks down at a length scale of $\xi = \hbar / (m c_e)$, this is the coherence length of the condensate. At this scale, the phonon energy is of order $E_{Lorentz} = m c_e^2$, which can be dubbed the Lorentz violation energy (i.e., where the phonon spectrum deviates from the linear dispersion). Note that, Lorentz violations do not necessarily occur at exactly the inter atomic length scale d and thus $E_{Lorentz}$ is generally distinct from the “Planck” energy scale $E_{Planck} = \hbar c_e / d$ – that is the energy required to resolve the individual atoms separated by a distance d (at such length-scales the hydrodynamic description becomes meaningless). Indeed, the ratio of the coherence length to the inter atomic distance is determined by the strength of the atomic interactions. Defining $g_0 = \hbar^2 d / m^3$, and setting $g \rho_e^2 = \varepsilon(\rho_e) = \rho_e c_e^2$, we get $(\xi/d)^2 = g_0/g$. In summary the relationships between different scales can be written in terms of the normalized strength of interactions g_0/g as:

$$\frac{E_{Planck}}{E_{Lorentz}} = \frac{\xi}{d} = \sqrt{\frac{g_0}{g}} = \left(\frac{M_Q}{m} \right)^{4/3}. \quad (3.9)$$

This ratio determines the relative importance of the quantum pressure term compared to the interaction energy. The corresponding ratio is (below, L is a length-scale on which the density changes):

$$\frac{\left(\frac{\hbar}{m} \nabla \sqrt{\rho} \right)^2}{\varepsilon(\rho)} \sim \frac{\hbar^2}{g m^2 \rho L^2} \sim \frac{\xi^2}{L^2} \lesssim \frac{\xi^2}{d^2} = \frac{g_0}{g}.$$

In the weak interaction limit, as in a dilute Bose gas, the coherence length ξ and the quantum mass scale M_Q are large compared to microscopic counterparts d and m . This signals that the system behaves like a macroscopic quantum object, hence the condensate fraction is closed to unity. In this regime, Lorentz violation occurs much before the interatomic scales are reached and the excitations are Bogoliubov quasiparticles with the non-linear spectrum. In the strong interaction regime, as in Helium-II or a strongly interacting BEC, the condensate fraction is small, however the Lagrangian (3.7) is still valid, as it produces correct equations for a zero entropy dissipationless classical fluid. In this regime, the quantum pressure is negligible down to the $\xi \sim d$ scale. This means that the collective excitations are sound waves all the way up to the effective Planck energy. Therefore, geometric theory of analogue gravity for the covariant sound waves, that we will summarize in the next section, applies as long as we stay in the hydrodynamic regime, that is to say at length scales larger than the inter atomic distance.

3.3 Background field formalism on the Keldysh contour for Bogoliubov quasiparticles

Here, we outline a procedure to extract a field theory of the excitations starting from Eq. (3.7). We show that an effective curvature and covariance emerge when the amplitude modes of the excitations are integrated out. Finally, we obtain an effective action for the superfluid system and the phonon bath. Unless noted otherwise, we

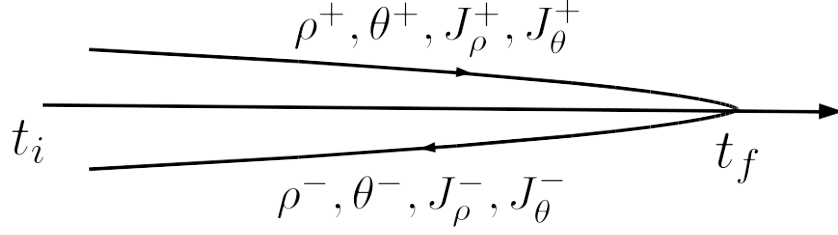


Figure 3.1: The Keldysh contour and its forward/backward branches labeled by the path index $s = \pm$: Each degree of freedom and the associated sources are defined twice, one on each branch. The values are matched at t_f , for example $\rho_f^+ = \rho_f^-$.

use the units, where

$$\hbar = c_e = k_B = 1. \quad (3.10)$$

We employ the closed-time path integral or the Keldysh functional integral [43–46] and the background field formalism [106, 107] to separate the superfluid background and the quantum field theory of excitations. Note that the procedure, outlined below in Eqs. (3.11) – (3.27) is completely general and does not rely on a particular form of the initial action, but we will apply it specifically to the superfluid Lagrangian (3.7).

Generally, given an initial density matrix $\hat{\boldsymbol{\varrho}}(t_i)$ and the evolution operator $\hat{\mathcal{U}}_{t',t}$ that takes the system from t to t' , the density matrix at any point in time t is

$$\hat{\boldsymbol{\varrho}}(t) = \hat{\mathcal{U}}_{t,t_i} \hat{\boldsymbol{\varrho}}(t_i) \hat{\mathcal{U}}_{t_i,t}^\dagger. \quad (3.11)$$

Suppose $\hat{\mathcal{O}}$ is an observable. In the Schrödinger picture, the expectation value of this operator at time t is

$$\langle \mathcal{O}(t) \rangle = \text{Tr} [\mathcal{O} \hat{\boldsymbol{\varrho}}(t)]. \quad (3.12)$$

In the Keldysh formalism, the time contour is made up of two branches that start at an early time t_i and meet at t_f as shown in Fig 3.1. Each degree of freedom in the system is defined twice, one on the forward and one on the backward branch of the time contour labeled by \pm respectively. The values of all variables are matched at the final point t_f where the branches meet. The observable can be coupled to the system via the source currents $J^\pm(\vec{r}, t)$ that are added to the Hamiltonian $\hat{H} \rightarrow \hat{H} + J^\pm \hat{\mathcal{O}}$. The forward/backward evolution operators associated with the modified Hamiltonian are denoted as $\hat{\mathcal{U}}(J^\pm)$. Then the forward/backward expectation values of the observable can be obtained from the following generating function

$$\mathcal{Z}[J^\pm] = \text{Tr} \left[\hat{\mathcal{U}}_{t_i, t_f}(J^-) \hat{\mathcal{U}}_{t_f, t_i}(J^+) \hat{\boldsymbol{\rho}}(t_i) \right], \quad (3.13)$$

by differentiating it with respect to the forward/backward source currents J^\pm

$$\langle \mathcal{O}^\pm(t) \rangle = \pm i \frac{\delta}{\delta J^\pm(t)} \mathcal{Z}[J^\pm] \Big|_{J^\pm=0}. \quad (3.14)$$

Note that, if we set $J^+ = J^-$ from the outset, the forward/backward evolution operators cancel due to unitarity and

$$\mathcal{Z}[\vec{J}^+ = \vec{J}^-] = \text{Tr} \hat{\boldsymbol{\rho}}(t_i) = 1. \quad (3.15)$$

This means taking the logarithm of the generating function as in ordinary field theory, is redundant in Keldysh theory.

The generating function Eq. (3.13) for the boson system in Eq. (3.7) can be written as a closed time path integral as [15, 47]:

$$\mathcal{Z}[J_\rho^\pm, J_\theta^\pm] = \int \mathcal{D}[\theta^\pm, \rho^\pm] \boldsymbol{\rho}(\rho_i^\pm, \theta_i^\pm) \times \exp \left[i \sum_{C=\pm} C \int dx \mathcal{L}(\rho^C, \theta^C) + J_\rho^C \rho^C + J_\theta^C \theta^C \right]. \quad (3.16)$$

where $dx \equiv dt d^3r$, the sum goes over the upper and lower Keldysh contours, the factor C is (± 1) for the upper/lower contour.

The simplest observables are the mean fields, that is the expectation values of the fields. Writing

$$\mathcal{Z}[J_\rho^\pm, J_\theta^\pm] = e^{iW[J_\rho^\pm, J_\theta^\pm]}, \quad (3.17)$$

the mean fields are generated by using Eq. (3.14) and Eq. (3.15)

$$\rho_0^\pm := \langle \rho^\pm \rangle = \pm \frac{\delta W}{\delta J_\rho^\pm} \Big|_{J_\rho^\pm=0} \quad \text{and} \quad \theta_0^\pm := \langle \theta^\pm \rangle = \pm \frac{\delta W}{\delta J_\theta^\pm} \Big|_{J_\theta^\pm=0}. \quad (3.18a)$$

Now, we can separate the system into a classical background and quantum excitations around it as follows. Suppose that the mean fields are given. Then one can express the sources in terms of the mean fields by constructing the *effective action*, that is the Legendre transform

$$\Gamma[\rho_0^\pm, \theta_0^\pm] = W[J_\rho^\pm, J_\theta^\pm] - \sum_{C=\pm} C \int dx (J_\rho^C \rho_0^C + J_\theta^C \theta_0^C). \quad (3.19)$$

Now, the sources can be expressed as

$$\frac{\delta \Gamma}{\delta \rho_0^\pm} = \mp J_\rho^\pm \quad \text{and} \quad \frac{\delta \Gamma}{\delta \theta_0^\pm} = \mp J_\theta^\pm. \quad (3.20a)$$

Exponentiating the effective action and using (3.19) one can eliminate the sources in (3.16) in favor of the mean fields. If we define the deviations from the mean fields:

$$\tilde{\rho}^\pm = \rho^\pm - \rho_0^\pm, \quad (3.21a)$$

$$\phi^\pm = \theta^\pm - \theta_0^\pm, \quad (3.21b)$$

we can write the following integral equation for the effective action

$$e^{i\Gamma[J_\rho^\pm, J_\theta^\pm]} = \int \mathcal{D}[\theta^\pm, \rho^\pm] \mathfrak{Q}(\rho_i^\pm, \theta_i^\pm) \times \exp \left[i \sum_{C=\pm} C \int dx \mathcal{L}(\rho^C, \theta^C) - \frac{\delta\Gamma}{\delta\rho_0^C} \tilde{\rho}^C - \frac{\delta\Gamma}{\delta\theta_0^C} \phi^C \right]. \quad (3.22)$$

The effective action, Γ , can be solved for iteratively and be expressed as a series (we restore the Planck constant below to emphasize the semiclassical nature of the expansion)

$$\Gamma = \Gamma_0 + \hbar\Gamma_{ph} + \hbar^2\Gamma_2 + \dots \quad (3.23)$$

the classical action

$$S[\rho^\pm, \theta^\pm] = \int dx \mathcal{L}(\rho^\pm, \theta^\pm), \quad (3.24)$$

being the zeroth term:

$$\Gamma_0 = S[\rho_0^+, \theta_0^+] - S[\rho_0^-, \theta_0^-]. \quad (3.25)$$

In this work we consider only the first order or one-loop correction Γ_{ph} to the classical action. This correction encapsulates the quantum field of Bogoluibov quasiparticles over the background, that become phonons at long wavelengths (hence we use the subscript ph , a shorthand for “*phonon*” corresponding to the first loop correction).

We substitute the lowest-order expression([3.25](#)) into Γ 's on the right hand side of Eq. (3.22). On the left-hand side, we substitute $\Gamma_0 + \Gamma_{ph}$, where Γ_{ph} is an unknown. Expanding S around ρ_0 and θ_0 , and matching the terms in the equation, we find the phonon effective action Γ_{ph} i.e. the leading-order correction in $\tilde{\rho}$ and ϕ to Γ . Defining

$$\tilde{\mathfrak{Q}}(\tilde{\rho}_i^\pm, \phi_i^\pm) = \mathfrak{Q}(\rho_i^\pm - \rho_0^\pm, \theta_i^\pm - \theta_0^\pm),$$

we write

$$e^{i\Gamma_{ph}[\rho_0^\pm, \theta_0^\pm]} = \int \mathcal{D}[\tilde{\rho}^\pm, \phi^\pm] \tilde{\mathbf{q}}(\tilde{\rho}_i^\pm, \phi_i^\pm) \times \exp \left\{ i \sum_{C=\pm} C \int dx \mathcal{L}^{C(2)}(\tilde{\rho}^C, \phi^C) \right\}, \quad (3.26)$$

where the \mathcal{L}^2 , depends on the path index $C = \pm$ not only through its arguments but explicitly as

$$\mathcal{L}^{\pm(2)}(\tilde{\rho}, \theta) = (\tilde{\rho}, \phi) \cdot \frac{\delta^2 \mathcal{L}}{\delta^2(\rho, \theta)} \Big|_{\rho_0^\pm, \theta_0^\pm} \cdot (\tilde{\rho}, \phi) \quad (3.27)$$

in multi-index notation. So far, the results are completely general. Now we use the explicit Lagrangian (3.7) and obtain the phonon effective Lagrangian, $\mathcal{L}^{(2)}$. After suppressing the time-path index $C = \pm$, it is

$$- \mathcal{L}^{(2)} = \tilde{\rho}(\partial_t + \vec{v}_0 \cdot \nabla)\phi + \frac{1}{2}\tilde{\rho} \left(\frac{c_0^2}{\rho_0} + \hat{K}_Q \right) \tilde{\rho} + \frac{1}{2}\rho_0(\nabla\phi)^2, \quad (3.28)$$

where we defined the “quantum pressure” operator,

$$\hat{K}_Q = \frac{1}{4m^2} \left[\frac{(\nabla\rho_0)^2}{\rho_0^3} - \frac{\nabla\rho_0}{\rho_0^2} \cdot \nabla - \frac{\nabla^2}{\rho_0} \right]. \quad (3.29)$$

3.3.1 Covariant phonon action

The one-loop correction can be computed exactly in the strong interaction limit, as the path integral reduces to a Gaussian integral. As noted in Sec. 3.2, at energy scales below $E_{Lorentz}$, the operator \hat{K}_Q in (3.28), that results from quantum pressure, can be neglected compared with the term c_0^2/ρ_0 . This yields the following Lagrangian

$$\mathcal{L}_{\hat{K}_Q \rightarrow 0}^{(2)} \rightarrow -\tilde{\rho}D_t\phi - \frac{1}{2}\tilde{\rho} \left(\frac{c_0^2}{\rho_0} \right) \tilde{\rho} - \frac{1}{2}\rho_0(\nabla\phi)^2, \quad (3.30)$$

where we defined the material derivative

$$D_t\phi = \partial_t\phi + \vec{v}_0 \cdot \nabla\phi.$$

Now, the density fluctuations, $\tilde{\rho}$, can be integrated out. To do the path integral over $\tilde{\rho}$, we can think of spacetime as divided into cubes with volume ξ^4/c_e and discretize the integral. Note that the integrand is a diagonal matrix over spacetime and the path integral reduces to a product of Gaussian integrals. At this point, we shorten the notations for the mean-field parameters ρ_0 , θ_0 and \vec{v}_0 , writing them as simply ρ , θ and \vec{v} for the sake of brevity. If we define the density matrix as

$$\mathfrak{Q}_\phi(\phi_i^+, \phi_i^-) = \tilde{\mathfrak{Q}}\left(\frac{\rho}{c^2}D_t\phi_i^+, \phi_i^+; \frac{\rho}{c^2}D_t\phi_i^-, \phi_i^-\right), \quad (3.31)$$

integrating out the $\tilde{\rho}$ field produces:

$$Z_{ph} = e^{i\Gamma_{ph}[\rho^\pm, \theta^\pm]} = \int \mathcal{D}'[\phi^\pm] \mathfrak{Q}_\phi e^{i(S_{ph}^+[\phi^+] - S_{ph}^-[\phi^-])}. \quad (3.32)$$

with the measure of the path integral being, again suppressing the \pm signs,

$$\mathcal{D}'[\phi] = \prod d\phi \sqrt{\frac{\rho}{2\pi c^2}}, \quad (3.33a)$$

and the following covariant action for phonons

$$S_{ph} = \frac{1}{2} \int dt d^3x \frac{\rho}{c^2} [(D_t\phi)^2 - c^2 (\nabla\phi)^2]. \quad (3.34)$$

This action can also be obtained through a classical treatment of the Lagrangian Eq. (3.7) [89]. The material derivative $D_t\phi = \partial_t\phi + \vec{v} \cdot \nabla\phi$ is the measure of the time rate of change of ϕ in a frame comoving with the fluid. This means the action in Eq. (3.34) describes non-dispersive waves with speed c in the fluid comoving frame. Galilean invariance of the fluid system requires that the sound wave velocity $\vec{u} = d\vec{x}/dt$ in the lab frame satisfy $(\vec{u} - \vec{v}) = c^2$. This means the sound rays with velocity with $d\vec{x}/dt = \vec{u}$ are null rays on the manifold with line element

$$ds^2 = -\frac{\rho}{c}[-(c^2 - v^2)dt^2 - 2\vec{v} \cdot \vec{dx}dt + \vec{dx} \cdot \vec{dx}]. \quad (3.35)$$

This is the line element for any analogue gravity system with background Galilean symmetry up to a conformal factor, for which the choice of ρ/c allows us to write the phonon action of Eq (3.34) in the following suggestive form [88, 89]

$$S_{ph} = \frac{1}{2} \int d^4x \sqrt{-g} g^{\mu\nu} \partial_\mu \phi \partial_\nu \phi. \quad (3.36)$$

Here, the metric can be read off from the line element Eq. (3.35) by writing $ds^2 = g_{\mu\nu} dx^\mu dx^\nu$ as

$$g_{\mu\nu} = \frac{\rho}{c} \begin{pmatrix} c^2 - v^2 & \vec{v}^T \\ \vec{v} & -\mathbf{I}_{3 \times 3} \end{pmatrix}, \quad (3.37)$$

here $(+ - - -)$ convention is used.

The volume measure factor turns out to be $\sqrt{-g} = \rho^2/c$. At static equilibrium the line element Eq. (3.35) is that of Minkowski space.

The measure in Eq. (3.33) is written as

$$\mathcal{D}'[\phi] = \prod_x \underbrace{(g^{00})^{1/2}}_{\text{“anomaly”}} (-g)^{1/4} d\phi. \quad (3.38)$$

We note that this measure is manifestly non-covariant due to the coordinate dependent factor g^{00} . For a field in curved spacetime the covariant measure ought to be $(-g)^{1/4}$ [108, 109]. This means, although the phonon action Eq. (3.34) is covariant, the path integral is not, leading to a quantum anomaly. We will come back to this issue in Sec. 3.4.3 where we derive the conservation law of the stress tensor.

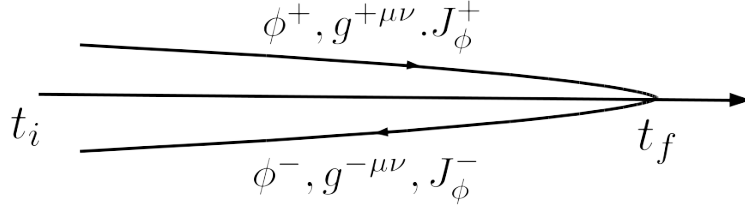


Figure 3.2: The Keldysh contour for the phonon field. The metric tensor depends on the background variables ρ_0^\pm and θ_0^\pm and therefore is also defined twice.

Before going into obtaining equations of motion from the effective action of the Keldysh field theory, it is worthwhile to list a number of properties that Keldysh theory obeys. We draw Fig. 3.2 to show the forward/backward fields and sources of the phonon field. We identified Eq. (3.32) with the closed-time-path partition function of phonons Z_{ph} . The first order correction Γ_{ph} to the classical action is then given as:

$$\Gamma_{ph} = -i \log Z_{ph}[g^+, g^-]. \quad (3.39)$$

As a consequence of unitarity, similar to Eq.(3.15),

$$Z_{ph}[g^\pm = g] = 1, \quad (3.40)$$

i.e. when the background is the same on the forward and backward directions, the product of backward and forward evolution operators is unitary. Also, from Eq. (3.32),

$$Z_{ph}[g^+, g^-; J^+, J^-] = (Z_{ph}[g^-, g^+; J_\phi^-, J_\phi^+])^*, \quad (3.41)$$

where J_ϕ^\pm are additional sources attached in order to compute expectation values of

ϕ . It follows from Eq. (3.40) and Eq. (3.41) that the effective action satisfies

$$\Gamma_{ph}[g, g] = 0, \quad (3.42a)$$

$$\Gamma_{ph}[g^+, g^-] = -\Gamma_{ph}^*[g^-, g^+]. \quad (3.42b)$$

These properties are handy while computing the Keldysh correlation functions.

3.4 Analogue Einstein equations and two-fluid hydrodynamics

In general relativity, the relationship between matter and spacetime curvature is governed by the Einstein's equation. Being covariant under coordinate transformations, the matter field obeys the covariant conservation law. However, this is not a total conservation law, as there is energy momentum exchange between fields and the spacetime curvature. There are pseudo-tensor constructions like Einstein pseudotensor or the Landau-Lifshitz pseudotensor that quantify the stress energy of the gravitational field [110, 111]. These pseudo-tensors, when added to the stress tensor of matter, become a totally conserved quantity.

In this section, in analogy with general relativity, we will start with the first loop effective action

$$\Gamma = S[\rho^+, \theta^+] - S[\rho^-, \theta^-] - i \log Z_{ph}[g^\pm], \quad (3.43)$$

where the metric g^\pm is a functional of ρ^\pm and θ^\pm according to Eq. (3.2). The effective action Eq. (3.43), albeit without using the Keldysh contour, is considered to compute backreaction corrections to acoustic black holes where the quantum effects, i.e. Hawking radiation, is important. [112] Unlike Ref. [112], in this chapter,

we explicitly integrated out the phonons through methods discussed in Sec. 3.3. First, this approach revealed the anomalous measure in Eq. (3.38). Secondly, the controlled series Eq. (3.23), produces higher order loop corrections. The contribution of these higher loops to the backreaction, especially near the horizon; where the acoustic approximation becomes less accurate, and the interplay between the Hawking radiation and covariance anomaly are interesting problems. However, all of these are subleading corrections at first order. Therefore we will not address these problems. Moreover, for the sake of computing the stochastic corrections, we extend the effective action by using the Keldysh formalism.

We will first write the stress-energy tensor for the covariant phonons starting from the effective action Eq. (3.19). Then we will write down an analogue Einstein equation that describes the evolution of metric tensor (3.2) due to the stress-energy of phonons, which play the part of matter. To complete the analogy, we will derive a total conservation law by using the covariant conservation law and the analogue Einstein's equation. Moreover, we will show that the conserved quantity is a canonical Noether current and therefore describes the total conservation of momentum and energy in the lab frame. This means two fluid hydrodynamics *directly* follows from the analogue gravity formalism.

3.4.1 Hilbert stress-energy operator of the covariant phonon field

The expectation value of the stress-energy operator can be defined by using Schwinger's variational principle [113] as

$$\langle \hat{T}_{\mu\nu} \rangle = -i \frac{2}{\sqrt{-g}} \frac{\delta \log Z_{ph}}{\delta (g^+)^{\mu\nu}} \Big|_{g^+=g^-} = \frac{2}{\sqrt{-g}} \frac{\delta \Gamma_{ph}}{\delta (g^+)^{\mu\nu}} \Big|_{g^+=g^-}. \quad (3.44)$$

Then, the stress-energy operator is defined (symmetrized for convenience) as

$$\hat{T}_{\mu\nu}(x) = \frac{1}{2} \{ \partial_\mu \hat{\phi}(x), \partial_\nu \hat{\phi}(x) \} - \frac{1}{2} g_{\mu\nu} \partial^\alpha \hat{\phi}(x) \partial_\alpha \hat{\phi}(x). \quad (3.45)$$

This expression is problematic because it contains a product of field operators at the same spacetime point and generally leads to divergences. These can be cured through a variety of regularization and renormalization schemes [113]. One of these methods is called point splitting where the field operators are taken on different spacetime points, and the limit of coincidence is taken after performing derivatives and averages. In semiclassical gravity diverging quantities are renormalized into coupling constants in Einstein's equation [49, 113].

Physically, the zero point quantum fluctuations that add up to an infinite vacuum energy. In the strongly interacting analoguesystem, the divergent quantities are believed to be already accounted for in the background as a part of the internal energy of the fluid [93]. This ensures the stability of the liquid droplets, by renormalizing the equilibrium pressure to zero. Recently, the role of zero point energy in the formation of stable macroscopic droplets in strongly interacting BEC's was investigated both theoretically [114] and experimentally [115]. Therefore, assuming that the vacuum energy is already renormalized into the background energy, we will

formally discard the divergent piece of the stress-energy expectation value. Note that, in field theory on flat spacetime, the divergence is tacitly discarded through the normal ordering of operators.

Let $\langle \hat{T}_{\mu\nu}(x) \rangle_{div}$ represent the divergent piece in the expectation value for the stress-energy operator. Throughout this chapter we will refer to the renormalized stress-energy as:

$$\begin{aligned} \langle \hat{T}_{\mu\nu}(x) \rangle = \frac{1}{2} (\delta_\mu^\alpha \delta_\nu^\beta + \delta_\nu^\alpha \delta_\mu^\beta - g_{\mu\nu} g^{\alpha\beta}) \times \\ \lim_{x', x'' \rightarrow x} \frac{\partial}{\partial x'^\alpha} \frac{\partial}{\partial x''^\beta} \langle \mathbb{T} \hat{\phi}(x') \hat{\phi}(x'') \rangle - \langle \hat{T}_{\mu\nu}(x) \rangle_{div}. \end{aligned} \quad (3.46)$$

where \mathbb{T} is the time ordering operator. The time ordered correlation function is equivalent to the forward-forward correlation function of the Keldysh theory [47]

$$\langle \mathbb{T} \hat{\phi}(x') \hat{\phi}(x'') \rangle = \langle \hat{\phi}^+(x') \hat{\phi}^+(x'') \rangle = \frac{\delta^2 Z_{ph}[J^+, J^-]}{\delta J^+(x') \delta J^+(x'')} \Big|_{J^+ = J^- = 0}. \quad (3.47)$$

3.4.2 Semiclassical analogue Einstein equations and the “phonon matter”

Having defined the stress tensor of the matter field (phonons), we now write down the equations of motion for the superfluid and the phonons and argue that it is analogous to the semi-classical Einstein’s equation.

After dropping the quantum pressure, and using Eq. (3.44), the Euler-Lagrange equations that follow from the effective action Eq. (3.43) in the limit $(\rho^\pm, \theta^\pm) \rightarrow (\rho,$

θ) are the fluid equations of motion Eq. (3.8) with semiclassical source terms

$$\partial_t \rho + \nabla \cdot (\rho \vec{v}) = \frac{1}{2} \nabla \cdot \left(\sqrt{-g} \langle \hat{T}_{\mu\nu} \rangle \frac{\delta g^{\mu\nu}}{\delta \vec{v}} \right), \quad (3.48a)$$

$$\partial_t \theta + \frac{1}{2} v^2 + \mu(\rho) = \frac{1}{2} \left(\sqrt{-g} \langle \hat{T}_{\mu\nu} \rangle \frac{\delta g^{\mu\nu}}{\delta \rho} \right). \quad (3.48b)$$

Here $\mu(\rho) = \partial \varepsilon / \partial \rho$ is the local chemical potential for the superfluid.

Given the initial density operator of phonons and initial values and boundary conditions for the background fields ρ and θ , one can compute the metric everywhere by solving Eq. (3.48) and plugging the solutions into the definition Eq. (3.2). The source terms on the right hand side must be self-consistent with this solution, as the metric appears both explicitly in (3.48) and also inside the definition of the stress tensor in Eq. (3.46). This is because the metric tensor determines how the sound field propagates, classically expressed as Eq. (3.1). In this respect, the Eqs. (3.48) resembles Einstein's equations where the Eulerian left hand sides provide dynamics to the metric tensor and are analogous to the Einstein tensor and the stress-tensor corresponds to the matter whose motion is dictated by the curvature.

3.4.3 Canonical versus covariant conserved currents

Here, we show that the covariant conservation law and the analogue Einstein equations Eq. (3.48) leads to a canonical conservation law for energy-momentum.

Classically, the stress tensor in Eq. (3.44), obeys the covariant conservation law

$$\nabla_\mu T^\mu{}_\nu = \partial_\mu T^\mu{}_\nu + T^\theta{}_\nu \Gamma^\mu_{\theta\mu} - T^\mu{}_\theta \Gamma^\theta_{\mu\nu} = 0, \quad (3.49)$$

owing to the fact that it is derived from the effective action [113], where ∇_μ denotes

the covariant derivative. Writing the definitions of Christoffel symbols Eq. (B.1) in terms of the metric and using Eq. (B.2) and Eq. (B.3), we get:

$$\nabla_\mu T^\mu{}_\nu = \frac{1}{\sqrt{-g}} \partial_\mu (T^\mu{}_\nu \sqrt{-g}) + \frac{1}{2} T_{\alpha\beta} \partial_\nu g^{\alpha\beta} = 0. \quad (3.50)$$

The partial derivative is streamlined with comma notation whenever convenient, i.e. for any quantity A , $\partial_\mu A = A_{,\mu}$. The Lagrangian density for phonons can be extracted from Eq. (3.36) as

$$\mathcal{L}_{ph} = \frac{1}{2} \sqrt{-g} g^{\mu\nu} \partial_\mu \phi \partial_\nu \phi. \quad (3.51)$$

Then the first term in Eq. (3.50) is related to the canonical stress tensor of phonons, and by inspecting the classical version of the Hilbert stress-energy tensor Eq. (3.45), it can be written as

$$\sqrt{-g} T^\mu{}_\nu = \frac{\partial \mathcal{L}_{ph}}{\partial \phi_{,\mu}} \phi_{,\nu} - \mathcal{L}_{ph} \delta^\mu{}_\nu. \quad (3.52)$$

By using the chain rule and the definition Eq. (3.44), the second piece in Eq. (3.50) reduces to

$$\frac{1}{2} \sqrt{-g} T_{\alpha\beta} \partial_\nu g^{\alpha\beta} = \frac{\partial \mathcal{L}_{ph}}{\partial \theta_{,\mu}} \theta_{,\mu\nu} + \frac{\partial \mathcal{L}_{ph}}{\partial \rho} \rho_{,\nu}. \quad (3.53)$$

Let \mathcal{L}_{cl} denote the Lagrangian density of the background after the quantum pressure term is dropped

$$- \mathcal{L}_{cl} = \rho \partial_t \theta + \frac{1}{2} \rho \vec{v}^2 + \varepsilon(\rho). \quad (3.54)$$

By using the equations of motion Eq. (3.48), in the Euler-Lagrange form, as shown in Appendix B we can write Eq. (3.50) as the conservation of the following current

$$\mathfrak{T}^\mu{}_\nu = \frac{\partial \mathcal{L}_{ph}}{\partial \phi_{,\mu}} \phi_{,\nu} + \frac{\partial (\mathcal{L}_{ph} + \mathcal{L}_{cl})}{\partial \theta_{,\mu}} \theta_{,\nu} - (\mathcal{L}_{ph} + \mathcal{L}_{cl}) \delta^\mu{}_\nu. \quad (3.55)$$

If we define the total Lagrangian of the background-phonon composite system

$$\mathcal{L}_{sys} = \mathcal{L}_{cl} + \mathcal{L}_{ph},$$

and noticing that $\partial\mathcal{L}_{cl}/\partial\rho_{,\mu}$ and $\partial\mathcal{L}_{cl}/\partial\phi_{,\mu}$ both vanish, \mathfrak{T} in Eq. (3.55) is precisely the conserved Noether current

$$\mathfrak{T}^\mu{}_\nu = \frac{\partial\mathcal{L}_{sys}}{\partial(\rho, \theta, \phi)_{,\mu}} \cdot (\rho, \theta, \phi)_{,\nu} - \mathcal{L}_{sys}\delta^\mu{}_\nu.$$

due to the spacetime translation invariance of the overall system represented by the effective action Eq. (3.43).

We define \mathcal{T} , the stress energy tensor of the analogue gravitational field as

$$\sqrt{-g}\mathcal{T}^\mu{}_\nu = \frac{\partial(\mathcal{L}_{ph} + \mathcal{L}_{cl})}{\partial\theta_{,\mu}} \theta_{,\nu} - \mathcal{L}_{cl}\delta^\mu{}_\nu. \quad (3.56)$$

This expression generates the familiar energy and momentum density in the background. For example the energy density of the background in the laboratory frame follows from Eq. (3.56) as

$$\sqrt{-g}\mathcal{T}^0{}_0 = \frac{1}{2}\rho\vec{v}^2 + \varepsilon(\rho). \quad (3.57)$$

Similarly, the laboratory frame momentum density of the background follows from Eq. (3.56) as

$$\sqrt{-g}\mathcal{T}^0{}_i = -\rho v_i. \quad (3.58)$$

The Noether current Eq. (3.55) can be written as the current due to the background and the excitations as Eq. (3.49) as the

$$\mathfrak{T}^\mu{}_\nu = \sqrt{-g}T^\mu{}_\nu + \sqrt{-g}\mathcal{T}^\mu{}_\nu. \quad (3.59)$$

This means the mixed canonical stress tensor of the excitations correspond to energy-momentum corrections due to excitations in the laboratory frame.

However, because of the covariance anomaly of the quantum phonon field that manifests itself in the path integral measure Eq. (3.38), the covariant derivative of the expectation value of the quantum stress operator must be equal to an anomalous current, i.e. $\nabla_\mu \langle \hat{T}^\mu_\nu \rangle = J_\nu^{anom}$. Furthermore this current should be Galilean covariant due to the overall Galilean invariance of the system. This is the second type of anomaly in the analogue gravity system, the first being the trace anomaly due to Hawking radiation, which occurs when there is a sonic horizon in the system [94]. In this work we assume that no sonic horizon exists and that the quantum pressure term is weak everywhere. We defer the rigorous analysis and computation of the anomalous current to another publication. Since anomalies are necessarily quantum effects, in the regimes we work, they should be washed out by thermal contributions. Then for the expectation

$$\mathfrak{T}^\mu_\nu = \sqrt{-g} \langle \hat{T}^\mu_\nu \rangle + \sqrt{-g} \langle \mathcal{T}^\mu_\nu [\hat{\phi}] \rangle, \quad (3.60)$$

the conservation law

$$\partial_\mu \mathfrak{T}^\mu_\nu = 0 \quad (3.61)$$

holds. In the next section we rewrite Eq. (3.61) and Eq. (3.48) in the two-fluid variables.

3.4.4 Mass-energy-momentum balance and the covariant conservation of stress-energy operator

In this section, we complete the connection of the analogue Einstein equation Eq. (3.48) and the covariant conservation law Eq. (3.50) and two-fluid hydrodynamics by identifying the normal and superfluid components in terms of the background fields and the stress tensor.

Inspecting the conservation law Eq. (3.60) that we derived in Sec. 3.4.3, we define the momentum density \vec{P} , energy density E and energy flux \vec{Q} due to phonons, in the lab frame

$$P_i := -\sqrt{-g} \left\langle \hat{T}_i^0 \right\rangle, \quad (3.62a)$$

$$E := \sqrt{-g} \left\langle \hat{T}_0^0 \right\rangle, \quad (3.62b)$$

$$Q_i := \sqrt{-g} \left\langle \hat{T}_0^i \right\rangle. \quad (3.62c)$$

Here, the quantities on the left hand side are momentum density, momentum flux tensor and energy density. Being Cartesian tensors, their indices are upped/lowered by using the Kronecker delta function. By Galilean transforming the quantities on the right hand side according to the usual tensor transformation rules, we observe that P_i is Galilean invariant while E and Q_i are not.

We define the following symmetric, Galilean invariant, Cartesian momentum flux tensor

$$\pi_{ij} := \frac{c}{\rho} \sqrt{-g} \left\langle \hat{T}_{ij} \right\rangle = \frac{c}{\rho} \sqrt{-g} \left\langle \hat{T}^\mu_j \right\rangle g_{i\mu}. \quad (3.63)$$

By using the expression for the metric Eq. (3.2) and the definitions in Eq. (3.62),

the mixed momentum flux tensor due to phonons is

$$-\sqrt{-g}\langle\hat{T}_j^i\rangle=\pi_{ij}+P_jv_i^s, \quad (3.64)$$

The equations of two fluid hydrodynamics are conservation laws for the density, momentum and energy for the superfluid and normal components of the system denoted by the superscripts s and n respectively. We make the following identification of velocity and density in Eq. (3.48) as the velocity of the superfluid component and the total density (i.e. superfluid plus normal) respectively.

$$\vec{v}:=\vec{v}_s, \quad (3.65a)$$

$$\rho:=\rho_s+\rho_n. \quad (3.65b)$$

Consequently, $\vec{v}_s=\nabla\theta$.

Now, we identify the analogue Einstein equations Eq. (3.48) as mass conservation and superflow equations respectively, by writing the phonon contribution in terms of energy and momenta defined in Eq. (3.62).

The inverse metric in Eq. (3.48) follows from Eq. (3.2) as

$$g^{\mu\nu}=\frac{1}{\rho c}\begin{pmatrix} 1 & \vec{v}_s^T \\ \vec{v}_s & -c^2\mathbf{I}_{3\times 3}+\vec{v}_s\vec{v}_s^T \end{pmatrix}. \quad (3.66)$$

If A is any tensor with two covariant indices contracted and $\kappa=\partial\ln c/\partial\ln\rho$ characterizes the logarithmic derivative of the energy of a linearly dispersing sound wave with respect to the density of the medium, then the derivative of the metric

Eq. (3.66) obeys the following rules

$$\frac{\delta g^{\mu\nu}}{\delta \rho} A_{\mu\nu\dots} = \frac{1}{\rho}(\kappa - 1)A^\mu_{\mu\dots} - 2\kappa c A^{00}_{\dots}, \quad (3.67a)$$

$$\frac{\delta g^{\mu\nu}}{\delta v_s^i} A_{\mu\nu\dots} = A^0_{i\dots} + A_i^0_{\dots}. \quad (3.67b)$$

The source current can be written as quasi-particle momentum by making the identification

$$-\frac{1}{2}\sqrt{-g}\langle\hat{T}_{\mu\nu}\rangle\frac{\delta g^{\mu\nu}}{\delta\vec{v}_s} = -\sqrt{-g}\langle\hat{T}^0_i\rangle = P_i. \quad (3.68)$$

Then the first analogue Einstein equation Eq. (3.48a) is recast as the continuity equation for mass

$$\partial_t \rho + \nabla \cdot (\rho \vec{v}_s + \vec{P}) = 0. \quad (3.69)$$

The source term in Eq. (3.48b) reads

$$\begin{aligned} \frac{1}{2}\sqrt{-g}\langle\hat{T}_{\mu\nu}\rangle\frac{\delta g^{\mu\nu}}{\delta\rho} &= \frac{\sqrt{-g}}{2\rho}[\kappa - 1]\langle\hat{T}^\mu_\mu\rangle_{anom} - \frac{\kappa}{\rho}\rho c\sqrt{-g}\langle\hat{T}^{00}\rangle \\ &:= -\frac{\kappa}{\rho}[E - \vec{v}_s \cdot \vec{P}] = -\frac{\kappa}{\rho}E_0 = -\frac{\partial E_0}{\partial\rho}. \end{aligned} \quad (3.70)$$

Here, the trace of the stress-operator is zero in the absence of an acoustic horizon where the Hawking radiation creates a trace anomaly. The frame shifted E_0 , by virtue of its tensorial expression being manifestly Galilean invariant, is the comoving frame energy density of quasiparticles. In these variables the Bernoulli Eq. (3.48b) takes its familiar form

$$\partial_t \theta + \frac{1}{2}v_s^2 + \mu(\rho) + \frac{\partial E_0}{\partial\rho} = 0. \quad (3.71)$$

A corollary of this equation is that the classical Lagrangian \mathcal{L} of the background is related to the isotropic pressure in the system

$$\mathcal{L}_d = -\rho\partial_t\theta - \rho\frac{1}{2}v_s^2 - \varepsilon(\rho) = [\rho\mu(\rho) - \varepsilon(\rho)] + \rho\frac{\partial E_0}{\partial\rho} - E_0 + E_0 = p + E_0. \quad (3.72)$$

From Eq. (3.61), the momentum conservation equation reads

$$\partial_\mu \mathfrak{T}^\mu{}_i = \partial_t \mathfrak{T}^0{}_i + \partial_j \mathfrak{T}^j{}_i = 0. \quad (3.73)$$

Writing \mathfrak{T} as in Eq. (3.60), computing \mathcal{T} according to Eq. (3.56) and using Eqs. (3.62), Eq. (3.64) and Eq. (3.72) we get

$$\partial_t(\rho v_{si} + P_i) + \partial_j([\rho v_{si} + P_i]v_{sj} + P_j v_{si} + \pi_{ij}) + \partial_i(p + E_0) = 0. \quad (3.74)$$

where repeated indices are summed.

Similarly, From Eq. (3.61), the energy conservation equation reads

$$\partial_\mu \mathfrak{T}^\mu{}_0 = \partial_t \mathfrak{T}^0{}_0 + \partial_j \mathfrak{T}^j{}_0 = 0. \quad (3.75)$$

Writing \mathfrak{T} as in Eq. (3.60), computing \mathcal{T} according to Eq. (3.56) and using Eqs. (3.62) and Eq. (3.71), we get

$$\partial_t \left(\frac{1}{2} \rho v^2 + \varepsilon(\rho) + E \right) + \partial_i \left(Q_i + [\rho v_{si} + P_i] \left[\frac{1}{2} v_s^2 + \mu(\rho) + \partial E_0 / \partial \rho \right] \right) = 0 \quad (3.76)$$

In summary, the analogue Einstein equation Eq. (3.48), the covariant conservation law of stress tensor Eq. (3.49) and the consequent conservation law Eq. (3.61) leads to the continuity of mass Eq. (3.69), Bernoulli equation Eq. (3.71) and the conservation of momentum Eq. (3.74). If we define the current density \vec{J} , energy density \mathcal{E} , momentum flux Π and the superfluid potential G as

$$J_i := \rho v_{si} + P_i, \quad (3.77a)$$

$$\mathcal{E} := \frac{1}{2} \rho v^2 + \varepsilon(\rho) + E, \quad (3.77b)$$

$$\Pi_{ij} := \rho v_{si} v_{sj} + P_i v_{sj} + P_j v_{si} + \pi_{ij} + [p + E_0] \delta_{ij}, \quad (3.77c)$$

$$G := \frac{1}{2} v_s^2 + \mu(\rho) + \frac{\partial E_0}{\partial \rho}. \quad (3.77d)$$

we rewrite Eq. (3.69), Eq. (3.74), Eq. (3.76) and Eq. (3.71) as the Landau- Khalatnikov equations for the superfluid

$$\partial_t \rho + \nabla \cdot \vec{J} = 0, \quad (3.78a)$$

$$\partial_t J_i + \nabla_j \Pi_{ij} = 0, \quad (3.78b)$$

$$\partial_t \mathcal{E} + \nabla \cdot (\vec{Q} + \vec{J}G) = 0, \quad (3.78c)$$

$$\partial_t \vec{v}_s + \nabla G = 0. \quad (3.78d)$$

The Eqs. (3.78a) and (3.78d) share the manifest Galilean invariance of Euler equations, because the P_i and E_0 are comoving frame momentum and energy of phonons. The Galilean invariance of Eqs. (3.78b) and (3.78c) follow immediately, because they are derived using the covariant conservation law Eq. (3.49), that is valid in all frames, and the analogue Einstein equations, which in the two-fluid language become Eqs. (3.78a) and (3.78d).

Finally, note that the dissipative effects due to the normal fluid are taken into account in the heat flux \vec{Q} and the momentum flux tensor π_{ij} . The dissipative components of these tensors can be computed according to linear response theory which we explain in the next section. In the limit $\vec{v}_s \rightarrow 0$, the Eqs. (3.78) become that of a normal fluid with $\rho \rightarrow \rho_n$ is the normal density and $P_i \rightarrow \rho_n v_{ni}$ defines the velocity of normal component. Assuming Stoke's constitutive law for stress, the momentum balance equation (3.78b) becomes the Navier-Stokes equation.

3.5 Stochastic analogue Einstein equations

Starting from the Lagrangian Eq. (3.7), we first derived the Euler equations Eq. (3.8) for the background and then compute the phonon contribution and called the overall system of equations the analogue Einstein (order one in metric perturbation) equations Eq. (3.48).

In this section we will go to second order in the metric perturbations and obtain dissipation and noise kernels due to phonons through a generalized linear response method. We will write an effective stochastic action for phonons that capture this noise and derive the stochastic analogue Einstein equation. This equation when linearized around a deterministic solution for the background fields ρ and θ , describes the motion of the stochastic corrections to the solution. Finally we show that in thermodynamic equilibrium the stochastic forcing term is balanced by the dissipation, that is the fluctuation-dissipation relation holds.

3.5.1 Linear response and the covariant stress-energy correlator

To see the semi-classical expansion due to metric perturbations, we first define the vector in time-path space composed of forward/backward metric tensors

$$\vec{g} = (g^{+\mu\nu}(x), g^{-\mu\nu}(x)). \quad (3.79)$$

Then the expansion of phonon effective action up to second order in metric perturbations is

$$\Gamma_{ph} = \frac{\delta\Gamma_{ph}}{\delta\vec{g}} \cdot \delta\vec{g} + \frac{1}{2} \delta\vec{g} \cdot \frac{\delta^2\Gamma_{ph}}{\delta\vec{g}\delta\vec{g}} \cdot \delta\vec{g} + O(\delta\vec{g}^3). \quad (3.80)$$

Here the boldface symbol δ is for variation with respect to the element $g^{+\mu\nu}$ is defined as

$$\frac{\delta\Gamma}{\delta g^{+\mu\nu}} = \frac{1}{\sqrt{-g(x)}} \frac{\delta\Gamma[g^+(x), g^-(x)]}{\delta g^{+\mu\nu}(x)} \Big|_{g^+=g^-=g}, \quad (3.81)$$

and the product of two time-path vectors $(\vec{\mathbf{A}} \cdot \vec{\mathbf{B}})$ sums over all path and tensor indices and integrates over position by using the metric $g^+ = g^- = g$, namely,

$$\vec{\mathbf{A}} \cdot \vec{\mathbf{B}} = \int d^4x \sqrt{-g(x)} \left(A^{+\mu\nu}(x) B_{\mu\nu}^+(x) + A^{-\mu\nu}(x) B_{\mu\nu}^-(x) \right). \quad (3.82)$$

Using Eq. (3.40), (3.41) and (3.42), it follows that the first order variation of the phonon effective action is

$$\frac{\delta\Gamma_{ph}}{\delta \vec{\mathbf{g}}} = \frac{1}{2} \left(\mathbf{T} \quad , -\mathbf{T} \right), \quad (3.83)$$

where

$$\mathbf{T} = \left\langle \hat{T}_{\mu\nu}(x) \right\rangle. \quad (3.84)$$

We define the deviations of the stress energy operator from its expectation value

$$\hat{t}_{\mu\nu}(x) = \hat{T}_{\mu\nu}(x) - \left\langle \hat{T}_{\mu\nu}(x) \right\rangle. \quad (3.85)$$

Following Martin and Verdaguer [116] we define the local stress deviation \mathbf{K} , the causal response kernel \mathbf{H} and the noise kernel \mathbf{N} that are bi-tensors made of correlators of \hat{t}

$$\hat{H}_{\mu\nu\alpha\beta}(x, y) = -i\theta(x^0 - y^0) \left\langle [\hat{t}_{\mu\nu}(x), \hat{t}_{\alpha\beta}(y)] \right\rangle, \quad (3.86a)$$

$$\hat{N}_{\mu\nu\alpha\beta}(x, y) = \frac{1}{2} \left\langle \{ \hat{t}_{\mu\nu}(x), \hat{t}_{\alpha\beta}(y) \} \right\rangle, \quad (3.86b)$$

$$\hat{K}_{\mu\nu\alpha\beta}(x, y) = \frac{-4}{\sqrt{g(x)g(y)}} \left\langle \frac{\delta^2 S_{ph}[\hat{\phi}]}{\delta g^{\mu\nu}(x) \delta g^{\alpha\beta}(y)} \right\rangle. \quad (3.86c)$$

These tensors are symmetric in the following way. If \mathbf{A} is any of the above kernels than

$$A_{\mu\nu\alpha\beta} = A_{\nu\mu\alpha\beta} = A_{\mu\nu\beta\alpha} \quad (3.87)$$

In Eq. (3.86a), \mathbf{H} is manifestly causal and $\mathbf{H}^{S,A}$ are symmetric/anti-symmetric parts of \mathbf{H} respectively,

$$H_{\mu\nu\alpha\beta}^{S,A}(x, y) = \pm H_{\alpha\beta\mu\nu}^{S,A}(y, x). \quad (3.88)$$

and they are

$$\hat{H}_{\mu\nu\alpha\beta}^S(x, y) = \mathbf{Im} \langle \mathbb{T}^* \{ \hat{t}_{\mu\nu}(x) \hat{t}_{\alpha\beta}(y) \} \rangle, \quad (3.89a)$$

$$\hat{H}_{\mu\nu\alpha\beta}^A(x, y) = \frac{-i}{2} \langle [\hat{t}_{\mu\nu}(x), \hat{t}_{\alpha\beta}(y)] \rangle. \quad (3.89b)$$

As we show in the Appendix C, the second order variation is a matrix in time-path space is

$$\frac{\delta^2 \Gamma_{ph}}{\delta \vec{\mathbf{g}} \delta \vec{\mathbf{g}}} = \frac{1}{4} \begin{pmatrix} i\mathbf{N} - \mathbf{H}^S - \mathbf{K} & -i\mathbf{N} - \mathbf{H}^A \\ -i\mathbf{N} + \mathbf{H}^A & i\mathbf{N} + \mathbf{H}^S + \mathbf{K} \end{pmatrix}. \quad (3.90)$$

All of these kernels are real. \mathbf{H}^A , the anti-symmetric component of the causal response function \mathbf{H} , changes sign in Eq. (3.90) when the forward/backward branches are switched. Therefore it breaks time-reversal symmetry and therefore gives rise to dissipative effects.

3.5.2 Global thermal equilibrium and fluctuation dissipation relation

Here we show, at global thermal equilibrium, that the noise kernel \mathbf{N} and the dissipation kernel \mathbf{H} are related in a stationary flow. For example, a flow through a

tube with varying cross section, but constant in time for each point in the tube and the temperature measured in the lab is uniform throughout the system.

The stationary flow with global thermal equilibrium is especially important because in the analogue gravity language it maps onto a hot curved spacetime at global thermal equilibrium. Such a space contains globally time-like Killing vectors κ^μ . [113, 117] The local temperature in the spacetime varies according to the norm of the time-like Killing vector and is dictated by Tolman's law:

$$T_{Tol} \sqrt{g_{\mu\nu} \kappa^\mu \kappa^\nu} = \text{constant}. \quad (3.91)$$

Once there are globally time-like Killing vectors, modes that solve the covariant wave equation Eq. (3.1) are classified as positive/negative Killing frequencies according to the value of their directional (Lie) derivative along the Killing vector, that is

$$\mathfrak{L}_\kappa u_n = -i\omega_n u_n, \quad (3.92a)$$

$$\mathfrak{L}_\kappa u_n^* = i\omega_n u_n^*, \quad \omega > 0. \quad (3.92b)$$

Now the field operator is written in the second quantization language and reads

$$\hat{\phi} = \sum_n \hat{a}_n^\dagger u_n^* + \hat{a}_n u_n, \quad (3.93)$$

where the vacuum state is uniquely defined. The Hamiltonian operator with eigenvalues equal to the Killing frequencies can be written in terms of the positive energy mode operators

$$\hat{H} = \sum_n \omega_n \hat{a}_n^\dagger \hat{a}_n. \quad (3.94)$$

As long as the conserved energy ω and the associated temperature is used, the methods of thermal field theory in flat spacetime is easily generalized to the curved

spacetime case [116]. In the fluid system, this is not a surprise, as in a stationary case, the Hamiltonian associated with the Lagrangian in Eq. (3.34) is time independent and second quantized in the form of Eq. (3.94).

In analogue gravity systems, this energy ω coincides with the lab frame energy of the mode [118]. Note that, this is not the comoving frame energy or the energy measured by observers in curved spacetime, which is not conserved. This means the temperature in the comoving frame and the lab frame are different and are related to each other through the Tolman law [93]. Stationary flow means the Killing vector is $\kappa = (1, 0, 0, 0)$. In global thermodynamic equilibrium, the positive energy modes u_i are distributed thermally according to the lab frame temperature so that we have

$$T_{Tol}\sqrt{g_{00}} = T_{Tol}\sqrt{\rho c(1 - v^2/c^2)} = T_{lab} = \frac{1}{\beta}. \quad (3.95)$$

Note that this analogue Tolman law is a purely classical effect that stems from the emergent Lorentz invariance of excitations in the strongly correlated superfluid. It is to be distinguished from the Unruh effect, where an accelerating observer detects a thermal radiation of phonons even if the lab frame's temperature is zero.

In equilibrium the eigenstates are distributed according to the lab frame temperature, with the density operator defined in Eq. (3.31) that reads

$$\hat{\rho}_\phi = \exp(-\beta\hat{H})/\text{Tr} \{ \hat{\rho}_\phi \}. \quad (3.96)$$

Then, the operator averages are best handled in imaginary time ($it = \tau$) formalism. For example for two operators \hat{O}_1 and \hat{O}_2 we have, suppressing the space indices,

$$\begin{aligned}
\langle \hat{O}_1(\tau) \hat{O}_2(\tau') \rangle &= \text{Tr} \left(\hat{O}_1(\tau) \hat{O}_2(\tau') \hat{\rho} \right) = \text{Tr} \left(U(i\tau) \hat{O}_1 U(-i\tau) U(i\tau') \hat{O}_2 U(-i\tau') U(-i\beta) \right) \\
&= \text{Tr} \left(\hat{O}_2(\tau' + \beta) \hat{O}_1(\tau) \hat{\rho} \right) = \langle \hat{O}_2(\tau' + \beta) \hat{O}_1(\tau) \rangle. \quad (3.97)
\end{aligned}$$

Stationarity allows the use of Fourier transformation in time domain, hence this equation can be written as

$$\langle \hat{O}_1(\omega) \hat{O}_2(-\omega) \rangle = e^{\beta\omega} \langle \hat{O}_2(-\omega) \hat{O}_1(\omega) \rangle. \quad (3.98)$$

Now we show that a fluctuation dissipation relation exists. Inspection of Eq. (3.104), (3.90) and (3.106) reveals that the time-reversal odd piece \mathbf{H}^A of the causal response causes dissipation and the fluctuation kernel \mathbf{N} causes noise.

Defining

$$F_{\mu\nu\alpha\beta}(\omega, \vec{x}, \vec{y}) = \int \frac{d\omega}{2\pi} e^{i(t-t')} \langle \hat{t}_{\mu\nu}(t, \vec{x}) \hat{t}_{\alpha\beta}(t', \vec{y}) \rangle, \quad (3.99)$$

and rewriting the definitions in Eq. (3.86) in frequency domain and using Eq. (3.98) we get:

$$\hat{H}_{\mu\nu\alpha\beta}^A(\omega, \vec{x}, \vec{y}) = -\frac{i}{2} F(\omega, \vec{x}, \vec{y}) (1 - e^{-\beta\omega}), \quad (3.100a)$$

$$\hat{N}_{\mu\nu\alpha\beta}(\omega, \vec{x}, \vec{y}) = \frac{1}{2} F(\omega, \vec{x}, \vec{y}) (1 + e^{-\beta\omega}). \quad (3.100b)$$

The fluctuation dissipation relation immediately follows as:

$$\hat{H}_{\mu\nu\alpha\beta}^A(\omega, \vec{x}, \vec{y}) = -i \tanh(\beta\omega/2) \hat{N}_{\mu\nu\alpha\beta}(\omega, \vec{x}, \vec{y}). \quad (3.101)$$

3.5.3 Hydrodynamic fluctuations around a deterministic solution

Suppose $\bar{\rho}$ and $\bar{\theta}$ are solutions to the analogue Einstein equations Eq. (3.48).

Define the classical and quantum corrections to the solutions

$$\rho^\pm = \bar{\rho} + \rho^\pm = \bar{\rho} + \rho^c \pm \rho^q \quad (3.102a)$$

$$\theta^\pm = \bar{\theta} + \theta^\pm = \bar{\theta} + \theta^c \pm \theta^q. \quad (3.102b)$$

Let the corresponding perturbations to the metric tensor be $h^c + h^q$ and $h^c - h^q$ so that

$$\vec{g} = (\bar{g}^{\mu\nu} + (h^q)^{\mu\nu} + (h^q)^{\mu\nu}, \bar{g}^{\mu\nu} + (h^c)^{\mu\nu} - (h^q)^{\mu\nu}). \quad (3.103a)$$

Breaking the deviations into classical and quantum parts amounts to (Keldysh) rotating the matrix in Eq. (3.90). The classical deviation can be thought of as a real displacement while the quantum deviation as a virtual displacement. Variation with respect to virtual displacement (\mathbf{h}^q) gives the classical equations of motion with one loop corrections as in Eq. (3.48). To find the fluctuations of the stress-energy, we can expand the effective actions as a Taylor series in the classical and quantum deviations to second order as

$$\Gamma_{ph}[\vec{g}] = \mathbf{T} \cdot \mathbf{h}^q - \frac{1}{2} \mathbf{h}^q \cdot (\mathbf{H} + \mathbf{K}) \cdot \mathbf{h}^c + \frac{i}{2} \mathbf{h}^q \cdot \mathbf{N} \cdot \mathbf{h}^q + O(\mathbf{h}^3), \quad (3.104)$$

where, all the kernels are functionals of the unperturbed metric g and $\vec{\mathbf{h}}$ is decomposed as $(\mathbf{h}^c, \mathbf{h}^q)$ and the dot product on the right hand side contracts spacetime indices with g and integrates over spacetime. We notice that the equation (3.104)

is in the same form as the Keldysh action for a quantum particle in a bath [15]. The well established technique to derive Langevin type equation from this action is to define an auxiliary stochastic tensor ξ to decouple the $O((h^q)^2)$ term (the Hubbard-Stratanovich decomposition).

$$\begin{aligned} \exp(i\Gamma_{ph}[\vec{\mathbf{g}}]) &= \frac{1}{\sqrt{\text{Det}(2\pi\mathbf{N})}} \int \mathcal{D}[\boldsymbol{\xi}] e^{-\frac{1}{2}\boldsymbol{\xi}\cdot\mathbf{N}^{-1}\cdot\boldsymbol{\xi}} e^{i\mathbf{Re}\{\Gamma_{ph}\}+i\boldsymbol{\xi}\cdot\mathbf{h}^q} \\ &= \langle e^{i\mathbf{Re}\{\Gamma_{ph}\}+i\boldsymbol{\xi}\cdot\mathbf{h}^q} \rangle_{\xi} = \langle \exp(i\Gamma_{ph}[\vec{\mathbf{g}}; \boldsymbol{\xi}]) \rangle_{\xi}. \end{aligned} \quad (3.105)$$

The mean and correlation function of the noise tensor field ξ is defined by the above Gaussian path integral, using the definition Eq. (3.106) of the noise kernel \mathbf{N} , which yields

$$\langle \xi_{\mu\nu}(x) \rangle_{\xi} = 0, \quad (3.106a)$$

$$\langle \xi_{\mu\nu}(x) \xi_{\alpha\beta}(y) \rangle_{\xi} = \frac{1}{2} \langle \{ \hat{t}_{\mu\nu}(x), \hat{t}_{\alpha\beta}(y) \} \rangle. \quad (3.106b)$$

The new phonon effective action

$$\Gamma_{ph}[\vec{\mathbf{g}}; \boldsymbol{\xi}[\vec{g}]] = (\mathbf{T} + \boldsymbol{\xi}) \cdot \mathbf{h}^q - \frac{1}{2} \mathbf{h}^q \cdot (\mathbf{H} + \mathbf{K}) \cdot \mathbf{h}^c + O(\mathbf{h}^3) \quad (3.107)$$

depends on the noise tensor ξ .

Then the background plus phonon effective action in Eq. (3.43) as a functional of noise tensor

$$\Gamma[\rho^{\pm}, \theta^{\pm}, \boldsymbol{\xi}] = S[\rho^{+}, \theta^{+}] - S[\rho^{-}, \theta^{-}] + \Gamma_{ph}[\vec{\mathbf{g}}; \boldsymbol{\xi}[\vec{g}]]. \quad (3.108)$$

3.5.4 Stochastic analogue Einstein equation

The Euler-Lagrange equations for the stochastic effective action $\Gamma[\rho^\pm, \theta^\pm, \boldsymbol{\xi}]$ in the limit $(\rho^\pm, \theta^\pm) \rightarrow (\rho, \theta)$ and hence $h^q \rightarrow 0$ are the following stochastic analogue Einstein equations for the two-fluid hydrodynamics

$$\partial_t \rho + \nabla \cdot (\rho \vec{v}) = \frac{1}{2} \nabla \cdot \left(\sqrt{-g} \left[\langle \hat{T}_{\mu\nu} \rangle + \xi_{\mu\nu} \right] \frac{\delta g^{\mu\nu}}{\delta \vec{v}} \right); \quad (3.109a)$$

$$\partial_t \theta + \frac{1}{2} v^2 + \mu(\rho) = \frac{1}{2} \left(\sqrt{-g} \left[\langle \hat{T}_{\mu\nu} \rangle + \xi_{\mu\nu} \right] \frac{\delta g^{\mu\nu}}{\delta \rho} \right). \quad (3.109b)$$

In this equation, the noise source $\boldsymbol{\xi}[\bar{g}]$ is computed by using the metric $\bar{g}(\bar{\rho}, \bar{v})$ that solves Eq. (3.48), while ρ and θ suffer deviations ρ^c, θ^c from the solution of Eq. (3.48) due to the existence of noise. The energy momentum tensor is also computed by taking these deviations in to account. Next we summarize the procedure to find the stochastic deviations ρ^c and θ^c of the background.

3.5.5 Procedure to compute background metric fluctuations from the analogue Einstein equation

Below, we outline the procedure to determine fluctuations of the metric, given initial data that consists of the initial conditions, boundary conditions, an initial state of the phonon density operator, and external sources, if any.

First, is to compute the deterministic solution $(\bar{\rho}, \bar{v})$ and the associated metric $\bar{g}_{\mu\nu}[\bar{\rho}, \bar{\theta}]$ as defined in Eq. (3.2), by solving the analogue Einstein equation (3.48) *self consistently*. In general this is equivalent to solving the two-fluid equations

Eq. (3.78) and is a difficult task. However, one can approach this problem perturbatively. If one has a solution to the Euler equations that describes the background without the phonons (Eq. (3.8) with no quantum pressure), then one can compute the expectation value of the stress-energy operator Eq. (3.46) by using the techniques in Ref. [113] and references therein. One then continues this process up to a desired order, so that the background is consistent with the metric on which the sources are computed.

Second, is to compute the correlators of the stress tensor in Eq. (3.86) to form the response and noise kernels. For the methods required to perform this, we refer the reader to Ref. [119, 120] and references therein.

Third, is to linearize the stochastic analogue Einstein equation (3.109) around the deterministic solution $\bar{\rho}, \bar{\theta}$. The resulting equation is linear in the stochastic corrections ρ^c and θ^c , to the background variables. The associated first-order corrections to the deterministic metric \bar{g} follow from the chain rule as

$$(h^c)^{\mu\nu} = \rho^c \frac{\delta \bar{g}^{\mu\nu}}{\delta \rho} + \bar{v}^c \cdot \frac{\delta \bar{g}^{\mu\nu}}{\delta \bar{v}}. \quad (3.110)$$

Then, the linearized stochastic analogue Einstein equation, that we dub the analogue Einstein-Langevin equation, follows from Eq. (3.109), where we linearize the stress tensor by using Eq. (3.104), as

$$\partial_t \rho^c + \nabla \cdot (\bar{\rho} \bar{v}^c) + \nabla \cdot (\rho^c \bar{v}) = \frac{1}{2} \nabla \cdot \left(\sqrt{-\bar{g}} \frac{\delta \bar{g}^{\mu\nu}}{\delta \bar{v}} \times \left[-\frac{1}{2} \int d^4 y (H + K)_{\mu\nu\alpha\beta}(x, y) (h^c)^{\alpha\beta}(y) + \xi_{\mu\nu} \right] \right) \quad (3.111)$$

and

$$\partial_t \theta^c + \bar{v} \cdot \bar{v}^c + \frac{\bar{c}^2}{\bar{\rho}} \rho^c = \frac{1}{2} \left(\sqrt{-\bar{g}} \frac{\delta \bar{g}^{\mu\nu}}{\delta \rho} \times \left[-\frac{1}{2} \int d^4 y (H + K)_{\mu\nu\alpha\beta}(x, y) (h^c)^{\alpha\beta}(y) + \xi_{\mu\nu} \right] \right). \quad (3.112)$$

Fourth and final, is to write down correlators of h^c . To do this, one first expresses the correlators of the background corrections ρ^c and θ_c in terms of the noise correlator \mathbf{N} by using the Green's functions of the linear equations Eq. (3.111) and Eq. (3.112). Then the correlators of h^c follow from Eq. (3.110).

3.6 Equilibrium ‘Minkowski’ fluctuations

In this section we illustrate the procedure of Sec. 3.5.5 for the static ($\vec{v}_s = 0$) thermodynamic equilibrium focusing on a qualitative analysis (detailed technical calculations and results for the correlators are cumbersome and will be presented elsewhere). The metric tensor for the static background reduces to that of Minkowski, if one sets

$$\bar{\rho} = \rho_e = c_e = \bar{c} = 1 \quad (3.113)$$

in addition to the choice of units in Eq. (3.10).

This renders Step 1 in Sec. 3.5.5 trivial. The analogue Einstein equations Eq. (3.48) and the covariant conservation law Eq. (3.49) are trivially satisfied. Nevertheless, it is instructive to outline how the expectation value of the stress-tensor is computed.

The isotropy and homogeneity of Minkowski space places strong restrictions on the stress-energy tensor and its correlators. For the stress tensor, homogeneity

means all components are constant in spacetime. The trace of the expectation value of stress energy vanishes for a massless scalar field. The energy density is positive. There is no isotropic Cartesian vector; therefore, the momentum density vanishes. The only isotropic rank-2 Cartesian tensor is the Kronecker delta; therefore, the spatial components are isotropic. The only rank-2 Minkowski tensor with the above properties is

$$\left\langle \hat{T}^\mu{}_\nu \right\rangle = \frac{\pi^2 T^4}{45} \begin{pmatrix} 3 & 0 & 0 & 0 \\ 0 & -1 & 0 & 0 \\ 0 & 0 & -1 & 0 \\ 0 & 0 & 0 & -1 \end{pmatrix}, \quad (3.114)$$

where the overall factor is the black body energy density and can be obtained from the standard momentum space integral that arise in Eq. (3.46), after dropping the infinite vacuum energy.

Similarly to the stress tensor, the symmetries greatly reduce the complexity of calculating its correlates as well. First of all, the homogeneity of spacetime requires that any function $f(x, y) = f(x - y)$. The stress tensor correlators can be expressed as momentum space integrals. In thermal equilibrium, all non-local behavior is due to the factor $\coth(\beta\omega/2)$, which behaves like

$$\coth(\beta\omega/2) \xrightarrow{k_B T \gg \hbar\omega} \frac{2k_B T}{\hbar\omega} \quad (3.115)$$

in the high-temperature limit and all kernels become local (memoryless) operators in spacetime.

In this limit, we linearize Eq. (3.109) around $\bar{\rho}$ and $\bar{\theta}$ to get Eq. (3.111) and

(3.112) for the static equilibrium. This linearized equation is in the Langevin form.

In Fourier domain it reads

$$\begin{pmatrix} -i\omega & -|\vec{k}|^2 \\ 1 & -i\omega \end{pmatrix} \begin{pmatrix} \rho^c \\ \theta^c \end{pmatrix} = \begin{pmatrix} R_{11} & R_{12} \\ R_{21} & R_{22} \end{pmatrix} \begin{pmatrix} \rho^c \\ \theta^c \end{pmatrix} + \begin{pmatrix} \zeta_1 \\ \zeta_2 \end{pmatrix}. \quad (3.116)$$

where \hat{R} 's are local operators, hence polynomials in \vec{k} and ω and ζ 's are stochastic sources.

The stochastic sources ζ 's are deduced from $\xi_{\mu\nu}$ by applying Eq. (3.67a), as

$$\zeta_1 = -ik^j \xi_{0j} \quad (3.117a)$$

$$\zeta_2 = \frac{1}{2}(\kappa - 1)\xi^\mu_\mu - \kappa\xi^{00} \quad (3.117b)$$

where $\kappa = \partial \ln c / \partial \ln \rho$ is the change of energy of phonons with density.

The diagonal terms R_{11} and R_{22} in Eq. (3.116) are equal and the symmetric part of the response kernel does not contribute to them:

$$R_{11} = R_{22} = -i\frac{(1-\kappa)}{2}k^j(H^A)^0_{j\mu} - i\kappa k^j(H^A)^0_{j^{00}}. \quad (3.118)$$

Whereas, the antisymmetric part of the response kernel does not contribute to the off diagonal components

$$R_{12} = k^i k^j (H^S + K)^0_{i\ j} \quad (3.119)$$

and

$$R_{21} = -\frac{(1-\kappa)^2}{4}(H^S + K)^\nu_{\nu\mu} - \kappa^2(H^S + K)^{0000} + \kappa(\kappa - 1)(H^S + K)^\mu_{\mu}{}^{00}. \quad (3.120)$$

Now one can solve Eq. (3.116) and express the correlators of stochastic corrections ρ^c and θ^c in terms of the noise correlators and the metric fluctuation follows by using Eq. (3.110).

We also note that, to lowest order in k , introducing some constants α, β, ν we have

$$R_{11} = R_{22} \rightarrow -\nu |\vec{k}|^2 \quad (3.121a)$$

$$R_{12} \rightarrow \alpha_{ij} k^i k^j \quad (3.121b)$$

$$R_{21} \rightarrow -\beta \quad (3.121c)$$

and the Eq. (3.116) takes the form of the linearized Navier-Stokes and continuity equations with stochastic forcing terms

$$\partial_t \rho^c + (\delta_{ij} + \alpha_{ij}) \nabla_i \vec{v}_j^c - \nu \nabla^2 \rho^c = \zeta_1, \quad (3.122a)$$

$$\partial_t \vec{v}^c - \nu \nabla^2 \vec{v}^c = -(1 + \beta) \nabla \rho^c + \nabla \zeta_2. \quad (3.122b)$$

The coefficient of viscosity ν can be extracted as

$$\nu = \frac{1}{3} \frac{\partial}{\partial k_j} \left[\frac{(1 - \kappa)}{2} (H^A)^0{}_{j\mu}{}^\mu - \kappa (H^A)^0{}_{j\mu}{}^{00} \right] \Big|_{\vec{k}=0}. \quad (3.123)$$

3.7 Conclusions and outlook

In this work, we develop a geometric generalization of the Landau-Khalatnikov two-fluid hydrodynamics for a strongly correlated bosonic superfluid and derive a system of coupled equations describing the motion of the superfluid background and the entropy-carrying normal fluid of phonon excitations. By exploiting the emergent covariance of the phonon field, we draw analogies between general relativity and the

two-fluid system including stochastic effects due to the fluctuations of the phonon “matter” field.

We emphasize that the methods and analogies used here are applicable to a variety of systems. Indeed, weakly interacting quasiparticles excited over a ground state is a common picture in many-body physics. Hydrodynamics captures the long-wavelength behavior of such systems. Galilean invariance requires that quasiparticle dynamics is defined on the frame comoving with the background fluid that represents the ground state manifold. This means, when referred to the lab frame, that the quasiparticle field experiences shifts due to the background flow – an effect captured in the definition of the metric tensor (3.2). From thereon, the quasiparticles can be described by quantum field theory on curved spacetime, thereby justifying the geometric formulation of the problem.

We would like to conclude with a brief summary of our work and promising directions for further research

In Sec. 3.2, following an earlier work [93], we discussed the applicability of the metric description for fluid by analyzing the length- and energy-scales. In analogy with cosmology [96, 121], the geometric description breaks down at an effective “Planck energy,” where the hydrodynamic description becomes inapplicable. However, the quantum description of the boson system is known at all energies contrary to the case in cosmology. This paves the way to understanding the cosmological phenomena through condensed matter systems [122–124].

In Sec. 3.3, we used the background field formalism to write down the Keldysh theory of quasiparticles. We use the Keldysh contour because the dynamical fluc-

tuations of the phonon field follow naturally from the Keldysh effective action that is “designed” to account for non-equilibrium phenomena. One interesting finding of this analysis is an additional “gravitational anomaly” , not present in the original work of Unruh [88] and Stone [89] : that is, despite the action for the phonons is covariant, as already noted in the literature, the measure of the path integral is not covariant. Hence, in contrast to classical phonon action, their full quantum theory is not covariant. We believe this anomaly should be taken into account, whenever quantum effects such as Hawking radiation, is important. It is curious to see if this anomaly is related to gravitational anomalies in high-energy phenomena. These interesting issues will be discussed in a future publication.

In Sec. 3.4, inspired by Ref. 93, we derive the analogue Einstein equation that governs the background and the excitations (matter). We establish the equivalence of the analogue Einstein equation and the covariant conservation law for the phonons, to the two-fluid conservation laws. Instead of assuming a specific form for the stress-energy tensor as in Ref. [96], we prove the equivalence of the two descriptions by reducing the covariant conservation law down to the Noether current of the two-fluid system and by using the equations of motion. We believe that the proof presented here is more general, than the specific superfluid model we study, and should be applicable to any emergent general-relativistic theory, which may be derived in the hydrodynamic, long-wave-length limit of a “parent” condensed matter system.

In Sec. 3.5, we take the analogy between the superfluid system and general relativity further to the domain of stochastic fluctuations. This allows the appli-

cation of a variety of methods that have been invented for stochastic gravity [49] to condensed matter systems. We write the response and dissipation kernels in the covariant language. In global thermal equilibrium, we discuss the notion of temperature on curved spacetime and show the appearance of analogue Tolman’s law. We prove the fluctuation-dissipation relation for a metric with globally time-like Killing vectors – that is, for a flow that can be brought to a stationary form after a Galilean transformation. Finally, we outline a procedure to calculate correlators of various observables, including fluctuations of the metric.

One interesting direction would be to consider the effects of higher order correlators of the stress-energy tensor and build a hierarchy of equations similar to the BBGKY hierarchy.

Finally, we linearize the stochastic analogue Einstein equation and obtain a Langevin-type equation for the stochastic corrections to the background. We show that the symmetries of the flow determine structure of the Langevin equation, by considering the Minkowski case. Classification of the flow induced spacetimes, the stress tensor and its fluctuations on the basis of the symmetry of the flow is a well defined mathematical problem. In general relativity these correspond to the Petrov classification of spacetimes and Segre classification of symmetric tensors [125]. Together with the machinery of general relativity such as conformal transformations and general coordinate transformations, the classification of the solutions of the two-fluid equations can be carried out in a similar spirit.

The main fundamental physical consequence of our analysis is the finding that sound waves propagating on a superfluid background at a finite temperature experi-

ence a random, stochastic metric on top a dynamical but deterministic background metric determined by the classical superfluid flow. Even in the absence of any flows and in equilibrium, where the average metric is that of flat Minkowski space, the phonon “rays” would experience random deviations from the flat background. This may lead to analogue gravitational lensing of acoustic waves due to the phenomenon called ‘intermittency’. In Ref. [126], Zeldovich considered light rays propagating in a random medium with a fluctuating metric, and showed that even if the average metric is flat, an observer receiving two distant rays would see the rays bend and the corresponding object shrink, due to the stochasticity. The effect seems unobservable in actual general relativity due to very weak metric fluctuations, if any [127]. However, similar fluctuations of “synthetic metric” can be greatly enhanced in a superfluid and it is conceivable that the corresponding analogue Zeldovich effect – bending of phonon “rays” propagating through a thermal superfluid – could become observable.

Chapter 4: Dynamical many-body localization in an integrable model

4.1 Introduction

Recently, there has been a lot of interest and progress in understanding Anderson-type localization properties of disordered, interacting many-body systems. Notably, the remarkable phenomenon of many-body localization (MBL) was discovered [32–39]. In an isolated system, MBL manifests itself in the localization of all eigenstates and leads to the breakdown of ergodicity and violation of the eigenvalue thermalization hypothesis [29, 31], forcing to revisit the very foundations of quantum statistical mechanics [128, 129].

In this work, we ask whether a driven interacting system can be *dynamically* many-body localized. We answer this question in the affirmative and present an exactly solvable model of a kicked chain of interacting linear rotors, which shows both dynamical MBL and delocalized regimes.

A quantum kicked-rotor is a canonical model of quantum chaos [25, 130] which exhibits dynamical localization in momentum space. The time dependent Schrödinger equation for a general kicked rotor is given by (here and below, we set $\hbar = 1$ and

the driving period $T = 1$),

$$\mathbf{i}\partial_t\psi(\theta, t) = [2\pi\alpha(-\mathbf{i}\partial_\theta)^l + K(\theta)\delta(t - n)]\psi(\theta, t). \quad (4.1)$$

In the ground-breaking paper [25], Fishman, Prange, and Grempel proved that the eigenvalue problem for the Floquet operator of a kicked rotor is equivalent to that of a particle hopping in a (quasi)periodic potential ((ir)rational α) in one-dimension [28] given by,

$$\sum_r W_{m+r}u_r + \tan[\omega - 2\pi\alpha m^l]u_m = Eu_m. \quad (4.2)$$

This mapping traced the origin of the dynamical localization in driven systems to Anderson localization in time-independent settings. While the quadratic rotor ($l = 2$) is nonintegrable, the linear rotor model ($l = 1$) in Eq. (4.1) was exactly solved in Refs. [25, 27, 28, 41, 131]. The corresponding integrable lattice version in Eq. (4.2) with $l = 1$ is dubbed Maryland model (MM) [132, 133] (See section A.1 for technical details of this mapping). For the linear rotor, both classical and quantum dynamics is integrable, and the dynamical localization (absence of chaos) is due to the existence of a complete set of integrals of motion [41]. However, the incommensurate MM is an Anderson insulator with no classical interpretation [28] even though the linear rotor manifests classical integrability. Thus, the dynamical localization for the quantum version of both linear ($l = 1$) and quadratic rotor ($l = 2$) seems to stem from the Anderson mechanism [28].

In this work, we generalize the linear kicked rotor model by considering an interacting chain of driven rotors in order to understand the anatomy of many-body

localization in the dynamical space. One of the remarkable features of this many-particle model is that it manifests both localization and delocalization in dynamical space depending on whether the components of $\vec{\alpha}$ are irrational or rational.

Let us emphasize from the outset that the model we consider is integrable for all parameters owing to the first order differential operator. This leads to integrals of motion (IOMs), which are *local* in the spatial (angular) variables. The underlying integrability is a special, non-universal feature of our model (4.3), which allows us to solve it exactly. However, the existence of the local-in- θ IOMs has no direct relation to dynamical MBL, which occurs in *momentum* space. The non-interacting version of these emergent IOM's for the linear kicked rotor was pointed out by Berry in Ref. ([41]).

As shown below, dynamical MBL is accompanied by the appearance of *additional* integrals of motion bounded in momentum space – a central result of this work. As argued below, these “emergent” IOMs and the dynamical MBL are universal phenomena, which would survive in non-integrable generalizations of the model (which however is not analytically solvable).

To capture the dynamical localization for this interacting model, we monitor three indicators: energy growth at long times, (momentum degrees of freedom at long times, and the existence of integrals of motion in momentum space. Below, we first present the details of our model in Section 4.2. The main analytical results are outlined in Section 4.3, and their numerical analysis and key conclusions are given in Section 4.4. An outline of technical derivation of the results is given in Section 4.5. The experimental proposal to realize our model (4.3), is explained in Section 4.6.

In section 4.7 we list our conclusions. Finally, Appendix A.1 and Appendix A.2 are devoted to the summary of the connection of the rotor problem to a lattice model and the correspondence between our model and a d -dimensional lattice, respectively.

Throughout the text, in all the summations $\sum_i \dots$ or $\sum_{ij} \dots$ we only consider $i \neq j$. So that, expressions like $\sum_j 1/(\alpha_i - \alpha_j)$ are not divergent. The denominator vanishes only when there is a resonance, such as $\alpha_i \rightarrow \alpha_j$.

4.2 The Model

We consider a many-body interacting generalization,

$$\begin{aligned}\hat{H}(t) &= \hat{H}_0 + \hat{V} \sum_{n=-\infty}^{\infty} \delta(t - n), \quad \text{with } \hat{V} = \sum_{i=1}^d K(\hat{\theta}_i), \\ \hat{H}_0 &= 2\pi \sum_{i=1}^d \alpha_i \hat{p}_i + \frac{1}{2} \sum_{i \neq j}^{d-1} J_{ij}(\hat{\theta}_i - \hat{\theta}_j)\end{aligned}\tag{4.3}$$

of the linear rotor model.

\hat{H}_0 is the static Hamiltonian describing d particles on a ring, each rotating $2\pi\alpha_i$ radians per one period of the kick. $\hat{\theta}_i$ is the position operator for the i th particle on the ring and \hat{p}_i is its momentum. These d particles interact through a translationally invariant two-body potential $J_{ij}(\hat{\theta}_i - \hat{\theta}_j)$. This form of the interaction ensures conservation of momentum. The rotors are driven by $\hat{V}(t)$, which contains periodic delta function impulses, where the strength of the impulse is given by a general periodic one-body potential $K(\hat{\theta}_i)$. The local potentials are periodic with 2π and therefore the most general form can be written as $K(\theta_j) = \sum_m k_m e^{im\theta_j}$. Here, k_m is the m th Fourier component of the potential that acts on the j th particle. The

periodic form of the interaction potential J can be written as $J_{ij} = \sum_m b_m^{ij} e^{im(\theta_i - \theta_j)}$. Here, b_m^{ij} is the m th Fourier component of the interaction potential between the i th and j th particle. Reversing i and j and replacing m with $-m$ in this Fourier expansion has no effect on the components; therefore, $b_m^{ij} = b_{-m}^{ji}$. This property will be handy while deriving formulas throughout the text.

Note that in our model the localization is a consequence of incommensurate driving period and angular velocities $\vec{\alpha}$. This situation is different from recent works using Floquet analysis to probe dynamical properties of MBL states of disordered Hamiltonians [134–137] (in these papers, a Floquet perturbation is imposed on a state, many-body localized in coordinate space, while our goal is to induce *dynamical* many-body localization in *momentum space* by the Floquet perturbation).

4.3 Main Results

4.3.1 Energy dynamics

Following the conjecture of D’Alessio and Polkovnikov [138], we test the dynamical localization by computing the energy growth as a function of time at long times. The average energy after N kicks (equivalent to time) can be written as, $E(N) = \langle \psi_N | \hat{H}_0 | \psi_N \rangle$. To compute it, we write

$$|\psi_N\rangle = \hat{U}_F^N |\psi_0\rangle, \quad \hat{U}_F = e^{-i\hat{V}} e^{-i\hat{H}_0}, \quad (4.4)$$

where \hat{U}_F is the Floquet evolution operator, which captures the state of the system after each kick. Owing to the linear dependence of the Hamiltonian on the

momentum, we can explicitly compute this expectation.

$$E(N) = E(0) + \sum_{i=1}^d \sum_m 2\pi\alpha_i \langle \hat{\Gamma}_{mi} \rangle_0 \frac{\sin(mN\pi\alpha_i)}{\sin(m\pi\alpha_i)}. \quad (4.5)$$

In the above expression, $E(0) = \langle \psi_0 | H_0 | \psi_0 \rangle$ corresponds to the average many-body energy over the initial state. $\hat{\Gamma}_{mi} = -\mathbf{i}mk_m e^{\mathbf{i}m(\hat{\theta}_i + \pi\alpha_i[N+1])}$ depends on the chosen form of $K(\hat{\theta})$ averaged over the initial state and due to its periodic nature is a bounded function of the number of kicks N . The growth of energy for large N is then completely dependent on the nature of α_i appearing in the ratio $\frac{\sin(mN\pi\alpha_i)}{\sin(m\pi\alpha_i)}$. Note that this expression is completely independent of interactions, which we prove in Section 4.5.1. This is a consequence of momentum conserving interactions and this property is no longer valid when the translational invariance of interactions is broken.

4.3.2 Momentum dynamics

Another indicator for dynamical localization is the spread in the momentum degrees of freedom. The i th momentum after N kicks, $p_i(N) = \langle \psi_N | \hat{p}_i | \psi_N \rangle$ is given by the following expression,

$$p_i(N) = \langle \hat{p}_i \rangle_0 + \sum_m \langle \hat{\Gamma}_{mi} \rangle_0 \frac{\sin(mN\pi\alpha_i)}{\sin(m\pi\alpha_i)} + \sum_{mj} \langle \hat{\Gamma}_{mij}^{int} \rangle_0 \frac{\sin(mN\pi\Delta\alpha_{ij})}{m\pi\Delta\alpha_{ij}}.$$

We have defined $\Delta\alpha_{ij} = \alpha_i - \alpha_j$. In the above expression, the first term is the i th momentum in the initial eigenstate $\langle p_i \rangle_0 = \langle \psi_0 | \hat{p}_i | \psi_0 \rangle$. The second term corresponds to the kicking potential as defined in Eq. (4.5). The last term depends explicitly on the form of interaction via $\hat{\Gamma}_{mij}^{int} = -\mathbf{i}mb_m^{ij} e^{\mathbf{i}m(\hat{\theta}_i - \hat{\theta}_j + \pi N\Delta\alpha_{ij})}$ and is a bounded

function of N . The growth of momenta at long times corresponding to the last term is completely determined by the ratio $\frac{\sin(mN\pi\Delta\alpha_{ij})}{m\pi\Delta\alpha_{ij}}$.

4.3.3 Integrals of motion

Recent works have shown that the existence of integrals of motion (IOM) can be used as a diagnostic to quantify both non-interacting Anderson localization [139] and many-body localization [40, 140]. In the context of dynamical localization for the model at hand, we work in the momentum basis and search for existence of IOMs in this basis. We begin by constructing IOMs by identifying operators \hat{C}_i that satisfies $[\hat{C}_i, \hat{U}_F] = 0$ and $[\hat{C}_i, \hat{C}_j] = 0$. The existence of these IOMs encode information about dynamical localization. Operators that commute with \hat{U}_F satisfy the property $\langle \hat{C}_i \rangle_{N+1} = \langle \hat{C}_i \rangle_N$ and are given by

$$\hat{C}_i = \hat{p}_i + \frac{1}{2} \sum_m \frac{mk_m e^{im(\hat{\theta}_i + \pi\alpha_i)}}{\sin(m\pi\alpha_i)} + \frac{1}{2} \sum_{mj} \frac{b_m^{ij} e^{im(\hat{\theta}_i - \hat{\theta}_j)}}{\pi(\alpha_i - \alpha_j)}. \quad (4.6)$$

This expression is a generalization of the constant of motion given by Berry [41]. The derivation of this expression is given in Sec. 4.5.2. Since \hat{C}_i is an IOM, \hat{p}_i is bounded in time as long as the series in the last two terms converges. The delocalization of \hat{p}_i with time will occur due to the diverging denominators in the $\hat{\theta}$ dependent terms.

We reiterate that the model always contains d integrals of motion, $\hat{B}_i = \hat{\theta}_i/\alpha_i \pmod{2\pi}$ ($[\hat{B}_i, \hat{U}_F] = 0$) which results in integrability for both localized and delocalized cases. For example, if $\alpha_i = r_i/s_i$ is rational, the existence of \hat{B}_i results in integrability even though $\hat{C}_{1\dots d}$ do not exist. Since \hat{B}_i is momentum independent, its existence cannot bind $p_i(N)$. For the fully localized case, we have additional

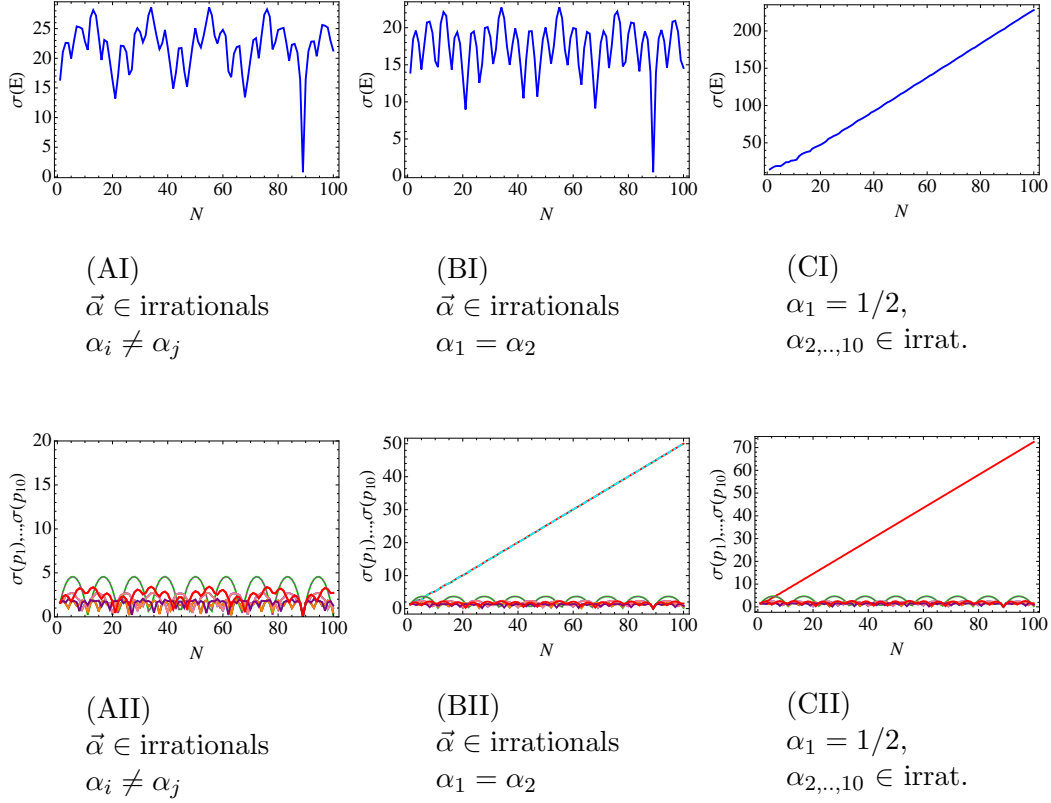


Figure 4.1: (Top panel) Plots showing evolution of the root mean square deviation of energy, $\sigma(E) = \sqrt{\langle H_0^2 \rangle - \langle H_0 \rangle^2}$, as a function of time, labeled by the number of kicks, N . (Bottom Panel) Plots showing evolution of the root mean square deviation of individual momenta in an ensemble of 10 particles $\sigma(p_i) = \sqrt{\langle p_i^2 \rangle - \langle p_i \rangle^2}$ as a function of time, labeled by the number of kicks, N . The initial states of the rotors are assumed to be definite momentum states. The total number of particles in this interacting ensemble is $d = 10$ and circular boundary conditions apply. We consider two body interaction term to be $J_{ij} = \cos(\theta_i - \theta_j)$. The periodic kicking potential is given by $K(\theta) = \sum_{m=1}^{\infty} k_m \cos(m\theta)$ for all particles. The m -th Fourier coefficient is fixed by $k_m = \tilde{z}/m^2$, where \tilde{z} is a random complex number with real and imaginary parts uniformly distributed in the interval $[0,1]$. We make sure that $K(\theta)$ is real. We choose $\vec{\alpha}$ corresponding to three scenarios: Figs. (AI, AII): If φ denotes the golden ratio, $\alpha_j = (j/d)\varphi - (1/2)\varphi$ are all irrationals for $j = 1 \dots 10$. Figs. (BI, BII): We consider α_j distinct irrationals as in Case A, but set $\alpha_1 = \alpha_2$, which results in the resonant growth of $\sigma(p_1)$ and $\sigma(p_2)$, while $\sigma(E)$ is bounded. Figs. (CI, CII): We consider α_j as in Case A and set $\alpha_1 = 1/2$, which results in the resonant growth of $\sigma(E)$ and $\sigma(p_i)$.

d IOM's $\hat{C}_{1\dots d}$ given in Eq. (4.6) that explicitly depend of \hat{p}_i and thus constrain it. Thus, \hat{C}_i 's can be thought of as “emergent” IOM's constraining the momentum growth, resulting in dynamical MBL and “emergent” superintegrability.

4.4 Dynamical many-body localization and the structure of $\vec{\alpha}$

Equipped with three analytical expression for the energy growth, momentum growth and IOMs [Eqs. (4.5), (4.6), and (4.6)], we now diagnose the dynamical localization for three distinct cases with varying structure of $\vec{\alpha}$. We note that, there are cases where $m\alpha_i$ can get arbitrarily close to integers (Liouville numbers) and total energy and momentum are no longer bounded. In the single rotor case, such a situation yields interesting consequences like marginal resonance and a mobility edge in the momentum lattice, [41, 141]. In this study we exclude this possibility and refer to generic irrationals only.

4.4.1 Case I: $\alpha_1 \dots \alpha_d$ are distinct generic irrationals

For irrational values of α_i , the total energy in Eq. (4.5) is always a bounded function of N since $m\alpha_i \notin \text{integer}$. In Fig. 4.1(AI), we fix initial states to be momentum eigenstates $\psi_0(\theta) = e^{ip_0\theta}$. For momentum eigenstates, $\langle \hat{\Gamma}_{mi} \rangle_0 \sim 0$. Thus, we plot the root mean square (RMS) of system's energy $\sigma(E) = \sqrt{\langle \hat{H}_0^2 \rangle - \langle \hat{H}_0 \rangle^2}$ as a function of N . Fig. 4.1 (AI) shows boundedness in the spread of the energy as a function N . The momentum growth shown in Eq. (4.6) has contributions from both interactions and the kicking potential. In Fig. 4.1 (AII) we plot RMS deviation of

momenta $\sigma(p_1) \dots \sigma(p_d)$ (we used $d = 10$ for the specific simulation) and show that the spread in the momenta is bounded as a function of N . For this case the integrals of motion in Eq. (4.6) exist and convergent. Thus, all the diagnostics for this case point towards a true many-body dynamical localization.

4.4.2 Case II: $\alpha_1 = \alpha_2$ and $\alpha_2 \dots \alpha_d$ are distinct generic irrationals

For this case, the energy remains a bounded function of N since $m\alpha_i$ are not integers. Thus, the RMS deviation $\sigma(E)$ is bounded as shown in Fig. (4.1 BI). However, the second term in the momentum expression (Eq. (4.6)) develops a resonance (for the momenta p_1 and p_2) since $\alpha_1 \rightarrow \alpha_2$. Due to this resonance term, $\sin(mN\pi\Delta\alpha_{12})/(m\pi\Delta\alpha_{12}) \sim N$ as $\alpha_1 \rightarrow \alpha_2$. This resonant growth is reflected in the RMS deviation of $\sigma(p_1)$ and $\sigma(p_2)$ growing linearly with N , while the $\sigma(p_3) \dots \sigma(p_{10})$ remain bounded as shown in Fig. 4.1 (BII). This is a striking scenario where the resonant momenta are not localized even if the total energy is bounded for large N . However, the delocalization of p_1 and p_2 in time is reflected in the break down of IOMs \hat{C}_1 and \hat{C}_2 due to diverging denominators in the resonant limit $\alpha_1 \rightarrow \alpha_2$. For this case, the bounded total energy fails to diagnose delocalization as shown in Fig. 4.1 (BI, BII). We note that this scenario has no analogue in the non-interacting limit. Notice that interactions we considered possess translational invariance, i.e. in the form $J(\theta_i - \theta_j)$ given in Eq. (4.3) and therefore interactions conserve momentum. The dichotomy between the energy growth and momentum growth is a result of conservation of momentum and the linear dependence of energy on mo-

momentum. If we allow interactions that break translational invariance, momentum is no longer conserved and resonance due to interactions triggers unbounded growth (delocalization) of both momenta and the total energy.

4.4.3 Case III: $\alpha_1 = 1/2$ and $\alpha_2 \dots \alpha_d$ are distinct generic irrationals

For rational $\alpha_1 = 1/2$, the system develops a different kind of resonance compared to Case II. We consider a kicking potential with $(k_2 \neq 0)$. The resonance condition $m\alpha_1 \in \text{integer}$ can be satisfied for $m = 2$ and the ratio $\frac{\sin(mN\pi\alpha_1)}{\sin(m\pi\alpha_1)}$ grows as N . It results in energy growth and delocalization of momenta p_1 as shown in the RMS deviations in Fig. 4.1 (CI, CII). This is a converse situation to Case II where the energy delocalizes with the delocalization of p_1 even though the momenta p_2, p_3, \dots, p_{10} are bounded. This situation is again captured by the IOMs, where \hat{C}_1 does not exist, while $\hat{C}_2 \dots \hat{C}_{10}$ are well defined and convergent as seen in Eq. (4.6).

We can generalize the above representative cases. For each rational α_i , its integral of motion \hat{C}_i breaks down and the corresponding momentum and energy diverge with time. For each pair $\alpha_i = \alpha_j$ both \hat{C}_i and \hat{C}_j break down and the corresponding momenta diverge in opposite directions, therefore $\hat{C}_i + \hat{C}_j$ is still an IOM and the total momentum and energy of the pair are bounded.

Other than the behaviour of energy in Case II in Section 4.4.2, the rest of our analysis apply equally to the interactions that break translational symmetry.

4.5 Derivation of main results

Having established the physical understanding of localization for this model, we now sketch the brief derivation leading to the final results in Eq. (4.5), Eq. (4.6) and Eq. (4.6). In the following we consider the expectation of a generic operator as a function of time, $X(N) = \langle \psi_N | \hat{X} | \psi_N \rangle$. We write the explicit evolution of the many-body wave function between two successive kicks, $|\psi_N\rangle = e^{-i\hat{V}} e^{-i\hat{H}_0} |\psi_{N-1}\rangle$. Notice that $\hat{H}_0 = 2\pi\vec{\alpha}\cdot\hat{\vec{p}} + \frac{1}{2} \sum_{i \neq j}^{d-1} J_{ij}(\hat{\theta}_i - \hat{\theta}_j)$ contains the many-body interaction term which may seem daunting, however, the linear momentum term allows a factorization in the Floquet operator. The Baker-Campbell-Hausdorff formula $\hat{Z} = \ln(e^{\hat{X}} e^{\hat{Y}})$ becomes tractable when $[\hat{X}, \hat{Y}] = s\hat{Y}$. In this case, the result simply reads $\hat{Z} = \hat{X} + s\hat{Y}/(1 - e^{-s})$. Now fix m and let $\hat{X} = i2\pi(\alpha_1\hat{p}_1 + \alpha_2\hat{p}_2)$ and $\hat{Y} = i\tilde{b}_m^{12} \exp(im[\hat{\theta}_1 - \hat{\theta}_2])$ where $\Delta\alpha_{12} = \alpha_1 - \alpha_2$. The result of the commutator reads $[\hat{X}, \hat{Y}] = i2\pi\Delta\alpha_{12}m\hat{Y}$, precisely the tractable case discussed above. Replacing s with $i2\pi\Delta\alpha_{12}m$ in the formula $\hat{Z} = \hat{X} + s\hat{Y}/(1 - e^{-s})$ and inverting both sides of the equality, we obtain the following factorization

$$e^{-i2\pi\vec{\alpha}\cdot\vec{p} - i\tilde{b}_m^{12} \exp(im[\theta_1 - \theta_2])} = e^{-i\tilde{b}_m^{12} \exp(im[\theta_1 - \theta_2])} e^{-i2\pi\vec{\alpha}\cdot\vec{p}}. \quad (4.7)$$

For this to hold, the Fourier coefficients must satisfy

$$\tilde{b}_m^{ij} = \frac{\sin(\pi m \Delta\alpha_{ij})}{\pi m \Delta\alpha_{ij}} b_m^{ij} e^{-im\pi\Delta\alpha_{ij}}. \quad (4.8)$$

This argument can be generalized to more particles and Fourier coefficients. Due to linearity summations over particle indices i, j and Fourier indices m are introduced.

All in all, we can factorize the evolution operator for our model in Eq. (4.3) as,

$$|\psi_N\rangle = e^{-i\hat{V} - \frac{i}{2} \sum_{ij} \tilde{J}_{ij}(\hat{\theta}_i - \hat{\theta}_j)} e^{-i2\pi\vec{\alpha} \cdot \hat{\vec{p}}} |\psi_{N-1}\rangle, \quad (4.9)$$

where we have defined the modified interaction term as,

$$\tilde{J}_{ij} = \sum_m \tilde{b}_m^{ij} e^{im(\theta_i - \theta_j)} \quad (4.10a)$$

$$= \sum_m \frac{\sin(\pi m \Delta\alpha_{ij})}{\pi m (\Delta\alpha_{ij})} b_m^{ij} e^{im(\theta_i - \theta_j - \pi \Delta\alpha_{ij})}. \quad (4.10b)$$

The advantage of this factorization is that the operator $e^{-i2\pi\vec{\alpha} \cdot \hat{\vec{p}}}$ is a translation operator in the position basis. We can rewrite Eq. (4.9) in the position basis by acting with $\langle\theta|$ from the left. We define $\langle\theta|\psi_N\rangle = \psi_N(\theta)$ and express $\langle\theta|e^{-i2\pi\vec{\alpha} \cdot \hat{\vec{p}}}|\psi_{N-1}\rangle = \psi_{N-1}(\vec{\theta} - 2\pi\vec{\alpha})$. For a single kick we then have,

$$\psi_N(\vec{\theta}) = e^{-iV(\vec{\theta}) - \frac{i}{2} \sum_{ij} \tilde{J}_{ij}(\theta_i - \theta_j)} \psi_{N-1}(\vec{\theta} - 2\pi\vec{\alpha}). \quad (4.11)$$

The above equation can be recursively iterated to yield,

$$\psi_N(\vec{\theta}) = e^{-i \sum_{n=0}^{N-1} [V(\vec{\theta} - 2\pi n\vec{\alpha}) + \sum_{ij} \tilde{J}_{ij}(\vec{\theta} - 2\pi n\vec{\alpha})]} \psi_0(\vec{\theta} - 2\pi N\vec{\alpha}). \quad (4.12)$$

4.5.1 Derivation of the evolution of energy and momentum averages

Now consider a generic operator $\hat{X} \equiv X(\hat{p}_1 \dots \hat{p}_d; \hat{\theta}_1 \dots \hat{\theta}_d)$. The expectation value of this operator after N kicks is

$$X(N) = \int d\vec{\theta} \psi_N^*(\vec{\theta}) X \left(\frac{\partial}{\partial \theta_1} \dots \frac{\partial}{\partial \theta_d}; \theta_1 \dots \theta_d \right) \psi_N(\vec{\theta}). \quad (4.13)$$

If we substitute $\hat{X} = \hat{p}_k$, we get

$$p_l(N) = \langle \hat{p}_l \rangle_0 - \sum_{n=1}^N \left\langle \partial_l V(\vec{\theta} + 2\pi n\vec{\alpha}) + \partial_l \frac{1}{2} \sum_{ij} \tilde{J}_{ij}(\vec{\theta} + 2\pi n\vec{\alpha}) \right\rangle_0.$$

Here, $\partial_l \equiv \partial/\partial\theta_l$ and $\langle \dots \rangle_0 \equiv \int d\vec{\theta} \dots |\psi_0|^2$. The contribution from the kicking potential is:

$$\left\langle -\partial_l \sum_n V(\vec{\theta} + 2\pi n \vec{\alpha}) \right\rangle_0 = \sum_m \langle \hat{\Gamma}_{ml} \rangle_0 \frac{\sin(mN\pi\alpha_l)}{\sin(m\pi\alpha_l)}. \quad (4.14)$$

The contribution from the interaction potential is

$$\left\langle -\partial_l \sum_n \frac{1}{2} \sum_{ij} \tilde{J}_{ij}(\hat{\theta}_i - \hat{\theta}_j + 2\pi n[\alpha_i - \alpha_j]) \right\rangle_0 = \sum_{jm} \langle \hat{\Gamma}_{mj}^{int} \rangle_0 \frac{\sin(mN\pi\Delta\alpha_{li})}{\pi m \Delta\alpha_{li}}.$$

Putting together above expressions, we obtain the expression for the momentum dynamics presented in Sec. (4.3.2).

$$p_i(N) = \langle \hat{p}_i \rangle_0 + \sum_m \langle \hat{\Gamma}_{mi} \rangle_0 \frac{\sin(mN\pi\alpha_i)}{\sin(m\pi\alpha_i)} + \sum_{mji} \langle \hat{\Gamma}_{mij}^{int} \rangle_0 \frac{\sin(mN\pi\Delta\alpha_{ij})}{m\pi\Delta\alpha_{ij}}. \quad (4.15)$$

Now we derive the expression for the energy growth. Substituting $\hat{X} = \hat{H}_0$ in Eq. (4.13), we have

$$\begin{aligned} E(N) = E(0) + \sum_{mi} 2\pi\alpha_i \langle \hat{\Gamma}_{mi} \rangle_0 \frac{\sin(mN\pi\alpha_i)}{\sin(m\pi\alpha_i)} + \frac{1}{2} \sum_{ij} \langle J_{ij}(\hat{\theta}_i - \hat{\theta}_j + 2\pi N\Delta\alpha_{ij}) - J_{ij}(\hat{\theta}_i - \hat{\theta}_j) \rangle_0 \\ + \sum_{ijm} 2\pi\alpha_i \langle \hat{\Gamma}_{mij}^{int} \rangle_0 \frac{\sin(mN\pi\Delta\alpha_{ij})}{m\pi\Delta\alpha_{ij}}. \end{aligned} \quad (4.16)$$

In the above equation, a cancellation occurs between the interaction terms in the last two lines of Eq. (4.16) owing to the following relation,

$$\begin{aligned} \frac{1}{2} \sum_{ij} \langle J_{ij}(\hat{\theta}_i - \hat{\theta}_j + 2\pi N\Delta\alpha_{ij}) - J_{ij}(\hat{\theta}_i - \hat{\theta}_j) \rangle_0 \\ = - \sum_{ijm} 2\pi\alpha_i \langle \hat{\Gamma}_{mij}^{int} \rangle_0 \frac{\sin(mN\pi\Delta\alpha_{ij})}{m\pi\Delta\alpha_{ij}}. \end{aligned} \quad (4.17)$$

This completes the derivation of the energy growth shown in Sec. (4.16)

$$E(N) = E(0) + \sum_{i=1}^d \sum_m 2\pi\alpha_i \langle \hat{\Gamma}_{mi} \rangle_0 \frac{\sin(mN\pi\alpha_i)}{\sin(m\pi\alpha_i)}. \quad (4.18)$$

The dropping out of interaction terms from the total energy can be interpreted in the following way. As seen from Eq. (4.15), the contribution of interaction to the momentum average picks up a negative sign when i and j are interchanged. This means interaction transfers momentum from one particle to the other at each kick, in other words momentum is conserved for each couple of rotors. Since the energy is linear in momenta, when the momenta of rotors are summed, the contribution of interactions vanishes. We emphasize that when the interactions break translational invariance, they no longer conserve momentum and in that case energy growth depends on interactions too.

4.5.2 Construction of integrals of motion

In this section, we outline the derivation involved in the construction of integrals of motion. By inspecting Eq. (4.14) and using the identity $\sin(m\pi\alpha) = [\exp(\mathbf{i}m\pi\alpha) - \exp(-\mathbf{i}m\pi\alpha)]/(2\mathbf{i})$, we can write

$$\begin{aligned} p_l(N+1) - p_l(N) = & \frac{1}{2} \sum_m \frac{mk_m}{\sin(m\pi\alpha_l)} \left(\left\langle e^{\mathbf{i}m(\hat{\theta}_l + \pi\alpha_l)} \right\rangle_N - \left\langle e^{\mathbf{i}m(\hat{\theta}_l + \pi\alpha_l)} \right\rangle_{N+1} \right) \\ & + \frac{1}{2} \sum_{mj} \frac{b_m^{lj}}{\pi\Delta\alpha_{lj}} \left(\left\langle e^{\mathbf{i}m(\hat{\theta}_l - \hat{\theta}_j)} \right\rangle_N - \left\langle e^{\mathbf{i}m(\hat{\theta}_l - \hat{\theta}_j)} \right\rangle_{N+1} \right), \end{aligned} \quad (4.19)$$

noting that, the expression is valid whenever the denominators $\sin(m\pi\alpha_l)$ and $\Delta\alpha_{lj} = \alpha_l - \alpha_j$ are non-zero, in other words, whenever the resonances are avoided.

The above expression can be organized in a way that it manifests the IOMs,

$$\left\langle \hat{p}_i + \frac{1}{2} \sum_m \frac{mk_m e^{im(\hat{\theta}_i + \pi\alpha_i)}}{\sin(m\pi\alpha_i)} + \frac{1}{2} \sum_{mj} \frac{b_m^{ij} e^{im(\hat{\theta}_i - \hat{\theta}_j)}}{\pi(\alpha_i - \alpha_j)} \right\rangle_{N+1} = \left\langle \hat{p}_i + \frac{1}{2} \sum_m \frac{mk_m e^{im(\hat{\theta}_i + \pi\alpha_i)}}{\sin(m\pi\alpha_i)} + \frac{1}{2} \sum_{mj} \frac{b_m^{ij} e^{im(\hat{\theta}_i - \hat{\theta}_j)}}{\pi(\alpha_i - \alpha_j)} \right\rangle_N \quad (4.20)$$

If we use the definition in Eq.(4.6) we get $\langle \hat{C}_l \rangle_{N+1} = \langle \hat{C}_l \rangle_N$, thereby proving that \hat{C}_l is an integral of motion.

4.5.3 Floquet Hamiltonian and quasienergy eigenstates

A special case of our model is when there are no resonances, namely, all IOMs associated with the momentum localization $\hat{C}_{1..d}$ are intact. In this case, of particular importance is the following combination of the integrals of motion

$$\hat{H}_F = \sum_i 2\pi\alpha_i \hat{C}_i. \quad (4.21)$$

Where \hat{H}_F is known as the Floquet Hamiltonian and is defined as,

$$e^{-iH_F} = e^{-i\hat{V}} e^{-i\hat{H}_0} = \hat{U}_F. \quad (4.22)$$

The quasienergy wave functions ψ_ω are simultaneous eigenstates of \hat{H}_F and \hat{C}_i 's.

The quasienergy- ω state centered around momenta $\langle \hat{p} \rangle = \vec{M}$ is

$$\psi_\omega(\vec{\theta}) = (2\pi)^{-N/2} \exp \left\{ i\vec{M} \cdot \vec{\theta} - \sum_{jm} \frac{k_m e^{im(\theta_j + \pi\alpha_j)}}{2\sin(m\pi\alpha_j)} - \sum_{ijm} \frac{b_m^{ij}}{4\pi m(\alpha_i - \alpha_j)} e^{im(\theta_i - \theta_j)} \right\}. \quad (4.23)$$

This satisfies $\hat{C}_i \psi_\omega = M_i \psi_\omega$. By writing $\hat{H}_F \psi_\omega = \omega \psi_\omega$ and using Eq. (4.21),

we see that the eigenvalue equation is satisfied when, $\omega = 2\pi \vec{\alpha} \cdot \vec{M} \pmod{2\pi}$.

We can also compute the momentum-momentum correlator, $\langle \hat{p}_i \hat{p}_j \rangle - \langle \hat{p}_i \rangle \langle \hat{p}_j \rangle$ for $i \neq j$ over quasienergy eigenstates. The correlator over this state follows as

$$\langle \hat{p}_i \hat{p}_j \rangle - \langle \hat{p}_i \rangle \langle \hat{p}_j \rangle = -\frac{1}{4} \sum_m \frac{|b_m^{ij}|^2}{\pi^2 (\alpha_i - \alpha_j)^2}. \quad (4.24)$$

In the case of a resonance $\alpha_i \rightarrow \alpha_j$, this correlator clearly diverges, while in the localized case it remains finite.

4.6 Experimental proposal

A natural venue for realizing the interacting kicked rotor model is superconducting grains. The Hamiltonian, Eq. (4.3) could be implemented using a chain of voltage-biased superconducting grains coupled to each other using Josephson junctions. Consider a chain of grains gated by a ground plane which resistively connected to ground (see, Fig. 4.2). We then supply a gate voltage V_i to each grain, and connect them to each other by Josephson junctions J_{ij} .

Because the voltage on the i -th grain is locked to be V_i , its phase winds with an angular velocity $\dot{\phi}_i = 2eV_i/\hbar$. Therefore, the resistance and gate capacitor can be ignored when writing the effective stationary part of the Hamiltonian:

$$H_0 = \sum_i q_i V_i - \sum_{ij} J_{ij} \cos(\phi_i - \phi_j). \quad (4.25)$$

In addition, the “kick” term is obtained by connecting each grain to a common macroscopic superconductor (which is itself grounded), for a short time and through a strong Josephson coupling.

$$V(t) = - \sum_{i,n} K(t - nT) \cos \phi_i, \quad (4.26)$$

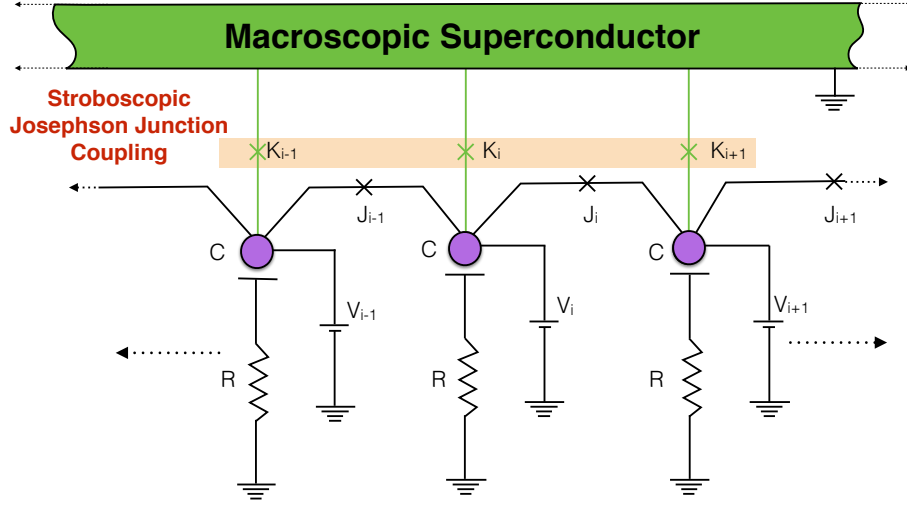


Figure 4.2: Schematic of chain of voltage-biased (V_i) superconducting grains coupled to each other (J_i) using Josephson junctions. Each grain is connected (K_i) to a grounded common macroscopic superconductor stroboscopically through a strong Josephson coupling.

with $K(t) = K$ when $|t| < \tau$. To make the kick term as close to a delta function as possible, we must have $2eV_i\tau \ll \hbar 2\pi$, and $K\tau \sim \hbar$, and $\tau \ll T$. A diagram of the circuit for a nearest-neighbor interaction is shown in Fig. 4.2. Identifying, $\phi_i = \theta_i$, $2\pi\alpha_i = 2eV_i/\hbar$ and $p_i = \hbar q_i/2e$ we see that we indeed obtain the Hamiltonian of Eq. (4.3).

4.7 Conclusions

In this work, we introduced the concept of *dynamical* many-body localization and presented an exactly-solvable model of driven linear rotors, which exhibits this phenomenon. Although the model possesses a full set of integrals of motion, it is shown that dynamical MBL is accompanied by the emergence of additional integrals

of motion, local in momentum space. We believe that this observation has important general implications for understanding dynamics of interacting many-body systems.

We have shown that these integrals of motion break down due to two types of resonances indicating delocalization in momentum space. One type of resonance originates from commensuration of the external driving period with the parameters of the system and the other from the static interactions. An interesting feature of this model is that the total energy in the system, that is linear in momenta, fails to be a good indicator of dynamical localization, since when momentum conserving interactions delocalize momentum, momenta of interacting pair grow in opposite directions.

Moreover, we have shown, by utilizing the lattice mapping introduced by Fishman and Grempel and Prange, that our model maps into a disordered lattice with as many dimensions as there are rotors. Based on this observation, we argue that what is observed is an Anderson type localization, particularly of the type seen in correlated disorder systems.

We also have proposed an experimental setup composed of Josephson junctions and superconducting grains to realize the model Hamiltonian.

Finally, we emphasize that the results presented here can apply to more generic non-integrable systems. For example, a recent work [142] considers interacting kicked Dirac particles with individual Hamiltonians, $H_0 = 2\pi\alpha\sigma_x p + M\sigma_z$, and provides a simple argument that this non-integrable system also exhibits MBL. First, this model also exhibits localization when α 's are generic distinct irrationals. Second, although the number of interacting particles that can be considered numer-

ically is limited, note that at large momenta the Dirac model crosses over to the linear model considered here. This suggests that MBL should be robust to a class of non-integrable generalizations, for any number of interacting rotors.

Chapter 5: Conclusions

Classical mechanics is built on assumptions that hold for macroscopic bodies, therefore, is applicable to a diverse set of phenomena that includes those that appear in anthropic scales, which makes the theory appealing to our intuition. For this very reason it historically precedes quantum mechanics that lies at the heart of our current understanding of nature.

Classical models have enormous utility for being well understood and intuitive. In this thesis we put forward three models for many-body quantum systems, solve them under certain assumptions and employ a classical analogy to help understand the underlying physics and/or make inference about a broader class of systems.

From a different perspective, these analogies contribute to resolve the problem of how classical dynamics emerge from quantum mechanics. Although the emergence of classical mechanics from quantum mechanics, commonly referred to as the classical limit, is controlled by a single parameter, the Planck constant, the qualitative picture the two theories paint is fundamentally different. The measurement problem, the failure of conventional quantization schemes for the gravitational field and the emergence of chaos from unitary quantum dynamics are all different cases of the ‘classical limit’ problem that plagues almost all fields of modern physics in

addition to rising foundational questions. All three of these issues are related to how we extract a set of observables (what we refer to as the ‘system’) from a very large number of interacting quantum degrees of freedom, a majority of which make up the ‘environment’ for the system. Therefore, the afore-mentioned issues can be considered in the context of the ‘quantum many-body problem’ as we argued in the introduction.

Below is a summary of the models considered in these thesis, the corresponding classical analogy, its advantages and/or its relation to a broader problem say of classicalization of particles/fields, emergence of spacetime or chaos.

In Part 2, we considered a quasi-one-dimensional superconductor. In the superconducting phase of matter, the complete many-body quantum field theory can be reduced to the solution of a PDE for the superconducting order parameter and the two-point function for the quasiparticles. This PDE parametrically depends on the disorder in the system. In the long wavelength limit, the appropriate Eilenberger equations of the system were solved. We discovered that this problem can be mapped to a one-dimensional classical particle moving in an external potential. In view of the recent interest in superconducting heterostructures, we studied the proximity effects in a normal segment, attached to a clean p -wave wire. We discovered that despite the presence of impurities, the proximity-induced superconducting correlations are long-range. We also found that impurity scattering leads to the appearance of a delocalized zero-energy peak that hints to the long sought zero-energy Majorana mode. The methods we employ can be applied to analyze a variety of situations with quasi one dimensional disordered superconductor and metal junctions,

which will form the building block of topological quantum computers.

In Part 3, we considered a strongly interacting Bose system. Similarly, the superfluid phase is described as a classical object: a perfect fluid. The environment is the gas of phonons which effect the background flow by applying stresses. This picture is called the two-fluid model. The phonons, possessing Lorentz symmetry, can be shown to travel on an emergent spacetime metric defined by the perfect fluid. With this observation we drew analogies between general relativity and the two-fluid system including stochastic effects due to the fluctuations of the phonon “matter” field. This gives an idea of how classical spacetime might emerge from quantum degrees of freedom in the low energy limit. Moreover, based on this analogy, we conjectured a lensing for a phonon wave packet due to stochastic fluctuations of the background fluid, similar to lensing of light rays due to a fluctuating metric field.

In Part 4 we considered the analogy between localization of electron states in a lattice and the quantum bounds to classical chaos, known as the Maryland model. To understand if the quantum suppression of chaos persists despite interactions, we introduced the concept of *dynamical* many-body localization and presented an exactly-solvable model of driven and interacting linear rotors, which exhibits this phenomenon. For each rotor, the rest of the rotors is the environment. The existence of dynamical MBL depends on whether the environment restores chaos or not. Although the model possesses a full set of integrals of motion, it is shown that dynamical MBL is accompanied by the emergence of additional integrals of motion, local in momentum space. In both cases the quantum evolution equations closely follow their classical counter parts. The additional integrals of motion break down

when interactions become resonant causing phase space diffusion or delocalization.

We also have proposed an experimental setup composed of Josephson junctions and superconducting grains to realize the model Hamiltonian. Finally, we emphasize that the results presented here can apply to more generic non-integrable systems. For example, a later work [\[142\]](#) considers interacting kicked Dirac particles with individual Hamiltonians, $H_0 = 2\pi\alpha\sigma_x p + M\sigma_z$, and provides a simple argument that this non-integrable system also exhibits MBL. This suggests that MBL should be robust to a class of non-integrable generalizations, for any number of interacting rotors.

Appendix A: Mapping between Quantum Kicked Rotor and the tight-binding model

In the first part of this section, we derive the known lattice mapping of the one dimensional kicked rotor [28]. Once we establish this derivation, we show that the many-body linear kicked rotor 4.3 also admits a lattice mapping of a particle on a d-dimensional lattice. We emphasize that existence of such a mapping in the many-body case is limited to the case of linear p model ($l = 1$).

A.1 Lattice model of single quantum kicked rotor

In the introduction we considered the time dependent Schrödinger equation for a kicked rotor. The kinetic part was considered to be \hat{p}^l . For the quadratic kicked rotor case $l = 2$ and the linear kicked rotor that we consider in this work is $l = 1$. Also $\hbar = 1$ and kicking period $T = 1$ are used in this equation.

$$\mathbf{i}\partial_t\psi(\theta, t) = [2\pi\alpha(-\mathbf{i}\partial_\theta)^l + K(\theta)\sum_n\delta(t-n)]\psi(\theta, t). \quad (\text{A.1})$$

The above equation can be solved for $\psi(\theta, t) = e^{-i\omega t}u(\theta, t)$, where the function u has the unit periodicity of the driving. Let u^\pm defines the state just before and after

the kick and are connected by the evolution operator in the following way,

$$u^+ = e^{-\mathbf{i}K(\theta)}u^-, \quad u^- = e^{\mathbf{i}(\omega - 2\pi\alpha\hat{p}^l)}u^+ \quad (\text{A.2})$$

Define the following: $\bar{u} = \frac{u^+ + u^-}{2}$, $\exp(-\mathbf{i}\hat{K}(\theta)) = (1 - \mathbf{i}\hat{W}(\theta))^{-1}(1 + \mathbf{i}\hat{W}(\theta))$, $\exp(-\mathbf{i}[2\pi\alpha\hat{p}^l - \omega]) = (1 - \mathbf{i}\hat{T}(\theta))^{-1}(1 + \mathbf{i}\hat{T}(\theta))$. Based on the above definitions, $u^\pm = (1 \mp \mathbf{i}\hat{T}(\theta))\bar{u}$ and

$$[\hat{T}(\theta) + \hat{W}(\theta)]\bar{u} = 0 \quad (\text{A.3})$$

is obtained.

Fourier transforming the above expression, we get the following tight binding model,

$$\sum_{n \neq m} W_{m-n} u_n + T_m u_m = E u_m. \quad (\text{A.4})$$

Here, the energies and hoppings are:

$$W_{m-n} = -E\delta_{m,n} - \quad (\text{A.5a})$$

$$\frac{1}{2\pi} \int_0^{2\pi} e^{-\mathbf{i}(m-n)\theta} \left\{ \tan \left(\frac{K(\theta)}{2} \right) \right\} d\theta,$$

$$T_m = \tan \left(\frac{1}{2} [\omega - 2\pi\alpha m^l] \right). \quad (\text{A.5b})$$

This completes the derivation for the lattice mapping for the single rotor case. In the following section, we generalize this derivation to demonstrate the existence of a lattice mapping for the interacting rotor model of Eq. (4.3).

A.2 d -dimensional lattice model

In this section we show that there exists a d - dimensional lattice model corresponding to the d particle interacting version of the kicked rotor model in Eq. (4.3).

Such a mapping has been previously identified for the case of a d rotors driven by an interaction potential [131]. Notice that in our case, the interactions are encoded in the static Hamiltonian \hat{H}_0 . However, we show that for the linear momentum dependence of the kinetic term, static interactions can be expressed as the driven interactions and the rest of the lattice mapping simply follows from Ref. ([131]). In order to establish this mapping, we use the factorization of the Floquet operator discussed in Section. (4.5). The time dependent Hamiltonian in Eq. (4.3) produces the same Floquet operator as,

$$\hat{H}(t) = 2\pi \sum_{i=1}^d \alpha_i \hat{p}_i + \hat{V}^F \sum_{n=-\infty}^{\infty} \delta(t - n), \quad (\text{A.6})$$

where we have defined,

$$\hat{V}^F = \sum_{i=1}^d K(\hat{\theta}_i) + \frac{1}{2} \sum_{i \neq j} \tilde{J}_{ij}(\hat{\theta}_i - \hat{\theta}_j) \quad (\text{A.7})$$

$$= \sum_{j=1}^d \sum_m k_m e^{im\hat{\theta}_j} + \frac{1}{2} \sum_{i \neq j} \sum_m \tilde{b}_m^{ij} e^{im(\hat{\theta}_i - \hat{\theta}_j)}. \quad (\text{A.8})$$

The factorization enables to treat on site and interaction potentials on equal footing.

The \tilde{b}^{ij} is defined in Eq. (4.8). Moreover, we write:

$$\hat{V}^F = \sum_{\vec{m}} V_{\vec{m}}^F e^{i\vec{m} \cdot \vec{\theta}}. \quad (\text{A.9})$$

Here, \vec{m} is a d -dimensional vector characterized by the integer m . The components of the potential $V_{\vec{m}}^F$ are as follows. For fixed i and j , for vectors \vec{m} parallel to a coordinate axis, i.e. $m_l = m\delta_{lj}$, $V_{\vec{m}}^F$ takes the value k_m . For vectors \vec{m} such that $m_l = m(\delta_{li} - \delta_{lj})$, $V_{\vec{m}}^F$ takes the value $\tilde{b}_m^{ij}/2$. For any other vector, $V_{\vec{m}}^F$ vanishes. Treating α 's and p 's as d -dimensional vectors as well, the Hamiltonian can be succinctly as:

$$\hat{H}(t) = 2\pi\vec{\alpha} \cdot \hat{\vec{p}} + \sum_{\vec{m}} V_{\vec{m}} e^{i\vec{m} \cdot \hat{\vec{\theta}}} \sum_{n=-\infty}^{\infty} \delta(t - n). \quad (\text{A.10})$$

Following Ref. ([131]), the above driven Hamiltonian can be mapped on to a d -dimensional lattice model, which is closely related to the lattice mapping outlined in the previous section for the single rotor case.

$$H_{\vec{m},\vec{n}} u_{\vec{n}} = T_{\vec{m}} u_{\vec{m}} + \sum_{\vec{n}} W_{\vec{m},\vec{n}} u_{\vec{n}} = E u_{\vec{m}}. \quad (\text{A.11})$$

Here, \vec{m} and \vec{n} are vectors that contain integers that correspond to the quantized eigenvalues of the angular momentum operator. The hopping and onsite terms are defined as,

$$W_{\vec{m}-\vec{n}} = -E\delta_{\vec{m},\vec{n}} + \frac{1}{(2\pi)^d} \int_0^{2\pi} e^{-i(\vec{m}-\vec{n}) \cdot \vec{\theta}} \left\{ -\tan\left(\frac{V^F(\vec{\theta})}{2}\right) \right\} d\vec{\theta}, \quad (\text{A.12a})$$

$$T_{\vec{m}} = \tan\left(\frac{1}{2}[\omega - 2\pi\vec{\alpha} \cdot \vec{m}]\right). \quad (\text{A.12b})$$

Here, we defined $E = -(1/[2\pi]^d) \int \tan(V^F(\vec{\theta})/2)$ so as to make $W_0 = 0$.

Appendix B: Derivation of the canonical conservation law

Here we derive the canonical conservation laws in Part 3, by using the covariant conservation law and the equations of motion for the two-fluid system. The Christoffel symbols are

$$\Gamma^\mu_{\nu\alpha} = \frac{1}{2}g^{\mu\beta} (g_{\beta\nu,\alpha} + g_{\beta\alpha,\nu} - g_{\nu\alpha,\beta}), \quad (\text{B.1})$$

where the comma notation means

$$g_{\beta\nu,\alpha} \equiv \frac{\partial}{\partial x^\alpha} g_{\beta\nu}.$$

For a symmetric tensor T^μ_θ , with the application of chain rule, we have

$$T^\mu_\theta \Gamma^\theta_{\mu\nu} = -\frac{1}{2}T_{\gamma\theta} (g^{\gamma\mu}_{,\nu} \delta^\theta_\mu + g^{\gamma\mu}_{,\mu} \delta^\theta_\nu - g^{\theta\mu}_{,\mu} \delta^\gamma_\nu) = -\frac{1}{2}T_{\gamma\theta} (g^{\gamma\mu}_{,\nu} \delta^\theta_\mu) = -\frac{1}{2}T_{\gamma\mu} g^{\gamma\mu}_{,\nu}. \quad (\text{B.2})$$

Similarly, we have

$$\Gamma^\mu_{\nu\mu} = \frac{1}{2}g^{\mu\beta} (g_{\beta\nu,\mu} + g_{\beta\mu,\nu} - g_{\nu\mu,\beta}) = \frac{1}{2}g^{\mu\beta} g_{\beta\mu,\nu} = \frac{1}{2g} g_{,\nu} = \partial_\nu \log \sqrt{-g}. \quad (\text{B.3})$$

Using Eq. (B.2) and Eq. (B.3) and relabeling dummy indices as required, we write the covariant conservation law Eq. (3.49) in the main text as Eq. (3.50).

Now, by using Eq. (3.52) and Eq. (3.53), the covariant conservation law Eq. (3.50) can be recast in the Noether current form that appears in Eq. (3.55) as follows.

$$\sqrt{-g}\nabla_\mu T^\mu{}_\nu = \left(\frac{\partial \mathcal{L}_{ph}}{\partial \phi_{,\mu}} \phi_{,\nu} - \mathcal{L}_{ph} \delta^\mu{}_\nu \right)_{,\mu} + \frac{\partial \mathcal{L}_{ph}}{\partial \theta_{,\mu}} \theta_{,\mu\nu} + \frac{\partial \mathcal{L}_{ph}}{\partial \rho} \rho_{,\nu} = 0. \quad (\text{B.4})$$

Using the Euler-Lagrange equation (classical limit of Eq. (3.48a))

$$\frac{\partial(\mathcal{L}_{ph} + \mathcal{L}_{cl})}{\partial \rho} = \left(\frac{\partial(\mathcal{L}_{ph} + \mathcal{L}_{cl})}{\partial \rho_{,\mu}} \right)_{,\mu} = 0,$$

and using the chain rule

$$\partial_\nu \mathcal{L}_{cl} = \frac{\partial \mathcal{L}_{cl}}{\partial \rho} \partial_\nu \rho + \frac{\partial \mathcal{L}_{cl}}{\partial \theta_{,\mu}} \theta_{,\mu\nu},$$

the covariant derivative in Eq. (B.4) becomes

$$\sqrt{-g}\nabla_\mu T^\mu{}_\nu = \left(\frac{\partial \mathcal{L}_{ph}}{\partial \phi_{,\mu}} \phi_{,\nu} - \mathcal{L}_{ph} \delta^\mu{}_\nu \right)_{,\mu} + \frac{\partial(\mathcal{L}_{ph} + \mathcal{L}_{cl})}{\partial \theta_{,\mu}} \theta_{,\mu\nu} - \partial_\mu \mathcal{L}_{cl} \delta^\mu{}_\nu = 0. \quad (\text{B.5})$$

Now using, the second Euler-Lagrange equation (classical limit of Eq. (3.48b)),

$$\left(\frac{\partial(\mathcal{L}_{ph} + \mathcal{L}_{cl})}{\partial \theta_{,\mu}} \right)_{,\mu} = \frac{\partial(\mathcal{L}_{ph} + \mathcal{L}_{cl})}{\partial \theta} = 0.$$

the Eq. (B.5) reduces to

$$\sqrt{-g}\nabla_\mu T^\mu{}_\nu = \left(\frac{\partial \mathcal{L}_{ph}}{\partial \phi_{,\mu}} \phi_{,\nu} - (\mathcal{L}_{cl} + \mathcal{L}_{ph}) \delta^\mu{}_\nu \right)_{,\mu} + \left(\frac{\partial(\mathcal{L}_{ph} + \mathcal{L}_{cl})}{\partial \theta_{,\mu}} \theta_{,\nu} \right)_{,\mu} = 0. \quad (\text{B.6})$$

The total derivative on the right hand side can be written as the divergence of the Noether current Eq. (3.55).

Appendix C: Noise and response kernels

Here, we write the first and second order variations of the effective phonon action in Part 3 as tensors and bi-tensor kernels. For example consider the second order variations of the phonon effective action with respect to the forward metric:

$$\begin{aligned} \frac{\delta^2 \Gamma_{ph}}{\delta(g^+)^{\mu\nu}(x)\delta(g^+)^{\alpha\beta}(y)} \Big|_{g^+=g^-} = \\ \frac{-i}{4} \sqrt{-g(x)} \langle \hat{T}_{\mu\nu}(x) \rangle \sqrt{-g(y)} \langle \hat{T}_{\mu\nu}(y) \rangle - i \frac{\delta^2 Z_{ph}}{\delta(g^+)^{\mu\nu}(x)\delta(g^+)^{\alpha\beta}(y)} \Big|_{g^+=g^-}. \end{aligned} \quad (\text{C.1})$$

In the last part we used the unitarity of the partition function in Eq. (3.40).

The second order variation of the phonon partition function contains the expectation value of a product of stress-energy operators.

$$\begin{aligned} \frac{\delta^2 Z_{ph}}{\delta(g^+)^{\mu\nu}(x)\delta(g^+)^{\alpha\beta}(y)} \Big|_{g^+=g^-} = \\ -\frac{1}{4} \sqrt{-g(x)} \sqrt{-g(y)} \langle \mathbb{T}^* \left\{ \hat{T}_{\mu\nu}(x) \hat{T}_{\alpha\beta}(y) \right\} \rangle + i \left\langle \frac{\delta^2 S_{ph}[\hat{\phi}]}{\delta g^{\mu\nu}(x) \delta g^{\alpha\beta}(y)} \right\rangle. \end{aligned} \quad (\text{C.2})$$

Here, the Weyl or \mathbb{T}^* ordered average of the product of stress operators is understood in the following way. The stress-energy operator contains terms quadratic in the field and its derivatives. It can be regularized by using the point splitting method [104, 113]. In this regularization scheme, to take an average as in Eq. (C.2), one first

writes the quadratic operator average as

$$\lim_{x', x'' \rightarrow x} \left\langle \mathbb{T}^* \left\{ \partial_\mu \hat{\phi}(x') \partial_\nu \hat{\phi}(x'') \right\} \right\rangle = \lim_{x', x'' \rightarrow x} \frac{\partial}{\partial x'^\mu} \frac{\partial}{\partial x''^\nu} \left\langle \mathbb{T} \left\{ \hat{\phi}(x') \hat{\phi}(x'') \right\} \right\rangle. \quad (\text{C.3})$$

Then, the time ordered operator average is computed and renormalized by subtracting the divergent terms. Lastly, the operators are acted on the result and the coincidence limit is taken.

Weyl ordering inherits all properties of time or path ordering, for example it is possible to rewrite the Weyl ordered average as

$$\begin{aligned} 2 \left\langle \mathbb{T}^* \left\{ \hat{T}_{\mu\nu}(x) \hat{T}_{\alpha\beta}(y) \right\} \right\rangle &= \left\langle \left\{ \hat{T}_{\mu\nu}(x), \hat{T}_{\alpha\beta}(y) \right\} \right\rangle \\ &+ \left\langle \mathbb{T}^* \left\{ \hat{T}_{\mu\nu}(x) \hat{T}_{\alpha\beta}(y) \right\} \right\rangle - \left\langle \tilde{\mathbb{T}}^* \left\{ \hat{T}_{\mu\nu}(x) \hat{T}_{\alpha\beta}(y) \right\} \right\rangle. \end{aligned} \quad (\text{C.4})$$

Here, $\{, \}$ is the anti-commutator and $\tilde{\mathbb{T}}$ is the reverse Weyl ordering computed by reversing the time ordering in Eq. (C.3). Using Eq. (3.41), we can decompose the Weyl ordered average into its real and imaginary parts

$$\left\langle \mathbb{T}^* \left\{ \hat{T}_{\mu\nu}(x) \hat{T}_{\alpha\beta}(y) \right\} \right\rangle = \frac{1}{2} \left\langle \left\{ \hat{T}_{\mu\nu}(x), \hat{T}_{\alpha\beta}(y) \right\} \right\rangle + i \mathbf{Im} \left\langle \mathbb{T}^* \left\{ \hat{T}_{\mu\nu}(x) \hat{T}_{\alpha\beta}(y) \right\} \right\rangle. \quad (\text{C.5})$$

Following Martin and Verdaguer [116] we define the (bi-tensor) real kernels.

$$\hat{H}_{\mu\nu\alpha\beta}^S(x, y) = \mathbf{Im} \left\langle \mathbb{T}^* \left\{ \hat{T}_{\mu\nu}(x) \hat{T}_{\alpha\beta}(y) \right\} \right\rangle, \quad (\text{C.6a})$$

$$\hat{H}_{\mu\nu\alpha\beta}^A(x, y) = \frac{-i}{2} \left\langle \left[\hat{T}_{\mu\nu}(x), \hat{T}_{\alpha\beta}(y) \right] \right\rangle, \quad (\text{C.6b})$$

$$\hat{H}_{\mu\nu\alpha\beta}(x, y) = \hat{H}_{\mu\nu\alpha\beta}^A(x, y) + \hat{H}_{\mu\nu\alpha\beta}^S(x, y), \quad (\text{C.6c})$$

$$= -i\theta(x^0 - y^0) \left\langle \left[\hat{T}_{\mu\nu}(x), \hat{T}_{\alpha\beta}(y) \right] \right\rangle \quad (\text{C.6d})$$

$$\hat{N}_{\mu\nu\alpha\beta}(x, y) = \frac{1}{2} \langle \{ \hat{t}_{\mu\nu}(x), \hat{t}_{\alpha\beta}(y) \} \rangle, \quad (\text{C.7a})$$

$$\text{where } \hat{t}_{\mu\nu}(x) = \hat{T}_{\mu\nu}(x) - \langle \hat{T}_{\mu\nu}(x) \rangle, \quad (\text{C.7b})$$

$$\hat{K}_{\mu\nu\alpha\beta}(x, y) = \frac{-4}{\sqrt{-g(x)}\sqrt{-g(y)}} \left\langle \frac{\delta^2 S_{ph}[\hat{\phi}]}{\delta g^{\mu\nu}(x) \delta g^{\alpha\beta}(y)} \right\rangle. \quad (\text{C.7c})$$

The kernels H^S and H^A are the symmetric and anti-symmetric bi-tensor parts of H , i.e.

$$H_{\mu\nu\alpha\beta}^{S,A}(x, y) = \pm H_{\alpha\beta\mu\nu}^{S,A}(y, x). \quad (\text{C.8})$$

With these, the second order variational derivative of the effective action on the forward branch reads

$$\frac{4}{\sqrt{-g(x)}\sqrt{-g(y)}} \frac{\delta^2 \Gamma_{ph}}{\delta (g^+)^{\mu\nu}(x) \delta (g^+)^{\alpha\beta}(y)} \Big|_{g^+=g^-} = i\hat{N}_{\mu\nu\alpha\beta}(x, y) - \hat{H}_{\mu\nu\alpha\beta}^S(x, y) - \hat{K}_{\mu\nu\alpha\beta}(x, y). \quad (\text{C.9})$$

Similarly, the second order variation with respect to the other combinations of the forward and backward values of the metric are

$$\frac{4}{\sqrt{-g(x)}\sqrt{-g(y)}} \frac{\delta^2 \Gamma_{ph}}{\delta (g^+)^{\mu\nu}(x) \delta (g^-)^{\alpha\beta}(y)} \Big|_{g^+=g^-} = -i\hat{N}_{\mu\nu\alpha\beta}(x, y) - \hat{H}_{\mu\nu\alpha\beta}^A(x, y), \quad (\text{C.10})$$

$$\frac{4}{\sqrt{-g(x)}\sqrt{-g(y)}} \frac{\delta^2 \Gamma_{ph}}{\delta (g^-)^{\mu\nu}(x) \delta (g^+)^{\alpha\beta}(y)} \Big|_{g^+=g^-} = -i\hat{N}_{\mu\nu\alpha\beta}(x, y) + \hat{H}_{\mu\nu\alpha\beta}^A(x, y), \quad (\text{C.11})$$

$$\frac{4}{\sqrt{-g(x)}\sqrt{-g(y)}} \frac{\delta^2 \Gamma_{ph}}{\delta (g^-)^{\mu\nu}(x) \delta (g^-)^{\alpha\beta}(y)} \Big|_{g^+=g^-} = i\hat{N}_{\mu\nu\alpha\beta}(x, y) + \hat{H}_{\mu\nu\alpha\beta}^S(x, y) + \hat{K}_{\mu\nu\alpha\beta}(x, y). \quad (\text{C.12})$$

The Eq. (3.90) is a compact way to write the above second order variations Eqs. (C.9)–(C.12).

Bibliography

- [1] K. Vogtman, A. Weinstein, and V.I. Arnol'd. *Mathematical Methods of Classical Mechanics*. Graduate Texts in Mathematics. Springer New York, 1997.
- [2] H. Goldstein, C.P. Poole, and J.L. Safko. *Classical Mechanics*. Addison Wesley, 2002.
- [3] R.M. Wald. *General Relativity*. University of Chicago Press, 2010.
- [4] B. Schutz. *A First Course in General Relativity*. Cambridge University Press, 2009.
- [5] R.K. Pathria and P.D. Beale. *Statistical Mechanics*. Elsevier Science, 1996.
- [6] R. Kubo. *Thermodynamics: An advanced course with problems and solutions*. North-Holland Pub. Co., 1976.
- [7] J.A. Wheeler and W.H. Zurek. *Quantum Theory and Measurement*. Princeton Legacy Library. Princeton University Press, 1983.
- [8] Wojciech Hubert Zurek. Decoherence, einselection, and the quantum origins of the classical. *Rev. Mod. Phys.*, 75:715–775, May 2003.
- [9] R.P. Feynman and A.R. Hibbs. *Quantum mechanics and path integrals*. International series in pure and applied physics. McGraw-Hill, 1965.
- [10] D.J. Griffiths. *Introduction to Quantum Mechanics*. Cambridge University Press, 2016.
- [11] P. A. M. Dirac. On the analogy between classical and quantum mechanics. *Rev. Mod. Phys.*, 17:195–199, Apr 1945.
- [12] George A. Baker. Formulation of quantum mechanics based on the quasi-probability distribution induced on phase space. *Phys. Rev.*, 109:2198–2206, Mar 1958.

- [13] John D. Trimmer. The present situation in quantum mechanics: A translation of schrödinger's "cat paradox" paper. *Proceedings of the American Philosophical Society*, 124(5):323–338, 1980.
- [14] Maximilian Schlosshauer. Decoherence, the measurement problem, and interpretations of quantum mechanics. *Rev. Mod. Phys.*, 76:1267–1305, Feb 2005.
- [15] A. Altland and B. Simons. *Condensed Matter Field Theory*. Cambridge University Press, 2006.
- [16] J. Sethna. *Statistical Mechanics: Entropy, Order Parameters and Complexity*. Oxford Master Series in Physics. OUP, 2006.
- [17] A.J. Leggett. *Quantum Liquids: Bose Condensation and Cooper Pairing in Condensed-matter Systems*. Oxford Graduate Texts. OUP, 2006.
- [18] N.B. Kopnin. *Theory of Nonequilibrium Superconductivity*. International Series of Monographs on Physics. Clarendon Press, 2001.
- [19] M.V Berry. Semiclassical mechanics of regular and irregular motion. In G. Iooss, R. H. G. Helleman, and R. Stora, editors, *Les Houches Lecture Series*, volume 36, pages 171–271. North Holland, 1983.
- [20] Michael Berry. Quantum chaology, not quantum chaos. *Physica Scripta*, 40(3):335, 1989.
- [21] M.V Berry, N.L Balazs, M Tabor, and A Voros. Quantum maps. *Annals of Physics*, 122(1):26 – 63, 1979.
- [22] Juan Maldacena, Stephen H. Shenker, and Douglas Stanford. A bound on chaos. *Journal of High Energy Physics*, 2016(8):106, 2016.
- [23] E. Ott. *Chaos in Dynamical Systems*. Cambridge University Press, 2002.
- [24] M.V Berry. Chaos and the semiclassical limit of quantum mechanics (is the moon there when somebody looks?). In R. J. Russell, P. Clayton, K. Wegter-McNelly, and J. Polkinghorne, editors, *Quantum mechanics: Scientific perspectives on Divine Action*, pages 41–54. CTNS Publications, 2001.
- [25] Shmuel Fishman, D. R. Grempel, and R. E. Prange. Chaos, quantum recurrences, and Anderson localization. *Phys. Rev. Lett.*, 49:509–512, Aug 1982.
- [26] C. Tian, A. Kamenev, and A. Larkin. Weak dynamical localization in periodically kicked cold atomic gases. *Phys. Rev. Lett.*, 93:124101, Sep 2004.
- [27] D. R. Grempel, Shmuel Fishman, and R. E. Prange. Localization in an incommensurate potential: An exactly solvable model. *Phys. Rev. Lett.*, 49:833–836, Sep 1982.

- [28] R. E. Prange, D. R. Grempel, and Shmuel Fishman. Solvable model of quantum motion in an incommensurate potential. *Phys. Rev. B*, 29:6500–6512, Jun 1984.
- [29] Mark Srednicki. Chaos and quantum thermalization. *Phys. Rev. E*, 50:888–901, Aug 1994.
- [30] Luca D’Alessio, Yariv Kafri, Anatoli Polkovnikov, and Marcos Rigol. From quantum chaos and eigenstate thermalization to statistical mechanics and thermodynamics. *Advances in Physics*, 65(3):239–362, 2016.
- [31] J. M. Deutsch. Quantum statistical mechanics in a closed system. *Phys. Rev. A*, 43:2046–2049, Feb 1991.
- [32] D.M. Basko, I.L. Aleiner, and B.L. Altshuler. Metal insulator transition in a weakly interacting many-electron system with localized single-particle states. *Annals of Physics*, 321(5):1126 – 1205, 2006.
- [33] Vadim Oganesyan and David A Huse. Localization of interacting fermions at high temperature. *Physical Review B*, 75(15):155111, 2007.
- [34] Arijeet Pal and David A Huse. Many-body localization phase transition. *Physical Review B*, 82(17):174411, 2010.
- [35] Jens H. Bardarson, Frank Pollmann, and Joel E. Moore. Unbounded growth of entanglement in models of many-body localization. *Phys. Rev. Lett.*, 109:017202, Jul 2012.
- [36] Shankar Iyer, Vadim Oganesyan, Gil Refael, and David A. Huse. Many-body localization in a quasiperiodic system. *Phys. Rev. B*, 87:134202, Apr 2013.
- [37] Bela Bauer and Chetan Nayak. Area laws in a many-body localized state and its implications for topological order. *Journal of Statistical Mechanics: Theory and Experiment*, 2013(09):P09005, 2013.
- [38] Bela Bauer and Chetan Nayak. Analyzing many-body localization with a quantum computer. *Physical Review X*, 4(4):041021, 2014.
- [39] John Z Imbrie. On many-body localization for quantum spin chains. *arXiv preprint arXiv:1403.7837*, 2014.
- [40] Anushya Chandran, Isaac H. Kim, Guifre Vidal, and Dmitry A. Abanin. Constructing local integrals of motion in the many-body localized phase. *Phys. Rev. B*, 91:085425, Feb 2015.
- [41] MV Berry. Incommensurability in an exactly-soluble quantal and classical model for a kicked rotator. *Physica D: Nonlinear Phenomena*, 10(3):369–378, 1984.

- [42] Gerard 't Hooft. A mathematical theory for deterministic quantum mechanics. *Journal of Physics: Conference Series*, 67(1):012015, 2007.
- [43] L.P. Kadanoff, G. Baym, and D. Pines. *Quantum Statistical Mechanics*. Advanced Books Classics Series. Perseus Books, 1994.
- [44] L.V. Keldysh. Diagram technique for nonequilibrium processes. *JETP*, 20(4):1018, 1965.
- [45] O.V. Konstantinov and V.I. Perel'. A diagram technique for evaluating transport quantities. *JETP*, 12(1):142, 1961.
- [46] Julian Schwinger. Brownian motion of a quantum oscillator. *Journal of Mathematical Physics*, 2(3):407–432, 1961.
- [47] A. Kamenev. *Field Theory of Non-Equilibrium Systems*. Cambridge University Press, 2011.
- [48] E. Calzetta and B. L. Hu. Closed-time-path functional formalism in curved spacetime: Application to cosmological back-reaction problems. *Phys. Rev. D*, 35:495–509, Jan 1987.
- [49] B L Hu and E Verdaguer. Stochastic gravity: a primer with applications. *Classical and Quantum Gravity*, 20(6):R1, 2003.
- [50] J. Rammer and H. Smith. Quantum field-theoretical methods in transport theory of metals. *Rev. Mod. Phys.*, 58:323–359, Apr 1986.
- [51] Liang Fu and C. L. Kane. Superconducting proximity effect and majorana fermions at the surface of a topological insulator. *Phys. Rev. Lett.*, 100:096407, Mar 2008.
- [52] Jay D. Sau, Roman M. Lutchyn, Sumanta Tewari, and S. Das Sarma. Generic new platform for topological quantum computation using semiconductor heterostructures. *Phys. Rev. Lett.*, 104:040502, Jan 2010.
- [53] Roman M. Lutchyn, Jay D. Sau, and S. Das Sarma. Majorana fermions and a topological phase transition in semiconductor-superconductor heterostructures. *Phys. Rev. Lett.*, 105:077001, Aug 2010.
- [54] Jason Alicea. Majorana fermions in a tunable semiconductor device. *Phys. Rev. B*, 81:125318, Mar 2010.
- [55] Yuval Oreg, Gil Refael, and Felix von Oppen. Helical liquids and majorana bound states in quantum wires. *Phys. Rev. Lett.*, 105:177002, Oct 2010.
- [56] M. Wimmer, A. R. Akhmerov, M. V. Medvedyeva, J. Tworzydło, and C. W. J. Beenakker. Majorana bound states without vortices in topological superconductors with electrostatic defects. *Phys. Rev. Lett.*, 105:046803, Jul 2010.

- [57] V. Mourik, K. Zuo, S. M. Frolov, S. R. Plissard, E. P. A. M. Bakkers, and L. P. Kouwenhoven. Signatures of majorana fermions in hybrid superconductor-semiconductor nanowire devices. *Science*, 336(6084):1003–1007, 2012.
- [58] M. T. Deng, C. L. Yu, G. Y. Huang, M. Larsson, P. Caroff, and H. Q. Xu. Anomalous zero-bias conductance peak in a nbinsb nanowirenb hybrid device. *Nano Letters*, 12(12):6414–6419, 2012. PMID: 23181691.
- [59] Anindya Das, Yuval Ronen, Yonatan Most, Yuval Oreg, Moty Heiblum, and Hadas Shtrikman. Zero-bias peaks and splitting in an al-inas nanowire topological superconductor as a signature of majorana fermions. *Nat Phys*, 8(12):887–895, 2012.
- [60] Piet W. Brouwer, Mathias Duckheim, Alessandro Romito, and Felix von Oppen. Topological superconducting phases in disordered quantum wires with strong spin-orbit coupling. *Phys. Rev. B*, 84:144526, Oct 2011.
- [61] A. R. Akhmerov, J. P. Dahlhaus, F. Hassler, M. Wimmer, and C. W. J. Beenakker. Quantized conductance at the majorana phase transition in a disordered superconducting wire. *Phys. Rev. Lett.*, 106:057001, Jan 2011.
- [62] Wade DeGottardi, Diptiman Sen, and Smitha Vishveshwara. Topological phases, majorana modes and quench dynamics in a spin ladder system. *New Journal of Physics*, 13(6):065028, 2011.
- [63] Alejandro M. Lobos, Roman M. Lutchyn, and S. Das Sarma. Interplay of disorder and interaction in majorana quantum wires. *Phys. Rev. Lett.*, 109:146403, Oct 2012.
- [64] P.W. Anderson. Theory of dirty superconductors. *Journal of Physics and Chemistry of Solids*, 11(1):26 – 30, 1959.
- [65] Klaus D. Usadel. Generalized diffusion equation for superconducting alloys. *Phys. Rev. Lett.*, 25:507–509, Aug 1970.
- [66] F. S. Bergeret, A. F. Volkov, and K. B. Efetov. Odd triplet superconductivity and related phenomena in superconductor-ferromagnet structures. *Rev. Mod. Phys.*, 77:1321–1373, Nov 2005.
- [67] Gert Eilenberger. Transformation of gorkov’s equation for type ii superconductors into transport-like equations. *Zeitschrift für Physik A Hadrons and nuclei*, 214(2):195–213, 1968.
- [68] Patrick Neven, Dmitry Bagrets, and Alexander Altland. Quasiclassical theory of disordered multi-channel majorana quantum wires. *New Journal of Physics*, 15(5):055019, 2013.

- [69] Simon Abay, Daniel Persson, Henrik Nilsson, Fan Wu, H. Q. Xu, Mikael Fogelström, Vitaly Shumeiko, and Per Delsing. Charge transport in inas nanowire josephson junctions. *Phys. Rev. B*, 89:214508, Jun 2014.
- [70] Valentin Stanev and Victor Galitski. Quasiclassical eilenberger theory of the topological proximity effect in a superconducting nanowire. *Phys. Rev. B*, 89:174521, May 2014.
- [71] Hoi-Yin Hui, Jay D. Sau, and S. Das Sarma. Generalized eilenberger theory for majorana zero-mode-carrying disordered p -wave superconductors. *Phys. Rev. B*, 90:064516, Aug 2014.
- [72] Christopher R. Reeg and Dmitrii L. Maslov. Zero-energy bound state at the interface between an s -wave superconductor and a disordered normal metal with repulsive electron-electron interactions. *Phys. Rev. B*, 90:024502, Jul 2014.
- [73] F. S. Bergeret, A. F. Volkov, and K. B. Efetov. Local density of states in superconductor-strong ferromagnet structures. *Phys. Rev. B*, 65:134505, Mar 2002.
- [74] I. Baladié and A. Buzdin. Local quasiparticle density of states in ferromagnet/superconductor nanostructures. *Phys. Rev. B*, 64:224514, Nov 2001.
- [75] F. S. Bergeret, A. F. Volkov, and K. B. Efetov. Scattering by magnetic and spin-orbit impurities and the josephson current in superconductor-ferromagnet-superconductor junctions. *Phys. Rev. B*, 75:184510, May 2007.
- [76] A A Golubov, Y Tanaka, Y Asano, and Y Tanuma. Odd-frequency pairing in superconducting heterostructures. *Journal of Physics: Condensed Matter*, 21(16):164208, 2009.
- [77] Yukio Tanaka, Masatoshi Sato, and Naoto Nagaosa. Symmetry and topology in superconductors odd-frequency pairing and edge states. *Journal of the Physical Society of Japan*, 81(1):011013, 2012.
- [78] Masashige Matsumoto and Manfred Sigrist. Quasiparticle states near the surface and the domain wall in a $p_x + i p_y$ -wave superconductor. *Journal of the Physical Society of Japan*, 68(3):994–1007, 1999.
- [79] Masashige Masashige Matsumoto, Mikito Koga, and Hiroaki Kusunose. Emergent odd-frequency superconducting order parameter near boundaries in unconventional superconductors. *Journal of the Physical Society of Japan*, 82(3):034708, 2013.
- [80] A. V. Zaitsev. Quasiclassical equations of the theory of superconductivity for contiguous metals and the properties of constricted microcontacts. *JETP*, 59:1015, 1984.

- [81] Gerhard Kieselmann. Self-consistent calculations of the pair potential and the tunneling density of states in proximity contacts. *Phys. Rev. B*, 35:6762–6770, May 1987.
- [82] Alban L. Fauchère, Wolfgang Belzig, and Gianni Blatter. Paramagnetic instability at normal-metal–superconductor interfaces. *Phys. Rev. Lett.*, 82:3336–3339, Apr 1999.
- [83] W. Belzig, C. Bruder, and Gerd Schön. Local density of states in a dirty normal metal connected to a superconductor. *Phys. Rev. B*, 54:9443–9448, Oct 1996.
- [84] A. Jeffrey and D. Zwillinger. *Table of Integrals, Series, and Products*. Table of Integrals, Series, and Products Series. Elsevier Science, 2007.
- [85] A. D. Sakharov. Vacuum quantum fluctuations in curved space and the theory of gravitation. *General Relativity and Gravitation*, 32(2):365–367, 2000.
- [86] Matt Visser. Sakharov’s induced gravity: A modern perspective. *Modern Physics Letters A*, 17(15n17):977–991, 2002.
- [87] Carlos Barcel, Stefano Liberati, and Matt Visser. Analogue gravity. *Living Reviews in Relativity*, 14(3), 2011.
- [88] W. G. Unruh. Experimental black-hole evaporation? *Phys. Rev. Lett.*, 46:1351–1353, May 1981.
- [89] Michael Stone. Acoustic energy and momentum in a moving medium. *Phys. Rev. E*, 62:1341–1350, Jul 2000.
- [90] H. Kleinert. Gravity as a theory of defects in a crystal with only second gradient elasticity. *Annalen der Physik*, 499(2):117–119, 1987.
- [91] Mark Van Raamsdonk. Building up spacetime with quantum entanglement. *International Journal of Modern Physics D*, 19(14):2429–2435, 2010.
- [92] Carlos Barcel, Stefano Liberati, Sebastiano Sonego, and Matt Visser. Causal structure of analogue spacetimes. *New Journal of Physics*, 6(1):186, 2004.
- [93] G.E. Volovik. *The Universe in a Helium Droplet*. International Series of Monographs on Physics. OUP, 2009.
- [94] L. J. Garay, J. R. Anglin, J. I. Cirac, and P. Zoller. Sonic analog of gravitational black holes in bose-einstein condensates. *Phys. Rev. Lett.*, 85:4643–4647, Nov 2000.
- [95] Jeff Steinhauer. Observation of quantum hawking radiation and its entanglement in an analogue black hole. *Nat Phys*, August 2016.

- [96] G.E. Volovik. Superfluid analogies of cosmological phenomena. *Physics Reports*, 351(4):195 – 348, 2001.
- [97] L.D. Landau and E.M. Lifshitz. *Fluid Mechanics*, volume 6. Elsevier Science, 1987.
- [98] I.M. Khalatnikov. *An Introduction to the Theory of Superfluidity*. Advanced Books Classics Series. Advanced Book Program, Perseus Pub., 2000.
- [99] L. P. Kadanoff and P. C. Martin. Hydrodynamic equations and correlation functions. *Annals of Physics*, 24:419–469, October 1963.
- [100] Christopher P. Herzog. The hydrodynamics of m-theory. *Journal of High Energy Physics*, 2002(12):026, 2002.
- [101] P. K. Kovtun, D. T. Son, and A. O. Starinets. Viscosity in strongly interacting quantum field theories from black hole physics. *Phys. Rev. Lett.*, 94:111601, Mar 2005.
- [102] Giuseppe Policastro, Dam T. Son, and Andrei O. Starinets. From ads/cft correspondence to hydrodynamics. *Journal of High Energy Physics*, 2002(09):043, 2002.
- [103] U. Weiss. *Quantum Dissipative Systems*. Series in modern condensed matter physics. World Scientific, 2008.
- [104] Rosario Martin and Enric Verdaguer. Stochastic semiclassical gravity. *Phys. Rev. D*, 60:084008, Sep 1999.
- [105] E. Madelung. Quantentheorie in hydrodynamischer form. *Zeitschrift für Physik*, 40(3):322–326, 1927.
- [106] M.E. Peskin and D.V. Schroeder. *An Introduction to Quantum Field Theory*. Advanced book classics. Addison-Wesley Publishing Company, 1995.
- [107] L. F. Abbott. Introduction to the background field method. *Acta Physica Polonica B*, 13(1):33, January 1982.
- [108] D. J. Toms. Functional measure for quantum field theory in curved spacetime. *Phys. Rev. D*, 35:3796–3803, Jun 1987.
- [109] S. W. Hawking. Zeta function regularization of path integrals in curved spacetime. *Comm. Math. Phys.*, 55(2):133–148, 1977.
- [110] J. Horský and J. Novotný. Conservation laws in general relativity. *Czechoslovak Journal of Physics B*, 19(4):419–442, 1969.
- [111] L.D. Landau and E.M. Lifshitz. *The Classical Theory of Fields*. Course of theoretical physics. Butterworth-Heinemann, 1975.

- [112] Roberto Balbinot, Serena Fagnocchi, Alessandro Fabbri, and Giovanni P. Propio. Backreaction in acoustic black holes. *Phys. Rev. Lett.*, 94:161302, Apr 2005.
- [113] N.D. Birrell and P.C.W. Davies. *Quantum Fields in Curved Space*. Cambridge Monographs on Mathematical Physics. Cambridge University Press, 1984.
- [114] D. S. Petrov. Quantum mechanical stabilization of a collapsing bose-bose mixture. *Phys. Rev. Lett.*, 115:155302, Oct 2015.
- [115] L. Chomaz, S. Baier, D. Petter, M. J. Mark, F. Wächtler, L. Santos, and F. Ferlaino. Quantum-fluctuation-driven crossover from a dilute bose-einstein condensate to a macrodroplet in a dipolar quantum fluid. *Phys. Rev. X*, 6:041039, Nov 2016.
- [116] Rosario Martin and Enric Verdaguer. On the semiclassical einstein-langevin equation. *Physics Letters B*, 465(14):113 – 118, 1999.
- [117] Bryce S. DeWitt. Quantum field theory in curved spacetime. *Physics Reports*, 19(6):295 – 357, 1975.
- [118] Jean Macher and Renaud Parentani. Black-hole radiation in bose-einstein condensates. *Phys. Rev. A*, 80:043601, Oct 2009.
- [119] Nicholas G. Phillips and B. L. Hu. Noise kernel in stochastic gravity and stress energy bitensor of quantum fields in curved spacetimes. *Phys. Rev. D*, 63:104001, Apr 2001.
- [120] A. Eftekharzadeh, Jason D. Bates, Albert Roura, Paul R. Anderson, and B. L. Hu. Noise kernel for a quantum field in schwarzschild spacetime under the gaussian approximation. *Phys. Rev. D*, 85:044037, Feb 2012.
- [121] G.E. Volovik. From quantum hydrodynamics to quantum gravity. In R.T. Jantzen H. Kleinert and R. Ruffini, editors, *Analog Models of and for General Relativity*, pages 1404–1423. World Scientific, 2008.
- [122] F. R. Klinkhamer and G. E. Volovik. Brane realization of q-theory and the cosmological constant problem. *JETP Letters*, 103(10):627–630, 2016.
- [123] V. V. Zavjalov, S. Autti, V. B. Eltsov, P. J. Heikkinen, and G. E. Volovik. Light higgs channel of the resonant decay of magnon condensate in superfluid *3he-b*. *Nature Communications*, 7:10294, 2016.
- [124] G. E. Volovik. Black hole and hawking radiation by type-ii weyl fermions. *JETP Letters*, pages 1–4, 2016.
- [125] A.Z. Petrov. *Einstein Spaces*. Elsevier Science, 2016.
- [126] Y. B. Zel’dovich. Observations in a Universe Homogeneous in the Mean. *Astron. Zh.*, 41:19, 1964.

- [127] D. Sokoloff and E. A. Illarionov. Intermittency and random matrices. *Journal of Plasma Physics*, 81(4):395810402, August 2015.
- [128] Ehud Altman and Ronen Vosk. Universal dynamics and renormalization in many-body-localized systems. *Annual Review of Condensed Matter Physics*, 6(1):383–409, 2015.
- [129] David Huse and Rahul Nandkishore. Many-body localization and thermalization in quantum statistical mechanics. *Annual Review of Condensed Matter Physics*, 6(1), 2015.
- [130] Alexander Altland and Martin R Zirnbauer. Field theory of the quantum kicked rotor. *Phys. Rev. Lett.*, 77(22):4536, 1996.
- [131] Shmuel Fishman, D. R. Grempel, and R. E. Prange. Localization in a d-dimensional incommensurate structure. *Phys. Rev. B*, 29(8):4272, 1984.
- [132] Barry Simon. Almost periodic schrödinger operators iv. the maryland model. *Annals of Physics*, 159(1):157 – 183, 1985.
- [133] G I Watson. Spectrum and bandwidth of an exactly soluble incommensurate model. *Journal of Physics A: Mathematical and General*, 25(2):345, 1992.
- [134] Achilleas Lazarides, Arnab Das, and Roderich Moessner. Fate of many-body localization under periodic driving. *Phys. Rev. Lett.*, 115:030402, Jul 2015.
- [135] Pedro Ponte, Z. Papić, François Huveneers, and Dmitry A. Abanin. Many-body localization in periodically driven systems. *Phys. Rev. Lett.*, 114:140401, Apr 2015.
- [136] Dmitry Abanin, Wojciech De Roeck, and François Huveneers. A theory of many-body localization in periodically driven systems. *arXiv preprint arXiv:1412.4752*, 2014.
- [137] Pedro Ponte, Anushya Chandran, Z Papić, and Dmitry A Abanin. Periodically driven ergodic and many-body localized quantum systems. *Annals of Physics*, 353:196–204, 2015.
- [138] Luca D’Alessio and Anatoli Polkovnikov. Many-body energy localization transition in periodically driven systems. *Annals of Physics*, 333:19–33, 2013.
- [139] Ranjan Modak, Subroto Mukerjee, Emil A Yuzbashyan, and B Sriram Shastri. Integrals of motion for one-dimensional Anderson localized systems. *New Journal of Physics*, 18(3):033010, 2016.
- [140] Maksym Serbyn, Z. Papić, and Dmitry A. Abanin. Local conservation laws and the structure of the many-body localized states. *Phys. Rev. Lett.*, 111:127201, Sep 2013.

- [141] R. E. Prange, D. R. Grempel, and Shmuel Fishman. Wave functions at a mobility edge: An example of a singular continuous spectrum. *Phys. Rev. B*, 28:7370(R), 1983.
- [142] Efim B. Rozenbaum and Victor Galitski. Dynamical localization of coupled relativistic kicked rotors. *Phys. Rev. B*, 95:064303, Feb 2017.